NASA TN D-971

TECHNICAL NOTE

D-971

TRANSONIC AERODYNAMIC LOADING CHARACTERISTICS OF A WING-BODY-TAIL COMBINATION HAVING A 52.5° SWEPTBACK WING OF ASPECT RATIO 3 WITH CONICAL WING CAMBER AND BODY INDENTATION FOR A DESIGN MACH NUMBER OF $\sqrt{2}$

By Marlowe D. Cassetti, Richard J. Re,
and William B. Igoe

Langley Research Center
Langley Air Force Base, Va.

NATIONAL AERONAUTICS AND SPACE ADMINISTRATION

WASHINGTON October 1961

NATIONAL AERONAUTICS AND SPACE ADMINISTRATION

TECHNICAL NOTE D-971

TRANSONIC AERODYNAMIC LOADING CHARACTERISTICS OF A WING-BODY-TAIL COMBINATION HAVING A 52.5° SWEPTBACK WING OF ASPECT RATIO 3 WITH CONICAL WING CAMBER AND BODY INDENTATION FOR A DESIGN MACH NUMBER OF $\sqrt{2}$

By Marlowe D. Cassetti, Richard J. Re,
and William B. Igoe

SUMMARY

An investigation has been made of the effects of conical wing camber and body indentation according to the supersonic area rule on the aerodynamic wing loading characteristics of a wing-body-tail configuration at transonic speeds. The wing aspect ratio was 3, taper ratio was 0.1, and quarter-chord-line sweepback was 52.5° with 3-percent-thick airfoil sections. The tests were conducted in the Langley 16-foot transonic tunnel at Mach numbers from 0.80 to 1.05 and at angles of attack from 0° to 14°, with Reynolds numbers based on mean aerodynamic chord varying from 7×10^6 to 8×10^6.

Conical camber delayed wing-tip stall and reduced the severity of the accompanying longitudinal instability but did not appreciably affect the spanwise load distribution at angles of attack below tip stall. Body indentation reduced the transonic chordwise center-of-pressure travel from about 8 percent to 5 percent of the mean aerodynamic chord.

INTRODUCTION

An investigation of the transonic aerodynamic characteristics of an airplane model having a 52.5° sweptback wing of aspect ratio 3 (reported in ref. 1) showed that the use of conical camber improved maximum lift-drag ratios attainable in the transonic region. It was inferred from force data that this gain in performance resulted from the improved wing lift distribution associated with the use of conical camber. Because of the scarcity of loads distribution data on conically cambered sweptback wings, the wing pressure loads on the wings of the model tested in reference 1 were also measured and are reported herein.

Similar loading investigations have previously been performed on conically cambered delta planform wings (for example, refs. 2 and 3).

A pressure instrumented model, the same as that used in the force tests of reference 1, was used in this investigation. The wing was cambered for a design Mach number of $\sqrt{2}$ according to the design charts of reference 4, and the body was indented according to the supersonic area rule of reference 5. For purposes of comparison, tests with a plane wing (no camber) and a nonindented body were also conducted. The models were tested in the Langley 16-foot transonic tunnel at Mach numbers from 0.80 to 1.05 and at angles of attack from 0° to 14°. Wing section pressures distributions were obtained for six spanwise stations on all configurations tested.

SYMBOLS

A	body cross-sectional area
A_{ij}	twist at ith spanwise station due to load at jth station
b	wing span
B_{ij}	twist at ith spanwise station due to moment at jth station
c	local chord measured streamwise in x,y plane
c'	mean aerodynamic chord
$\bar{c}$	average wing chord, S/b
c_m	wing section pitching-moment coefficient about local quarter-chord point
C_m	wing pitching-moment coefficient about $0.25c'$
c_n	wing section normal-force coefficient
C_N	wing normal-force coefficient, $\int_{\substack{\text{wing-body} \\ \text{juncture}}}^{1.0} c_n \frac{c}{\bar{c}} \, d\left(\frac{y}{b/2}\right)$
C_p	pressure coefficient, $\frac{\Delta p}{q}$
l	body length

M	free-stream Mach number
Δp	local static pressure minus free-stream static pressure
q	free-stream dynamic pressure
S	total wing area
x'	axial coordinate measured with respect to body nose
x	local axial coordinate measured with respect to wing section leading edge
$\frac{x_{cp}}{c'}$	wing chordwise center-of-pressure position, fraction of wing mean aerodynamic chord measured from leading edge of c'
y	spanwise coordinate measured with respect to plane of symmetry
$\frac{y_{cp}}{b/2}$	wing spanwise center-of-pressure position, fraction of wing semispan
z	coordinate normal to x and y, measured with respect to body center line
α	angle of attack of body center line

MODELS AND APPARATUS

Models

A photograph of the model with the plane wing, indented body, and horizontal and vertical tails is shown in figure 1(a). A sketch of the same configuration giving geometrical details is shown in figure 1(b). A tabulation of the model geometric characteristics is presented in table I.

Wings.- Both a plane and a conically cambered wing were tested, each having the same thickness distribution. The plane wing had NACA 65A003 airfoil sections axially. The cambered-wing ordinates were calculated by the method of reference 4 for a design Mach number of $\sqrt{2}$ at a lift coefficient of 0.2, and are shown as mean camber lines in figure 2. The camber method of reference 4 gave camber only over the outboard 20 percent of each local semispan so that the inboard 80 percent

of each local semispan of the wing was identical to the plane wing. The wings were of steel construction with static pressure orifices located at six spanwise stations (16, 32, 48, 64, 80, and 95 percent of the semispan). A listing of the chordwise orifice locations is presented in table II.

Bodies.- Table III presents the ordinates of the indented and nonindented bodies. Both were bodies of revolution for the forward 75 percent of the body length and had elliptical cross sections over the rearward 25 percent (to accommodate the model sting support).

The indented body had a cross-sectional area distribution calculated for $M = \sqrt{2}$ indentation according to the supersonic area rule of reference 5. The body was indented for only 80 percent of the area calculated for the presence of the horizontal and vertical tails. Cross-sectional area distributions for the two configurations are presented in figure 3.

Tails.- The geometric characteristics of the vertical and horizontal tails are listed in table I. It should be noted that the horizontal tail used on the indented body was different from that used on the nonindented body.

Apparatus

The tests were made in the Langley 16-foot transonic tunnel. A complete description of the wind tunnel and its airflow characteristics is contained in reference 6. The model was sting-supported as shown in figures 1(a) and 1(b). The sting-support system pivoted in a manner such that the model was kept on or near the tunnel center line throughout the angle-of-attack range.

The wing static pressures were recorded on multiple-tube mercury-manometer boards. A pendulum-type strain-gage inclinometer was located inside the model to determine the angle of attack.

TESTS

Three principal model configurations were tested. These were the cambered wing with the indented body, the plane wing with the indented body, and the cambered wing with the nonindented body. For most of the tests, both the vertical and horizontal tails were attached to the model and set at zero deflection. For some configurations and test Mach numbers, data at high angles of attack were obtained with the horizontal-tail incidence at -4° and -8°.

Boundary-layer transition was fixed on all configurations by means of a 0.1-inch-wide strip of distributed roughness particles of No. 220 carborundum grains. On the wings and tails, the strips were located on the upper and lower surfaces at the 2.5-percent-chord line. On the body, a strip around the nose was located at 2.5 percent of the body length.

Tests were conducted at Mach numbers from 0.80 to 1.05 and at angles of attack from 0° to 14° except when restricted by allowable model support loads. The Reynolds numbers based on mean aerodynamic chord varied from 7×10^6 to 8×10^6.

CORRECTIONS AND ACCURACY

Reference 7 indicates that tunnel-wall interference in the Langley 16-foot transonic tunnel is negligible for the size of model which was tested and therefore no such correction has been made. No correction has been made for model aeroelasticity; however, the wing was statically loaded and the measured influence coefficients are presented in figure 4. These coefficients were obtained by the method described in reference 8.

No difference in wing pressure distributions could be detected in tests with differing tail incidences. Therefore, the wing pressure data contained within this report are presented as independent of the tail settings actually used during the tests. In addition, a comparison of wing pressures measured with the tails on and off showed negligible differences. It is therefore considered that the effects on the data of the use of horizontal tails of different size can be ignored.

The accuracy of the data has been estimated as follows:

C_p	± 0.005
M	± 0.01
α, deg	± 0.2

PRESENTATION OF RESULTS

The results of this investigation are presented in the following figures:

DISCUSSION OF RESULTS

Effect of Camber on Local Separation

The effect of camber on local wing flow separation can be seen in a comparison of the chordwise pressure distributions for the plane and cambered wings when tested with the indented body (figs. 5 and 6). Up to an angle of attack of 10°, camber delayed wing-tip stall and spanwise stall progression. In general, beyond 10°, where separation is more fully developed, the distributions are quite similar for both wings.

The beneficial effects due to camber are apparent in the region of $M = 0.80$ to 0.90 as a reduction in the severity of the break in the wing normal-force coefficient with angle of attack (figs. 11(a) and (b)) and as a reduction in the severity of longitudinal instability as illustrated by the variation in wing pitching-moment coefficient with wing normal-force coefficient (figs. 12(a) and (b)).

Effect of Camber on Spanwise Loading

At 0° angle of attack the spanwise load distributions for the cambered wing in combination with the indented body (fig. 9) indicate that the basic loading due to camber is rather small. Thus at angles of attack of 2° and 4°, it is not surprising that the general shape of the spanwise loadings for the cambered wing is similar to that of the plane wing (fig. 8). At an angle of attack of 6°, the cambered wing had a more elliptic spanwise loading than the plane wing because the cambered wing maintained a higher loading over the tip station. Above an angle of attack of 6°, the shape of the spanwise loading is quite distorted due to local flow separation.

The apparent similarity of the loading characteristics for both the plane and cambered wings is illustrated by the similar location of the spanwise center of pressure and its variation with Mach number at constant normal-force coefficient (fig. 15).

Effect of Body Indentation on Chordwise Center-of-Pressure Travel

In the Mach number range of 0.90 to 0.98, the rearward chordwise center-of-pressure travel for the nonindented-body configuration was about 8 percent c' and for the indented-body configurations was about 5 percent c' (fig. 15). This beneficial effect of body indentation is due to higher negative pressure peaks near the wing leading edge and better chordwise pressure recovery at the 32- and 48-percent-semispan stations for the indented body configurations. These pressure differences are difficult to see in the pressure distributions of figures 5, 6, and 7 because of the small plotting scale. However, the effects of these differences are more evident in c_m as can be seen in table IV. At $M = 0.98$ for these wing stations, the local chordwise center of pressure (defined as $(0.25 - c_m/c_n)$) is 3 to 4 percent farther forward for the cambered wing in combination with the indented body than for the cambered wing in combination with the nonindented body.

CONCLUSIONS

An investigation of the aerodynamic loading characteristics of a 52.5° sweptback wing of aspect ratio 3, tested with indented and nonindented bodies, has led to the following conclusions:

1. Conical camber delayed wing-tip stall and reduced the severity of longitudinal instability.

2. Conical camber did not appreciably change the spanwise loading at angles of attack below tip stall of the plane wing.

3. Body indentation reduced the transonic chordwise center-of-pressure travel from about 8 percent to 5 percent of the mean aerodynamic chord.

Langley Research Center,
National Aeronautics and Space Administration,
Langley Air Force Base, Va., August 10, 1961.

REFERENCES

1. Igoe, William B., Re, Richard J., and Cassetti, Marlowe D.: Transonic Aerodynamic Characteristics of a Wing-Body Combination Having a 52.5° Sweptback Wing of Aspect Ratio 3 With Conical Camber and Designed for a Mach Number of $\sqrt{2}$. NASA TN D-817, 1961.

2. Mugler, John P., Jr.: Pressure Measurements at Transonic and Low Supersonic Speeds on a Thin Conical Cambered Low-Aspect-Ratio Delta Wing in Combination With Basic and Indented Bodies. NACA RM L57G19, 1957.

3. Mugler, John P., Jr.: Analysis of Pressure Data Obtained at Transonic Speeds on a Thin Low-Aspect-Ratio Cambered Delta Wing-Body Combination. NACA RM L58F24, 1958.

4. Boyd, John W., Migotsky, Eugene, and Wetzel, Benton E.: A Study of Conical Camber for Triangular and Sweptback Wings. NACA RM A55G19, 1955.

5. Whitcomb, Richard T., and Sevier, John R., Jr.: A Supersonic Area Rule and an Application to the Design of a Wing-Body Combination With High Lift-Drag Ratios. NASA TR R-72, 1960. (Supersedes NACA RM L53H31a.)

6. Ward, Vernon G., Whitcomb, Charles F., and Pearson, Merwin D.: Air-Flow and Power Characteristics of the Langley 16-Foot Transonic Tunnel With Slotted Test Section. NACA RM L52E01, 1952.

7. Whitcomb, Charles F., and Osborne, Robert S.: An Experimental Investigation of Boundary Interference on Force and Moment Characteristics of Lifting Models in the Langley 16- and 8-Foot Transonic Tunnels. NACA RM L52L29, 1953.

8. Arabian, Donald D.: Investigation at Transonic Speeds of Loading Over a 30° Sweptback Wing of Aspect Ratio 3, Taper Ratio 0.2, and NACA 65A004 Airfoil Section Mounted on a Body. NASA TN D-421, 1960. (Supersedes NACA RM L57G09a.)

TABLE I

MODEL GEOMETRICAL CHARACTERISTICS

Wing:	
Airfoil section, plane wing	NACA 65A003
Aspect ratio	3.0
Taper ratio	0.1
Area, sq in.	1,176.0
Vertical tail:	
Airfoil section	NACA 65A003
Taper ratio	0.2
Area, sq in.	293.9
Horizontal tail for indented body:	
Airfoil section	NACA 65A003
Aspect ratio	3.0
Taper ratio	0.2
Area, sq in.	293.9
Sweep of quarter-chord line, deg	45
Span, in.	29.70
Mean aerodynamic chord, in.	11.37
Root chord, in.	16.50
Horizontal tail for nonindented body:	
Airfoil section:	
Root	NACA 64A006
Tip	NACA 64A003
Aspect ratio	3.0
Taper ratio	0.2
Sweep of quarter-chord line, deg	45
Area, sq in.	236.1
Span, in.	26.61
Mean aerodynamic chord, in.	10.18
Root chord, in.	14.78

TABLE II

STATIC PRESSURE ORIFICE LOCATIONS FOR PLANE AND CAMBERED WINGS

$\frac{y}{b/2}$ / x/c	0.16		0.32		0.48		0.64		0.80		0.95	
	Upper surface	Lower surface	Upper surface	Lower surface	Upper surface	Lower surface	Upper surface	Lower surface	Upper surface	Lower surface	Upper surface	Lower surface
0	x		x		x		x		x			
.0125	x	x	x	x	x	x	x	x	x	x	x	
.025	x	x	x	x	x	x	x	x	x	x	x	x
.05	x	x	x	x	x	x	x	x	x	x	x	x
.10	x	x	x	x	x	x	x	x	x	x	x	x
.15	x		x		x		x		x		x	
.20	x	x	x	x	x	x	x	x	x	x	x	x
.30	x	x	x	x	x		x		x		x	
.40	x	x	x	x	x	x	x	x	x	x	x	x
.45	x		x		x		x		x		x	
.50	x	x	x	x	x	x	x	x	x	x	x	x
.55	x	x	x	x	x	x	x	x	x	x	x	x
.60	x	x	x	x	x	x	x	x	x	x	x	x
.65	x	x	x	x	x	x	x	x	x	x	x	x
.70	x	x	x	x	x	x	x	x	x	x	x	x
.75	x	x	x	x	x	x	x	x	x	x	x	x
.80	x	x	x	x	x	x	x	x	x	x	x	x
.85		x	x	x	x	x	x	x	x	x		x
.90	x	x	x	x	x	x	x	x	x	x	x	
.95	x	x	x	x	x		x	x	x			

TABLE III

BODY ORDINATES

[All dimensions are in inches]

Body station, x	Indented body		Nonindented body	
	y	z	y	z
Circular cross section				
0	0		0	
.50	.24		.24	
.75	.32		.32	
1.00	.39		.39	
2.00	.66		.66	
4.00	1.09		1.09	
6.00	1.46		1.46	
8.00	1.78		1.78	
10.00	2.07		2.07	
14.00	2.59		2.59	
18.00	3.03		3.03	
22.00	3.40		3.40	
26.00	3.73		3.73	
30.00	4.00		4.00	
35.00	4.28		4.28	
40.00	4.45		4.51	
45.00	4.46		4.64	
50.00	4.36		4.73	
55.00	4.27		4.76	
60.00	4.24		4.74	
65.00	4.30		4.65	
70.00	4.21		4.50	
75.00	4.08		4.29	
Elliptical cross section				
80.00	3.85	3.90	3.99	4.04
84.00	3.49	3.68	3.60	3.82
88.00	2.98	3.38	3.25	3.65
92.00	2.59	3.12	2.86	3.45
96.00	2.21	2.99	2.48	3.25
100.00	1.88	2.81	2.12	3.05

TABLE IV

WING SECTION COEFFICIENTS

(a) Indented body and plane wing

M	α, deg	$\frac{y}{b/2}$ = 0.16		$\frac{y}{b/2}$ = 0.32		$\frac{y}{b/2}$ = 0.48		$\frac{y}{b/2}$ = 0.64		$\frac{y}{b/2}$ = 0.80		$\frac{y}{b/2}$ = 0.95	
		c_n	c_m	c_n	c_m	c_n	c_m	c_n	c_m	c_n	c_m	c_n	c_m
0.80	0	-.0036	.0009	-.0117	.0018	-.0160	.0003	-.0154	-.0002	-.0279	-.0037	-.0301	-.0041
	2	.0833	-.0091	.0991	-.0031	.1026	-.0034	.1279	-.0019	.1435	-.0043	.1367	-.0040
	4	.1827	-.0208	.2191	-.0060	.2430	-.0087	.3153	-.0109	.2841	-.0117	.2761	-.0085
	6	.2804	-.0317	.3354	-.0015	.3649	-.0034	.4951	-.0564	.4839	-.0761	.4203	-.0135
	8	.3935	-.0431	.4962	-.0055	.5319	-.0165	.8223	-.1499	.4996	-.0027	.1063	-.0129
	10	.4989	-.0527	.6373	-.0072	.7333	-.0500	.9890	-.2098	.4663	-.0700	.1442	-.0269
	12	.6015	-.0533	.7702	-.0086	.9062	-.1074	.7910	-.1328	.4713	-.0791	.1841	-.0304
	14	.7006	-.0596	.9233	-.0346	1.0041	-.1718	.7928	-.1389	.4988	-.0776	.2038	-.0691
0.85	0	-.0017	.0008	-.0086	.0019	-.0110	.0009	-.0131	.0002	-.0236	-.0028	-.0195	-.0026
	2	.0854	-.0104	.1002	-.0040	.1039	-.0039	.1282	-.0024	.1467	-.0057	.1375	-.0043
	4	.1848	-.0232	.2250	-.0082	.2458	-.0105	.3150	-.0109	.2881	-.0122	.2669	-.0088
	6	.2913	-.0364	.3546	-.0083	.3698	-.0062	.5127	-.0597	.4882	-.0802	.2274	-.0143
	8	.4017	-.0493	.4992	-.0114	.5456	-.0216	.8201	-.1487	.5127	-.0942	.1167	-.0146
	10	.5120	-.0613	.6476	-.0165	.7475	-.0577	1.0338	-.2249	.4865	-.0747	.2015	-.0268
	12	.5953	-.0566	.7620	-.0112	.9117	-.1146	.7337	-.1345	.4584	-.0754	.1820	-.0516
	14	.6970	-.0652	.9118	-.0412	.9928	-.1673	.7626	-.1397	.5131	-.0846	.2096	-.0429
0.90	0	-.0007	.0011	-.0092	.0026	-.0127	.0012	-.0143	.0010	-.0232	-.0032	-.0168	-.0040
	2	.0893	-.0118	.1013	-.0042	.1093	-.0055	.1366	-.0030	.1543	-.0059	.1483	-.0062
	4	.1906	-.0265	.2330	-.0110	.2557	-.0125	.3099	-.0162	.3040	-.0101	.2692	-.0060
	6	.3020	-.0427	.3669	-.0157	.3853	-.0127	.5272	-.0630	.5423	-.0936	.1642	-.0151
	8	.4125	-.0598	.5132	-.0229	.5622	-.0344	.8129	-.1453	.5366	-.0965	.1421	-.0125
	10	.5299	-.0775	.6652	-.0341	.7528	-.0707	1.0562	-.2304	.5342	-.0882	.1387	-.0303
	12	.6121	-.0718	.7649	-.0226	.8790	-.0960	.7671	-.1287	.4960	-.0983	.1867	-.0552
	14	.6828	-.0842	.8994	-.0488	1.0096	-.1729	.7693	-.1403	.5804	-.1130	.2153	-.0449
0.92	0	.0002	.0016	-.0077	.0023	-.0072	.0002	-.0107	.0012	-.0216	-.0028	-.0175	-.0040
	2	.0901	-.0131	.1063	-.0070	.1124	-.0068	.1373	-.0031	.1564	-.0047	.1485	-.0048
	4	.1916	-.0290	.2418	-.0144	.2610	-.0150	.3054	-.0154	.3127	-.0138	.2903	-.0042
	6	.3069	-.0483	.3731	-.0220	.3918	-.0156	.5373	-.0669	.5818	-.1012	.1719	-.0169
	10	.5336	-.0847	.6711	-.0442	.7590	-.0823	1.0549	-.2322	.5754	-.0945	.1405	-.0375
	12	.6476	-.1005	.8232	-.0624	.9738	-.1416	1.1508	-.2576	.5267	-.0909	.2128	-.0644
0.94	0	-.0016	.0018	-.0083	.0021	-.0103	.0010	-.0153	.0013	-.0251	-.0027	-.0143	-.0036
	2	.0950	-.0158	.1081	-.0101	.1177	-.0103	.1469	-.0058	.1690	-.0024	.1594	-.0014
	4	.2000	-.0345	.2487	-.0193	.2707	-.0208	.3111	-.0194	.3263	-.0118	.2899	-.0066
	6	.3100	-.0516	.3804	-.0274	.4003	-.0228	.5425	-.0723	.5807	-.0934	.1780	-.0184
	8	.4208	-.0697	.5259	-.0357	.5823	-.0528	.7978	-.1400	.5813	-.1005	.1613	-.0128
	10	.5314	-.0886	.6664	-.0510	.7617	-.0928	1.0365	-.2279	.6386	-.1066	.1604	-.0341
	12	.6429	-.1064	.8129	-.0679	.9565	-.1462	1.1240	-.2497	.5584	-.0923	.2046	-.0642
0.98	0	-.0009	.0001	-.0076	.0025	-.0099	.0030	-.0110	.0023	-.0312	-.0070	.0013	-.0003
	2	.0883	-.0125	.1020	-.0069	.1132	-.0097	.1430	-.0138	.1662	-.0229	.2213	.0028
	4	.1890	-.0285	.2368	-.0161	.2551	-.0198	.3092	-.0317	.3630	-.0280	.4032	-.0856
	6	.3008	-.0507	.3685	-.0288	.3966	-.0304	.5469	-.0791	.5603	-.0968	.2062	-.0283
	8	.4116	-.0712	.5048	-.0397	.5753	-.0589	.7646	-.1399	.6493	-.1264	.1985	-.0318
	10	.5152	-.0885	.6411	-.0531	.7343	-.0946	.9727	-.2126	.7137	-.1423	.2167	-.0410
	12	.6233	-.1054	.7860	-.0709	.9206	-.1516	1.0880	-.2460	.7375	-.1375	.2198	-.0527
1.00	0	-.0008	-.0002	-.0069	.0015	-.0070	.0008	-.0109	.0018	-.0287	-.0056	-.0293	-.0006
	2	.0909	-.0131	.1038	-.0055	.1122	-.0054	.1419	-.0096	.1660	-.0210	.1690	.0095
	4	.1937	-.0299	.2402	-.0152	.2551	-.0157	.3230	-.0328	.3634	-.0370	.3525	-.0696
	6	.2962	-.0489	.3625	-.0261	.3891	-.0280	.5363	-.0777	.5485	-.0594	.2260	-.0407
	8	.3926	-.0628	.4906	-.0374	.5609	-.0583	.7423	-.1366	.6368	-.1252	.2227	-.0420
	10	.4756	-.0718	.6261	-.0528	.7180	-.0934	.9340	-.2039	.7385	-.1429	.2464	-.0520
1.05	0	.0011	-.0006	-.0075	.0013	-.0097	.0016	-.0116	.0018	-.0316	-.0071	-.0917	.0077
	2	.0944	-.0181	.1067	-.0127	.1146	-.0124	.1443	-.0123	.1600	-.0248	.1299	-.0093
	4	.1903	-.0360	.2318	-.0263	.2516	-.0288	.3188	-.0348	.3709	-.0460	.3123	-.0539
	6	.2902	-.0515	.3641	-.0360	.3996	-.0398	.5360	-.0738	.5523	-.1036	.2610	-.0546
	8	.3970	-.0725	.4807	-.0464	.5515	-.0698	.7044	-.1228	.6423	-.1296	.2694	-.0595
	10	.4895	-.0871	.6162	-.0619	.7100	-.1020	.8783	-.1805	.7182	-.1438	.2906	-.0641

TABLE IV.- Continued

WING SECTION COEFFICIENTS

(b) Indented body and cambered wing

M	α, deg	$\frac{y}{b/2}$ = 0.16		$\frac{y}{b/2}$ = 0.32		$\frac{y}{b/2}$ = 0.40		$\frac{y}{b/2}$ = 0.64		$\frac{y}{b/2}$ = 0.80		$\frac{y}{b/2}$ = 0.95	
		c_n	c_m	c_n	c_m	c_n	c_m	c_n	c_m	c_n	c_m	c_n	c_m
0.80	0	-.0128	.0015	-.0111	.0028	-.0257	-.0020	-.0266	-.0094	-.0743	-.0204	-.1797	-.0049
	2	.0787	-.0095	.0839	-.0051	.0870	-.0085	.1138	-.0142	.0994	-.0234	.0533	-.0247
	4	.1692	-.0201	.1896	-.0112	.2088	-.0122	.2575	-.0171	.2569	-.0210	.2297	-.0197
	6	.2650	-.0313	.3030	-.0170	.3251	-.0188	.3942	-.0190	.3938	-.0260	.3817	-.0253
	8	.3694	-.0432	.4314	-.0233	.4712	-.0268	.6192	-.0557	.5481	-.0894	.1943	-.0236
	10	.4807	-.0530	.5829	-.0147	.6704	-.0487	.8382	-.1067	.4781	-.0798	.1316	-.0141
	12	.5771	-.0564	.7295	-.0099	.8379	-.0853	.7583	-.1317	.4546	-.0829	.1765	-.0357
	14	.6787	-.0628	.8807	-.0375	.9961	-.1759	.7469	-.1403	.5102	-.0813	.1654	-.0193
0.85	0	-.0086	.0012	-.0136	.0036	-.0235	-.0022	-.0263	-.0099	-.0779	-.0192	-.1776	-.0024
	2	.0829	-.0110	.0880	-.0064	.0933	-.0092	.1701	-.0146	.1068	-.0244	.0644	-.0267
	4	.1766	-.0235	.1954	-.0130	.2122	-.0131	.2671	-.0178	.2737	-.0347	.2431	-.0158
	6	.2698	-.0346	.3105	-.0188	.3352	-.0173	.4054	-.0177	.4097	-.0251	.4046	-.0408
	8	.3793	-.0481	.4437	-.0293	.4828	-.0279	.6287	-.0594	.5892	-.1004	.1965	-.0704
	10	.4923	-.0614	.5905	-.0240	.6909	-.0615	.8403	-.1457	.4987	-.0869	.1454	-.0164
	12	.5887	-.0652	.7264	-.0195	.8429	-.0923	.7720	-.1554	.4670	-.0969	.1777	-.0154
	14	.6777	-.0658	.8577	-.0410	.9957	-.1754	.7435	-.1468	.5077	-.0826	.1703	-.0348
0.90	0	-.0091	.0010	-.0119	.0036	-.0244	-.0026	-.0271	-.0093	-.0852	-.0194	-.1744	-.0027
	2	.0824	-.0128	.0860	-.0073	.0949	-.0101	.1211	-.0150	.1077	-.0227	.0741	-.0241
	4	.1787	-.0269	.1974	-.0159	.2193	-.0169	.2760	-.0203	.2861	-.0251	.2556	-.0176
	6	.2794	-.0414	.3200	-.0234	.3629	-.0211	.4280	-.0197	.4355	-.0345	.4435	-.0478
	8	.3927	-.0583	.4638	-.0380	.4941	-.0269	.6102	-.0637	.6564	-.1150	.2109	-.0248
	10	.5064	-.0753	.6045	-.0389	.7094	-.0780	.8269	-.1315	.5251	-.0913	.1983	-.0149
	12	.6219	-.0941	.7552	-.0552	.8940	-.1260	1.0529	-.0149	.5272	-.0996	.1428	-.0344
0.92	0	-.0106	.0020	-.0121	.0038	-.0248	-.0028	-.0254	-.0099	-.0807	-.0190	-.1763	.0001
	2	.0842	-.0138	.0917	-.0086	.0963	-.0109	.1245	-.0154	.1159	-.0260	.0868	-.0237
	4	.1849	-.0300	.2076	-.0184	.2271	-.0190	.2853	-.0219	.2885	-.0227	.2561	-.0064
	6	.2871	-.0479	.3298	-.0295	.3672	-.0266	.4390	-.0228	.4510	-.0335	.5165	-.0090
	8	.4012	-.0645	.4722	-.0450	.5011	-.0366	.6213	-.0667	.6745	-.1190	.2163	-.0422
	10	.5152	-.0839	.6133	-.0488	.7217	-.0887	.8366	-.1315	.5900	-.0959	.1665	-.0145
	12	.6317	-.1011	.7611	-.0672	.9163	-.1401	1.0248	-.0145	.5714	-.0943	.1434	-.0322
0.94	0	-.0053	.0012	-.0133	.0048	-.0222	-.0028	-.0172	-.0099	-.0852	-.0074	-.1942	.0083
	2	.0962	-.0178	.0957	-.0112	.1034	-.0137	.1378	-.0178	.1180	-.0239	.0967	-.0249
	4	.1963	-.0358	.2113	-.0237	.2413	-.0278	.3040	-.0293	.2912	-.0199	.2705	-.0062
	5	.2364	-.0421	.2621	-.0276	.2967	-.0315	.3763	-.0344	.3820	-.0262	.3695	.0066
	8	.4023	-.0705	.4652	-.0402	.5165	-.0576	.6524	-.0664	.6749	-.1102	.4350	-.0278
	10	.5182	-.0904	.6192	-.0590	.7195	-.0954	.8462	-.1394	.5884	-.1045	.1764	-.0424
	12	.6256	-.1038	.7442	-.0720	.9115	-.1501	1.0086	-.0223	.6307	-.1029	.1563	-.0316
0.98	0	-.0020	-.0020	-.0088	.0036	-.0256	.0012	-.0139	-.0089	-.0831	-.0234	-.1816	-.0120
	2	.0876	-.0148	.0881	-.0089	.0935	-.0126	.1364	-.0156	.1291	-.0364	.1404	-.0381
	4	.1815	-.0293	.1979	-.0187	.2238	-.0244	.2970	-.0296	.3098	-.0557	.3579	-.0431
	6	.2842	-.0481	.3177	-.0322	.3660	-.0350	.4624	-.0439	.5239	-.0987	.6044	-.0485
	8	.3835	-.0623	.4459	-.0470	.5077	-.0523	.6397	-.0560	.6627	-.0921	.4409	-.0881
	10	.5042	-.0865	.5988	-.0747	.6732	-.0743	.8770	-.1592	.7044	-.1368	.2521	-.0415
	12	.6276	-.1040	.7172	-.0748	.8900	-.1573	.9664	-.1946	.7534	-.1486	.2215	-.0421
1.00	0	-.0046	-.0002	-.0090	.0030	-.0242	-.0016	-.0166	-.0094	-.0756	-.0267	-.1887	-.0120
	2	.0934	-.0182	.0940	-.0096	.0981	-.0120	.1386	-.0238	.1308	-.0464	.1421	-.0410
	4	.1893	-.0334	.2040	-.0201	.2284	-.0230	.3004	-.0377	.3304	-.0680	.2941	-.0562
	6	.2856	-.0483	.3179	-.0304	.3604	-.0319	.4633	-.0402	.5379	-.0721	.4956	-.0634
	8	.3829	-.0627	.4454	-.0471	.4976	-.0470	.6261	-.0566	.6010	-.0487	.5134	-.1053
	10	.4904	-.0829	.5847	-.0764	.6675	-.0765	.8471	-.1531	.6827	-.1258	.2794	-.0548
	12	.5981	-.1014	.7102	-.0777	.8782	-.1582	.9406	-.1989	.7566	-.1531	.2612	-.0582
1.05	0	-.0008	-.0003	-.0082	.0016	-.0207	-.0030	-.0158	-.0098	-.0771	-.0256	-.2535	-.0287
	2	.0888	-.0183	.0906	-.0138	.0999	-.0173	.1335	-.0246	.1204	-.0475	-.0177	-.0838
	4	.1824	-.0356	.2031	-.0277	.2263	-.0304	.2897	-.0392	.3154	-.0696	.1916	-.0879
	6	.2719	-.0496	.3134	-.0401	.3576	-.0417	.4453	-.0476	.5103	-.0827	.4271	-.1020
	8	.3699	-.0658	.4357	-.0553	.4923	-.0523	.6304	-.0541	.6786	-.1053	.5942	-.1147
	10	.4801	-.0851	.5655	-.0817	.6616	-.0853	.8271	-.1316	.7288	-.1442	.3347	-.0724

TABLE IV.- Concluded

WING SECTION COEFFICIENTS

(c) Nonindented body and cambered wing

M	α, deg	$\frac{y}{b/2}$ = 0.16		$\frac{y}{b/2}$ = 0.32		$\frac{y}{b/2}$ = 0.48		$\frac{y}{b/2}$ = 0.64		$\frac{y}{b/2}$ = 0.80		$\frac{y}{b/2}$ = 0.95	
		c_n	c_m	c_n	c_m	c_n	c_m	c_n	c_m	c_n	c_m	c_n	c_m
0.80	0	-.0177	.0062	-.0129	.0037	-.0266	-.0025	-.0321	-.0089	-.0789	-.0210	-.1850	.0025
	2	.0742	-.0062	.0844	-.0060	.0864	-.0083	.1111	-.0135	.1007	-.0262	.0627	-.0243
	4	.1635	-.0169	.1861	-.0117	.2041	-.0118	.2514	-.0168	.2519	-.0237	.2216	-.0177
	6	.2589	-.0294	.2992	-.0182	.3215	-.0171	.3895	-.0171	.3970	-.0296	.3819	-.0327
	8	.3659	-.0418	.4399	-.0214	.4737	-.0322	.6106	-.0497	.5537	-.0884	.2026	-.0241
	10	.4722	-.0524	.5730	-.0186	.6565	-.0478	.8255	-.1464	.4813	-.0796	.1458	-.0145
	12	.5663	-.0575	.7151	-.0095	.8192	-.0770	.7567	-.1313	.4496	-.0898	.1666	-.0303
	14	.6723	-.0664	.8529	-.0255	1.0109	-.1660	.7572	-.1388	.4977	-.0826	.1778	-.0324
0.85	0	-.0138	.0055	-.0112	.0033	-.0254	-.0024	-.0302	-.0088	-.0786	-.0214	-.1762	-.0021
	2	.0763	-.0070	.0859	-.0067	.0876	-.0091	.1144	-.0139	.1062	-.0274	.0627	-.0249
	4	.1704	-.0198	.1928	-.0136	.2089	-.0127	.2594	-.0173	.2713	-.0289	.2396	-.0165
	6	.2638	-.0322	.3077	-.0205	.3338	-.0170	.4012	-.0160	.4139	-.0285	.4024	-.0371
	8	.3753	-.0484	.4400	-.0299	.4795	-.0329	.6208	-.0485	.6067	-.1029	.2010	-.0227
	10	.4950	-.0642	.5907	-.0267	.6852	-.0637	.8352	-.1402	.4926	-.0816	.1560	-.0168
	12	.5843	-.0664	.7166	-.0164	.8104	-.0775	.7911	-.1339	.4591	-.1027	.1829	-.0344
	14	.6803	-.0738	.8525	-.0330	1.0064	-.1731	.7485	-.1441	.5176	-.0872	.1774	-.0329
0.90	0	.0013	.0019	-.0097	.0039	-.0257	-.0022	-.0260	-.0090	-.0787	-.0203	-.1764	.0004
	2	.0828	-.0094	.0920	-.0084	.0946	-.0101	.1213	-.0146	.1105	-.0271	.0769	-.0241
	4	.1822	-.0261	.2026	-.0173	.2194	-.0155	.2765	-.0187	.2839	-.0256	.2604	-.0152
	6	.2825	-.0414	.3256	-.0268	.3501	-.0208	.4397	-.0125	.4582	-.0178	.4627	-.0285
	8	.3979	-.0628	.4682	-.0447	.5028	-.0422	.6166	-.0482	.7185	-.1230	.2301	-.0293
	10	.5196	-.0831	.6133	-.0469	.7180	-.0854	.8228	-.1212	.5345	-.0894	.1639	-.0165
	12	.6375	-.1053	.7741	-.0641	.9198	-.1365	1.0253	-.1908	.5432	-.0981	.1509	-.0375
0.92	0	-.0046	.0037	-.0121	.0043	-.0282	-.0022	-.0281	-.0088	-.0792	-.0248	-.1735	-.0011
	2	.0872	-.0115	.0939	-.0092	.0975	-.0111	.1251	-.0152	.1139	-.0270	.0927	-.0251
	4	.1880	-.0291	.2106	-.0206	.2273	-.0179	.2900	-.0192	.2962	-.0236	.2721	-.0137
	6	.2934	-.0478	.3408	-.0339	.3711	-.0254	.4620	-.0153	.4789	-.0033	.4907	-.0384
	8	.4082	-.0706	.4843	-.0558	.5289	-.0563	.6401	-.0544	.7665	-.1262	.2286	-.0313
	10	.5311	-.0941	.6251	-.0592	.7358	-.1002	.8250	-.1208	.5647	-.0964	.1681	-.0167
0.98	0	-.0079	.0051	-.0070	.0045	-.0296	.0030	-.0247	-.0077	-.0936	-.0209	-.1689	-.0012
	2	.0891	-.0135	.0952	-.0136	.1021	-.0164	.1422	-.0279	.1057	-.0247	.1566	-.0287
	4	.1929	-.0320	.2131	-.0301	.2437	-.0348	.3129	-.0466	.3507	-.0727	.4079	-.0532
	6	.2912	-.0520	.3350	-.0449	.3821	-.0447	.4871	-.0545	.5780	-.0837	.5576	-.0374
1.00	0	-.0060	.0060	-.0106	.0046	-.0196	.0007	-.0217	-.0091	-.0791	-.0329	-.2149	-.0114
	2	.0816	-.0111	.0915	-.0116	.0993	-.0151	.1327	-.0266	.1185	-.0480	.0948	-.0545
	4	.1848	-.0288	.2082	-.0282	.2332	-.0316	.2999	-.0449	.3278	-.0742	.2358	-.0991
	6	.2846	-.0504	.3270	-.0437	.3766	-.0457	.4790	-.0561	.5574	-.0884	.4354	-.1030
1.05	0	-.0062	.0052	-.0059	.0033	-.0190	-.0018	-.0215	-.0099	-.0964	-.0224	-.2735	-.0199
	2	.0829	-.0134	.0912	-.0145	.1007	-.0198	.1308	-.0285	.1233	-.0578	-.0291	-.0609
	4	.1830	-.0327	.2033	-.0321	.2337	-.0370	.2930	-.0483	.3276	-.0847	.1784	-.0940

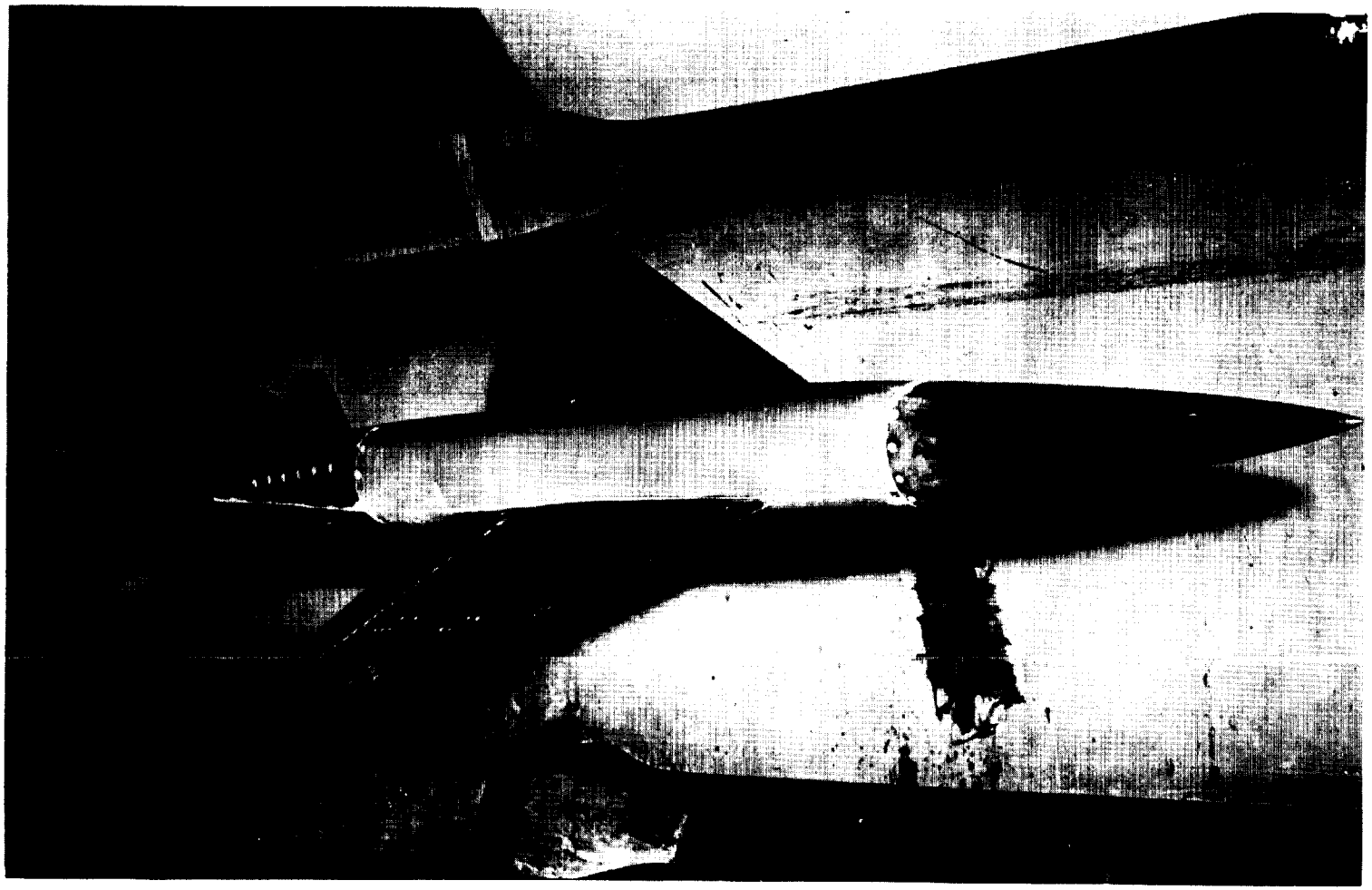

(a) Model mounted in Langley 16-foot transonic tunnel. L-58-301a

Figure 1.- Photograph and sketch of complete model.

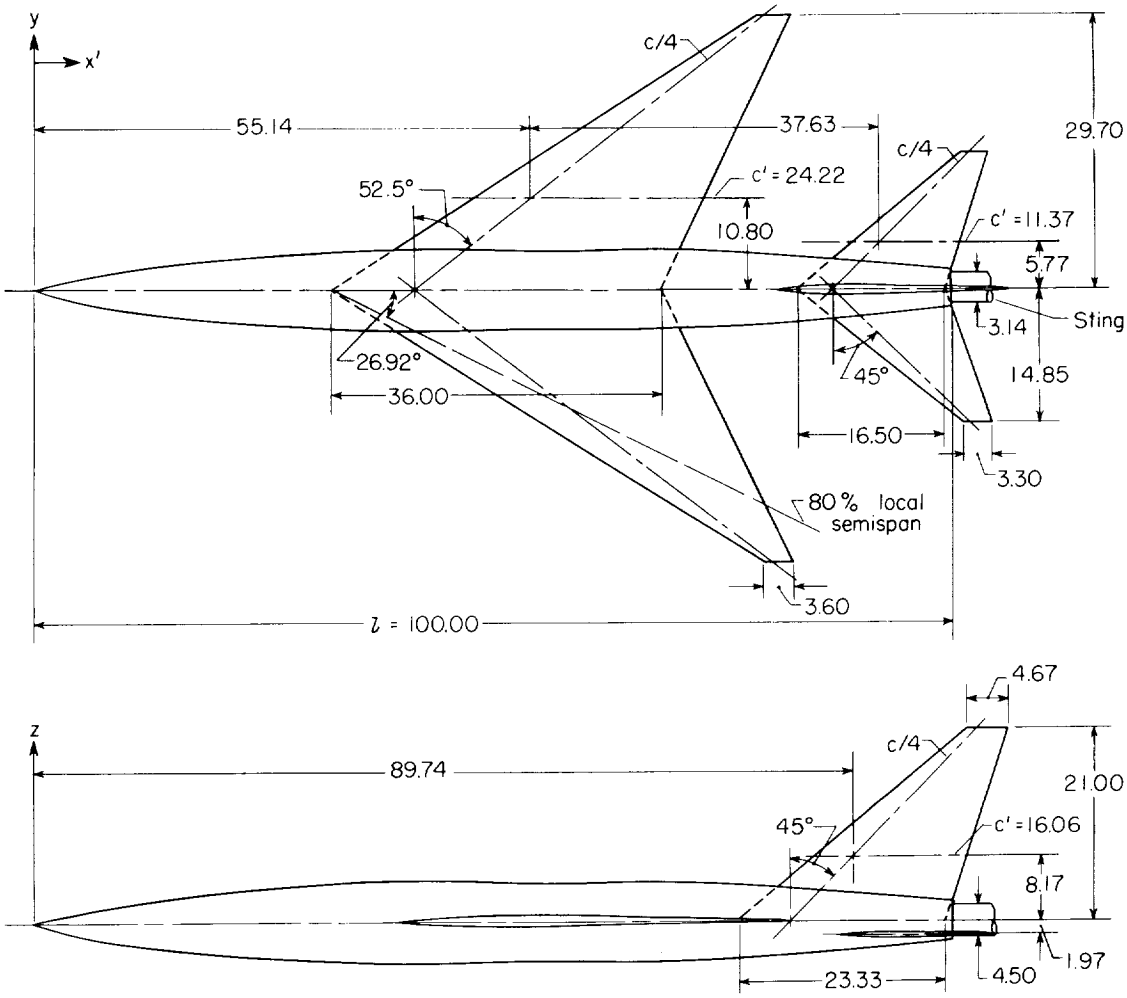

(b) Sketch of model with plane wing and indented body. All dimensions are in inches unless otherwise noted.

Figure 1.- Concluded.

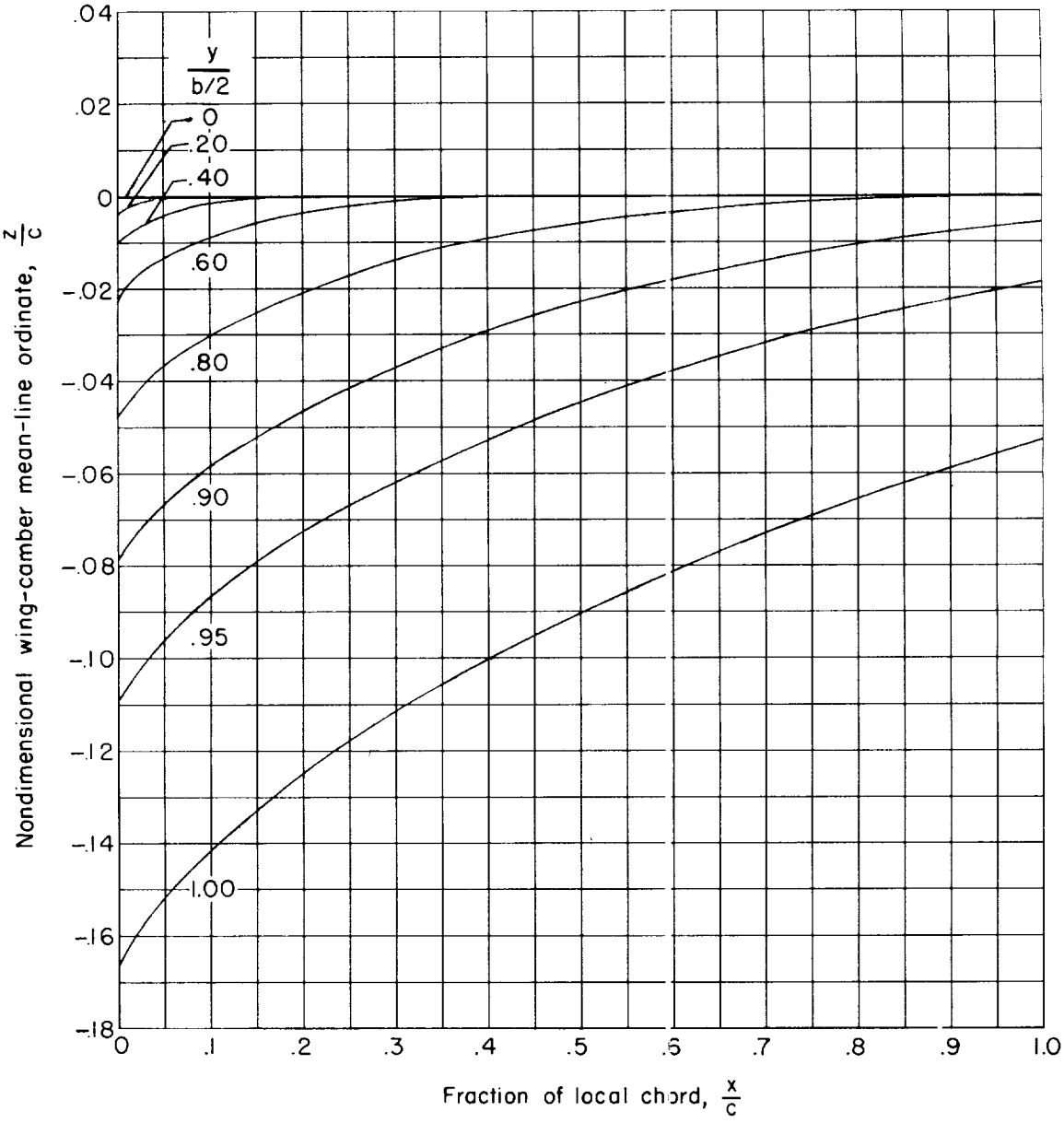

Figure 2.- Nondimensional wing camber ordinates for the conically cambered wing.

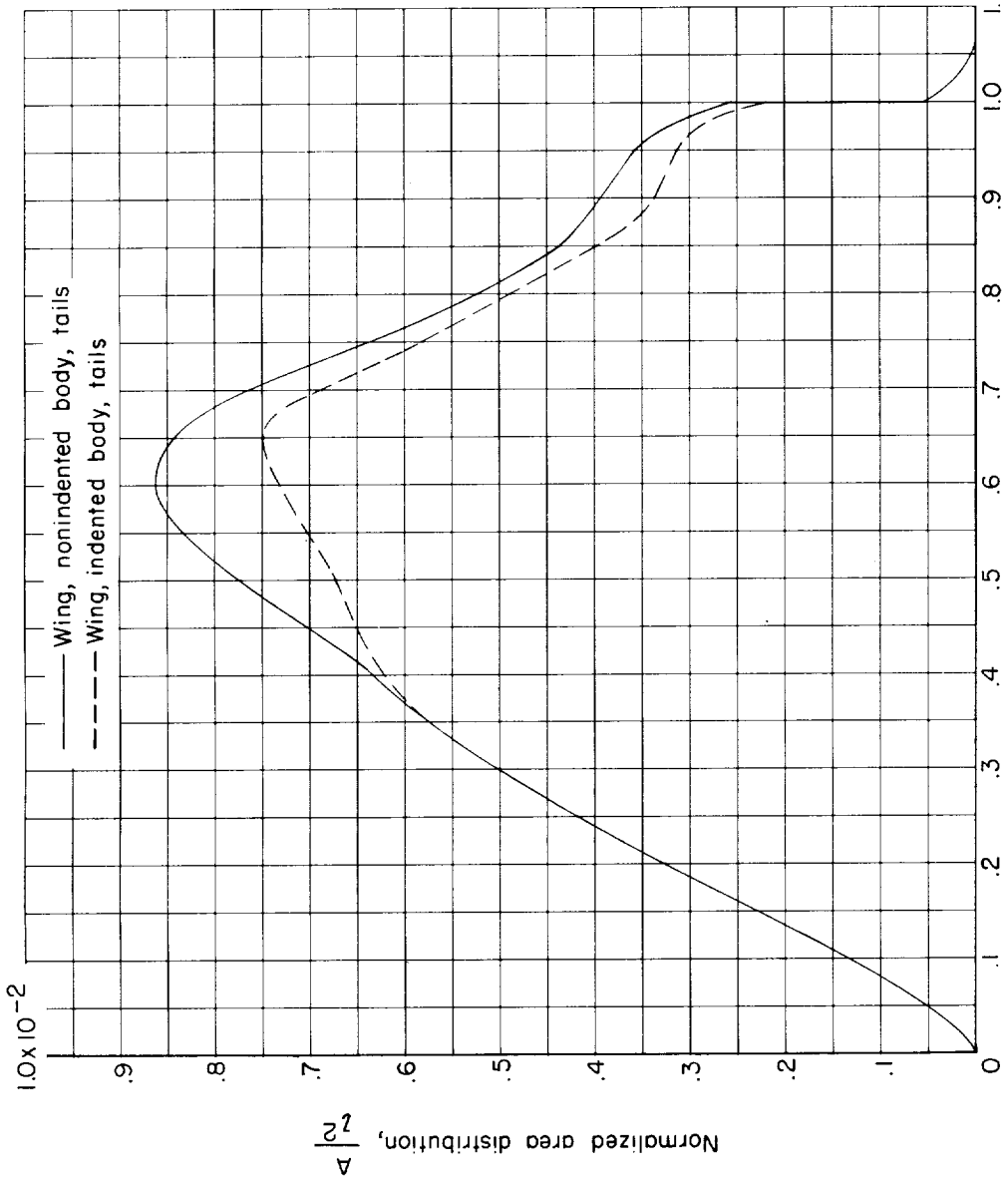

Figure 3.- Normalized axial distribution of cross-sectional area for complete models.

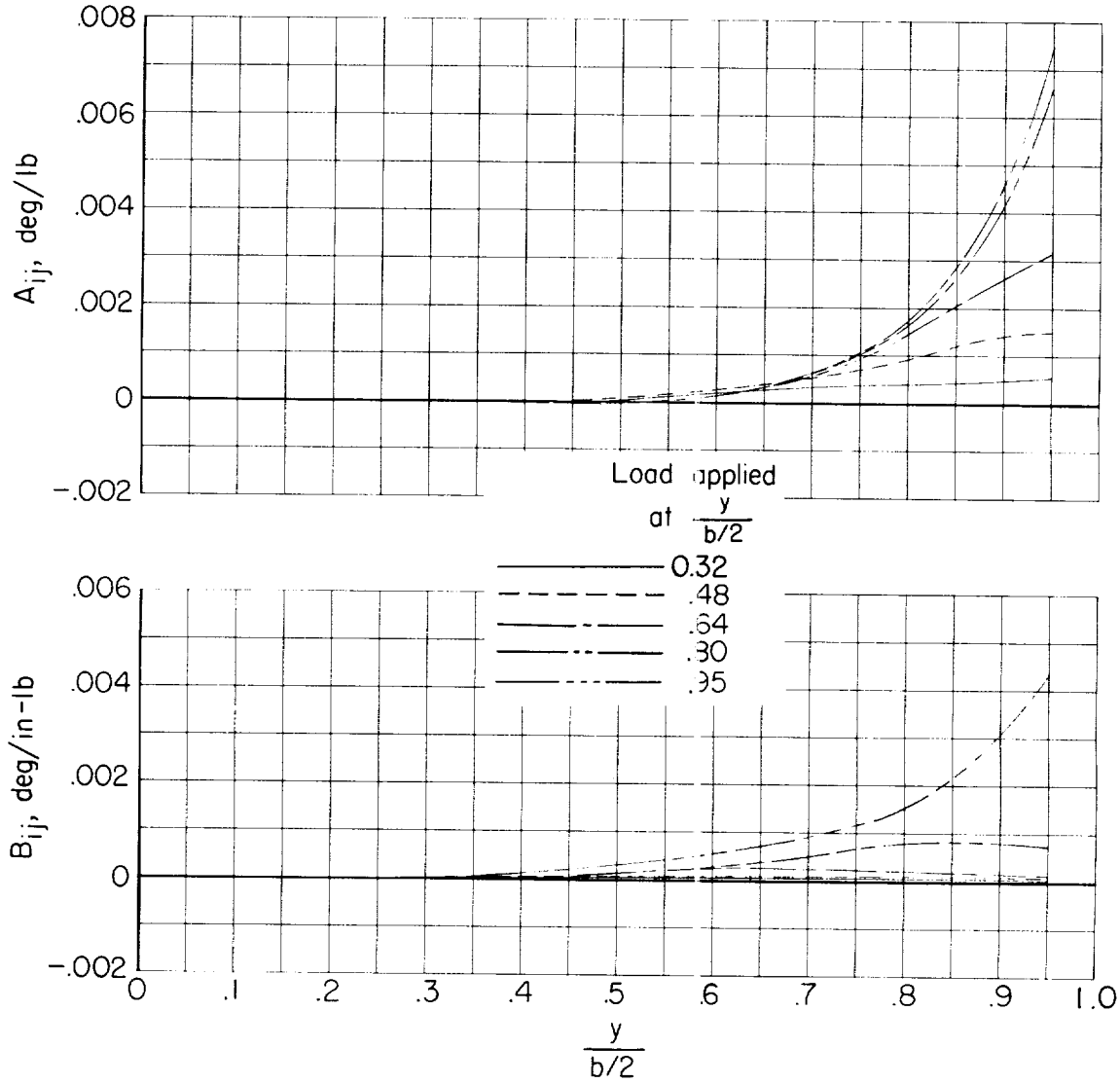

Figure 4.- Wing-twist characteristics for combined normal-force and pitching-moment loadings at five spanwise locations. (Wing attachment point at $\frac{y}{b/2} = 0.088$.)

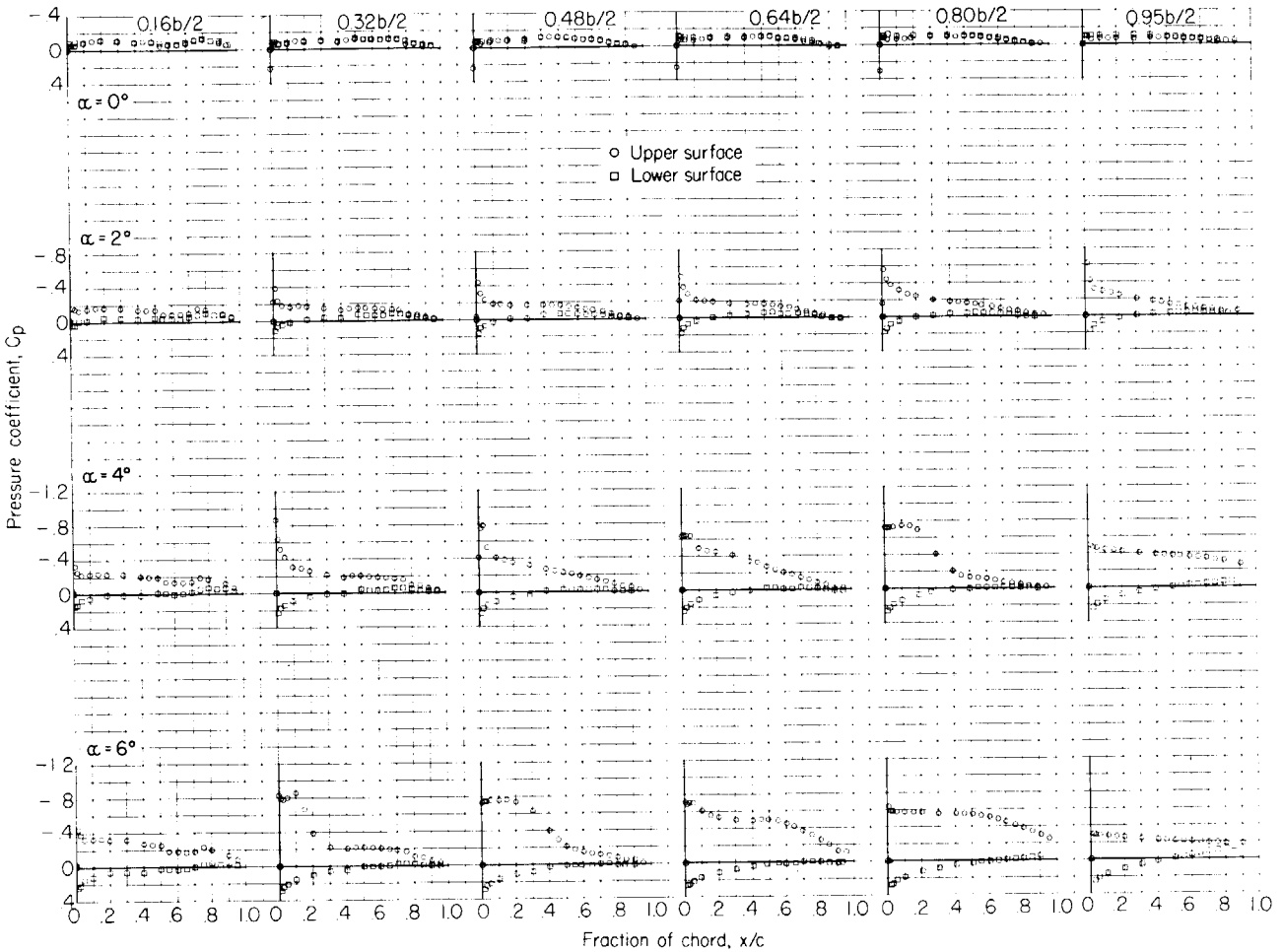

(a) M = 0.80.

Figure 5.- Chordwise pressure distributions for the plane wing in combination with the indented body.

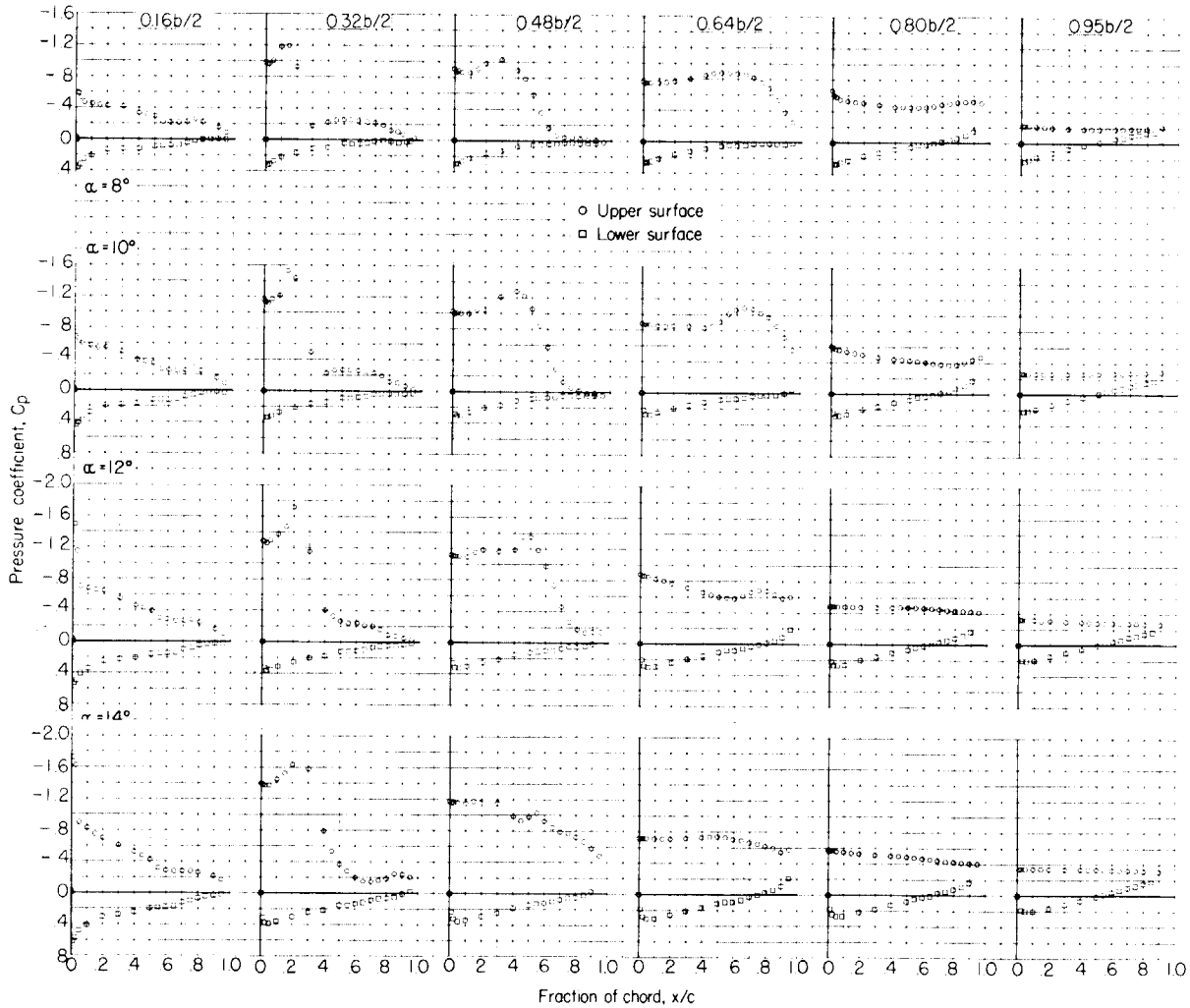

(a) Concluded.

Figure 5.- Continued.

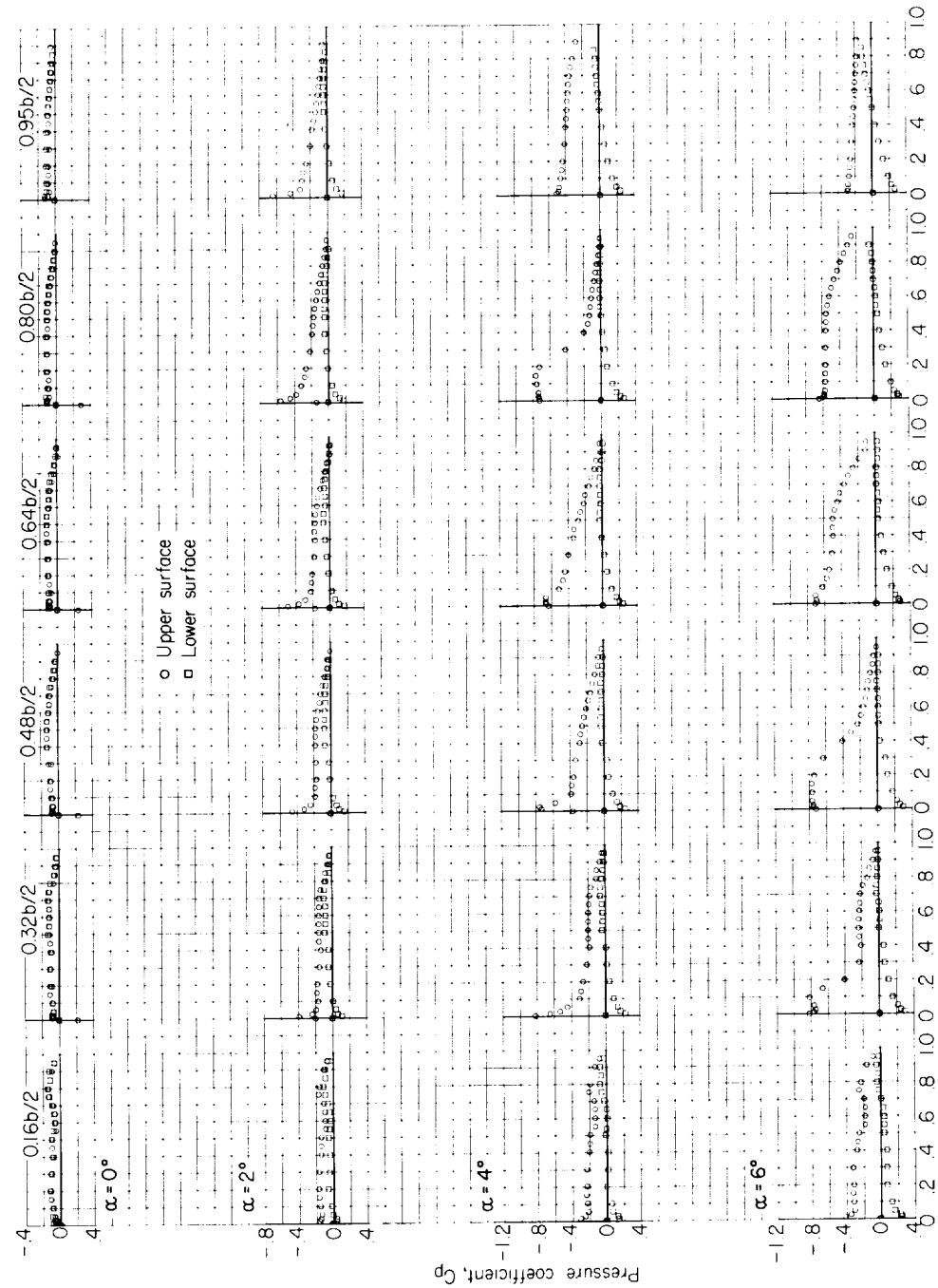

(b) M = 0.85.

Figure 5.- Continued.

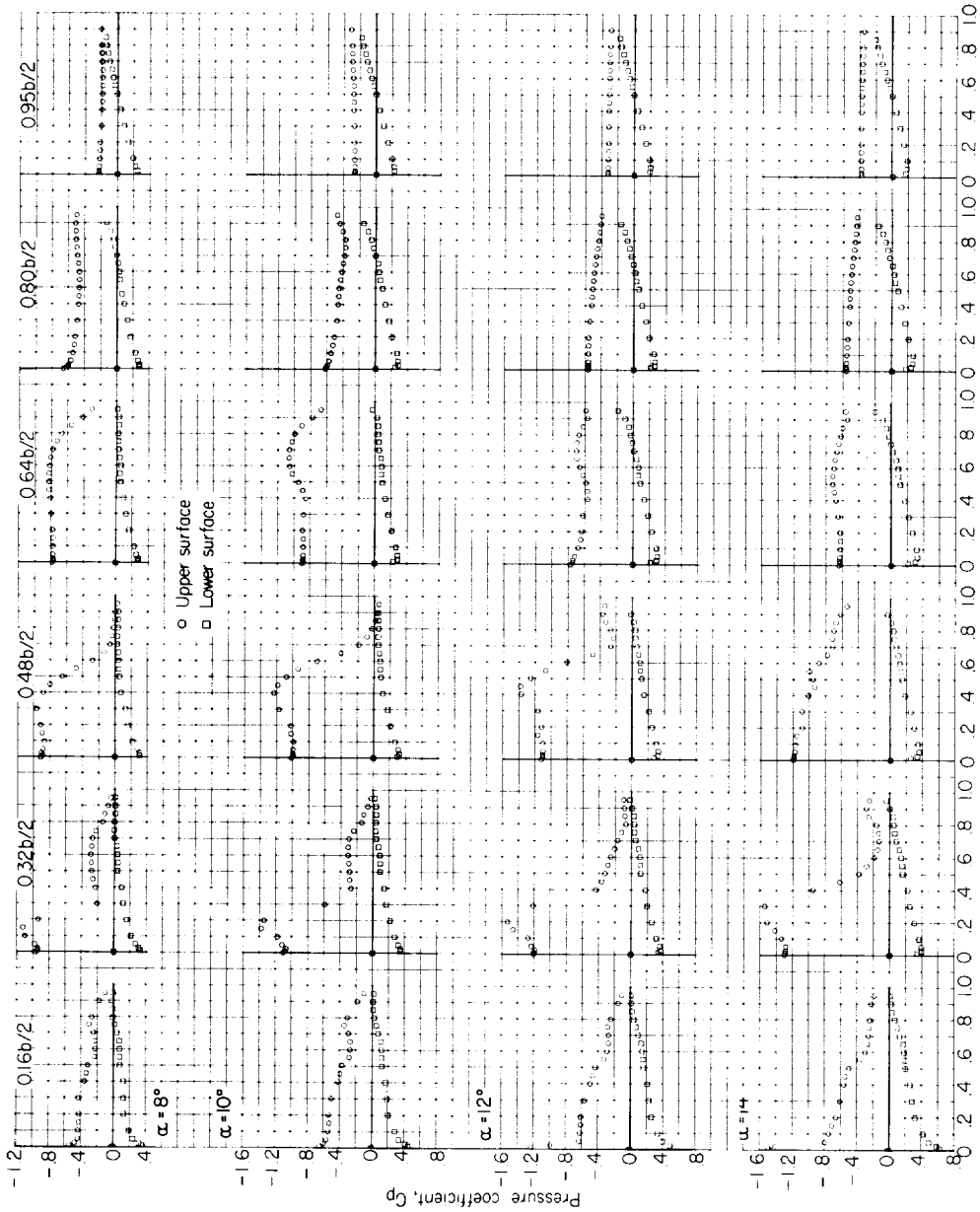

(b) Concluded.

Figure 5.- Continued.

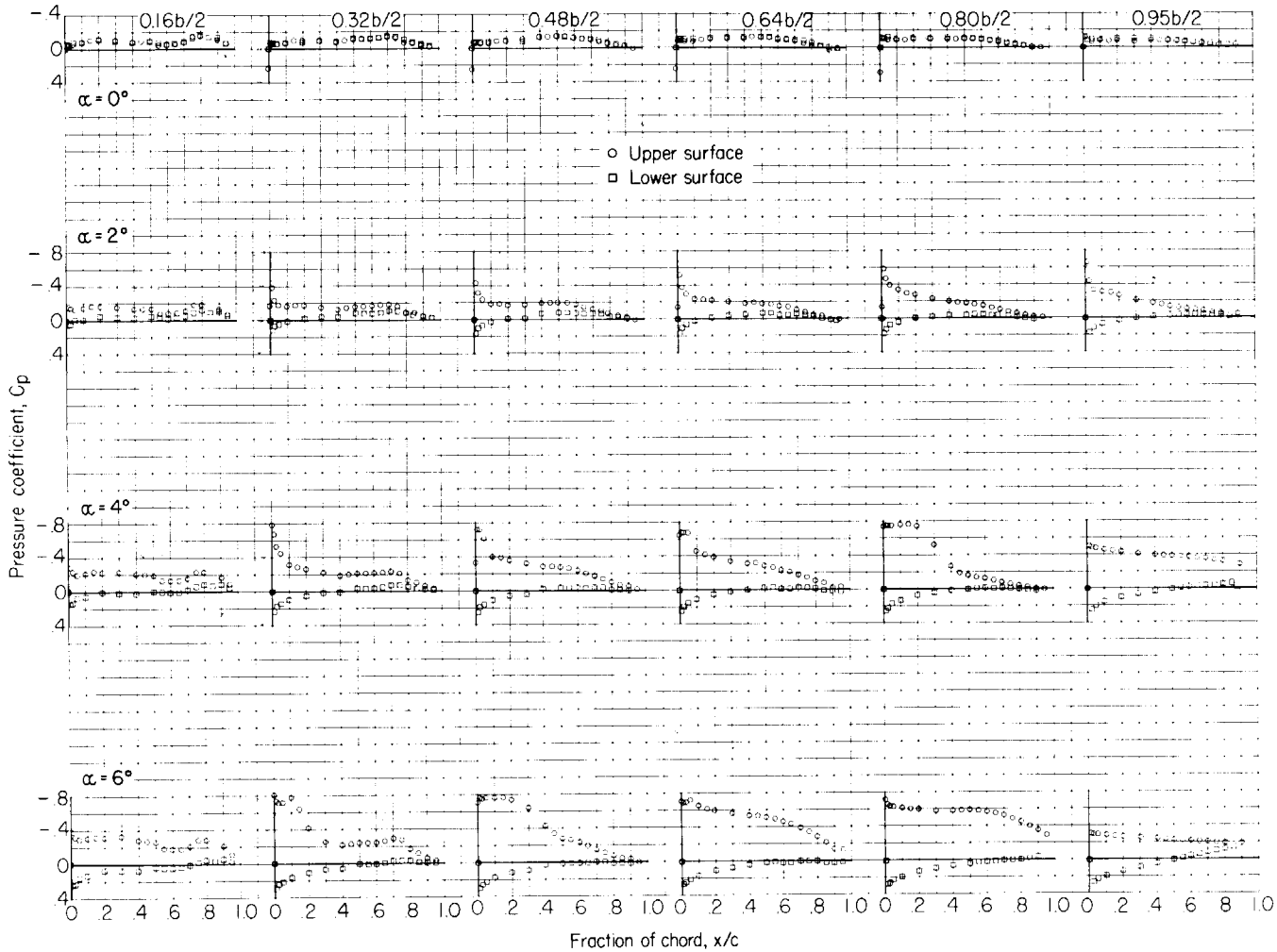

(c) M = 0.90.

Figure 5.- Continued.

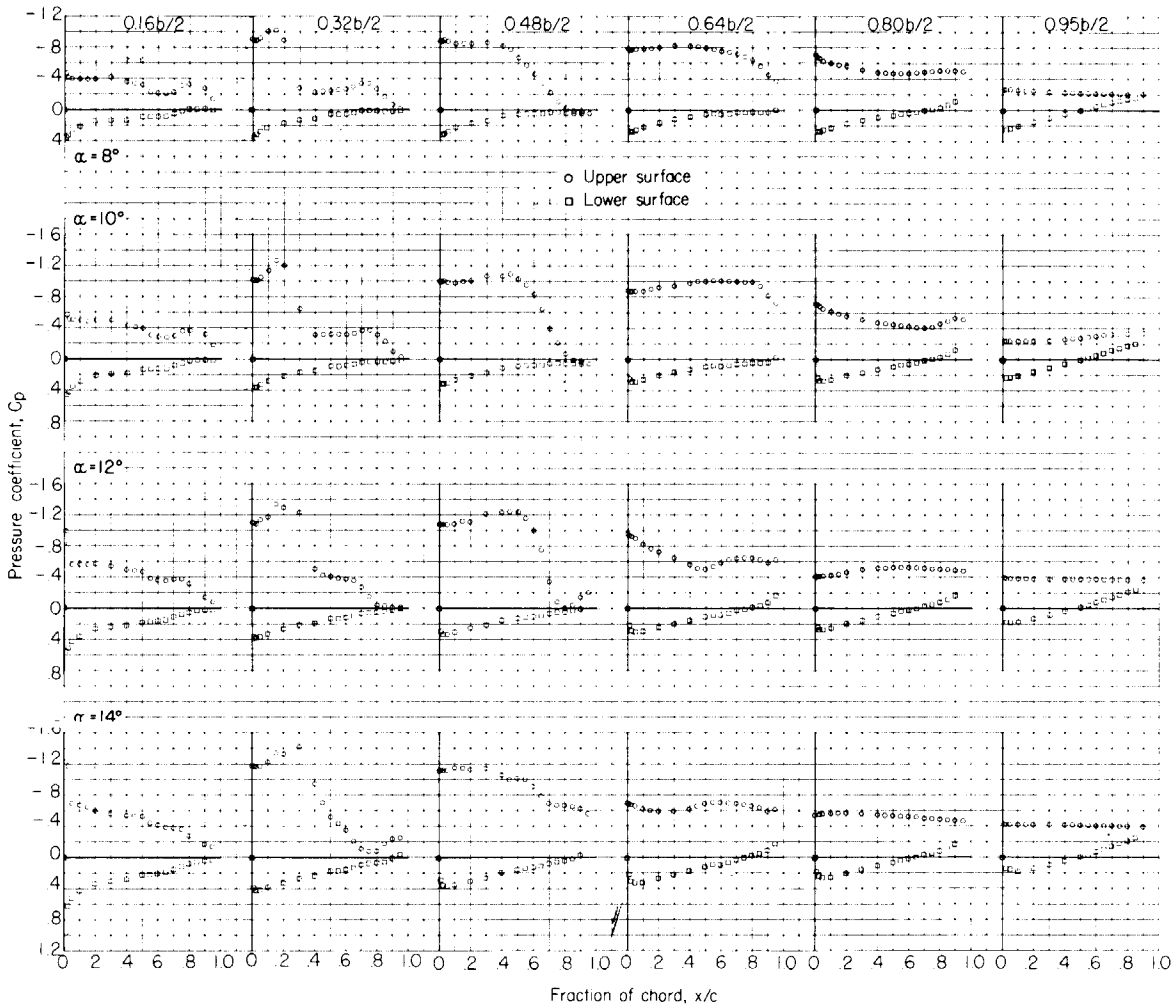

(c) Concluded.

Figure 5.- Continued.

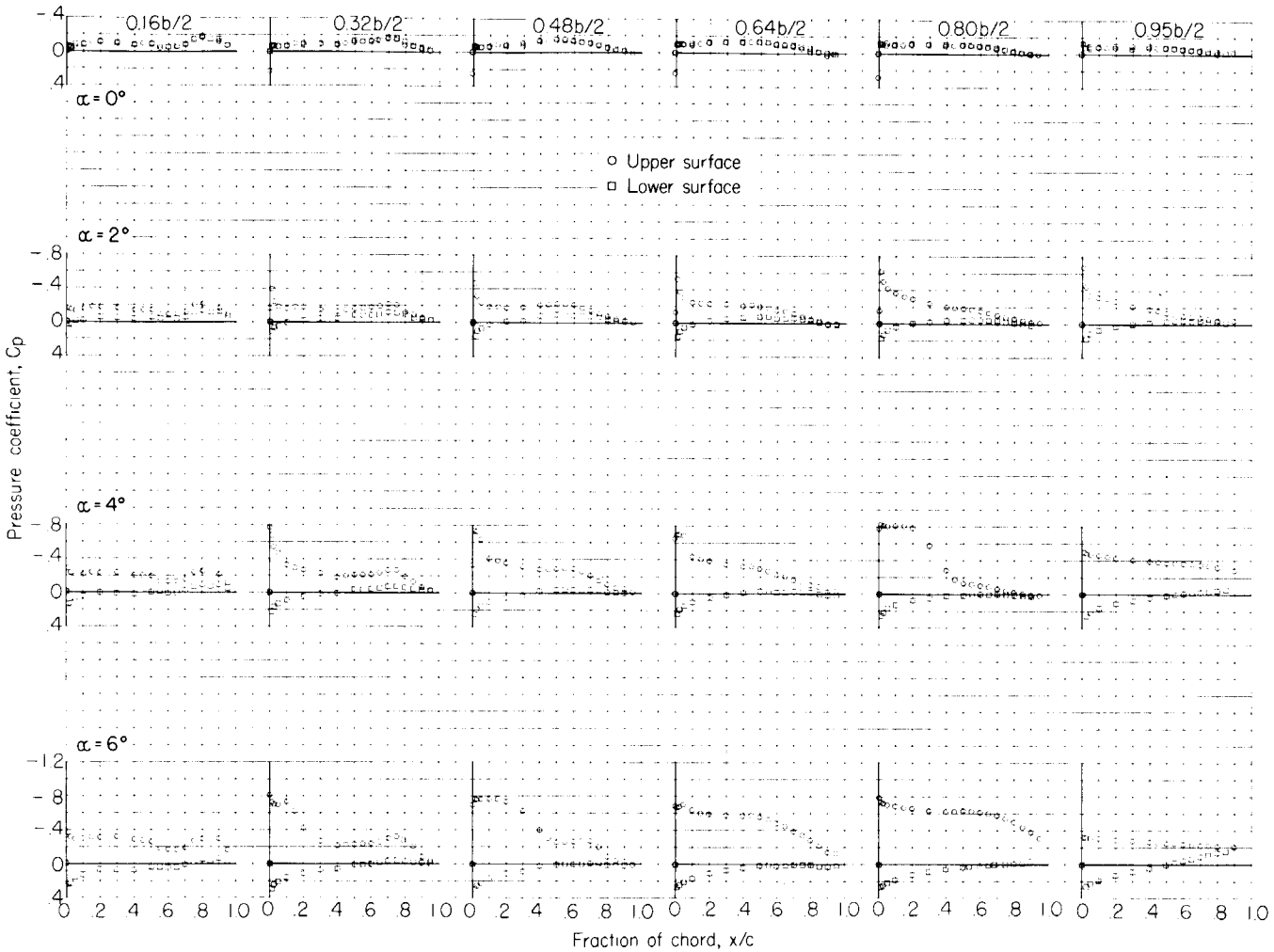

(d) M = 0.92.

Figure 5.- Continued.

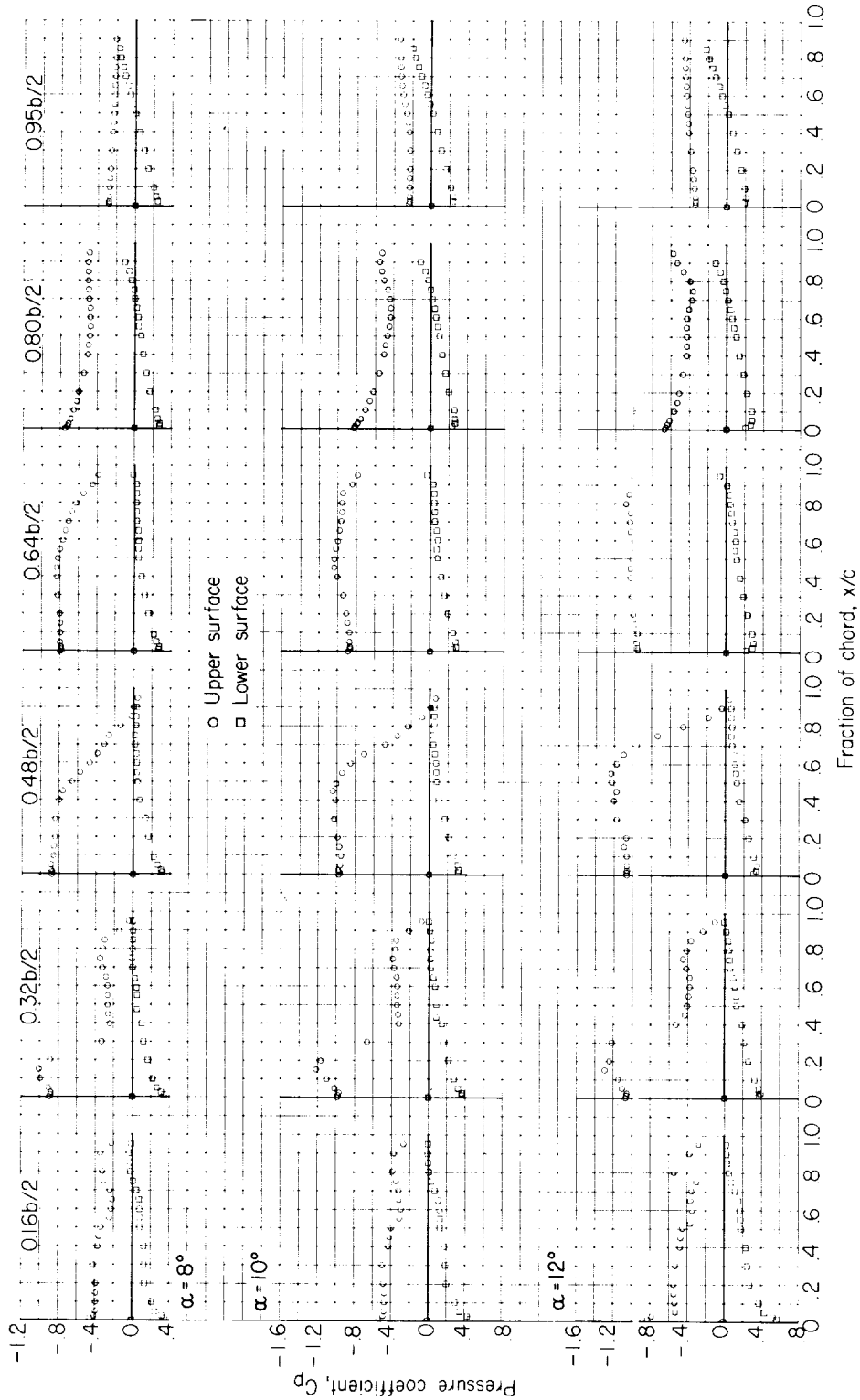

(d) Concluded.

Figure 5.- Continued.

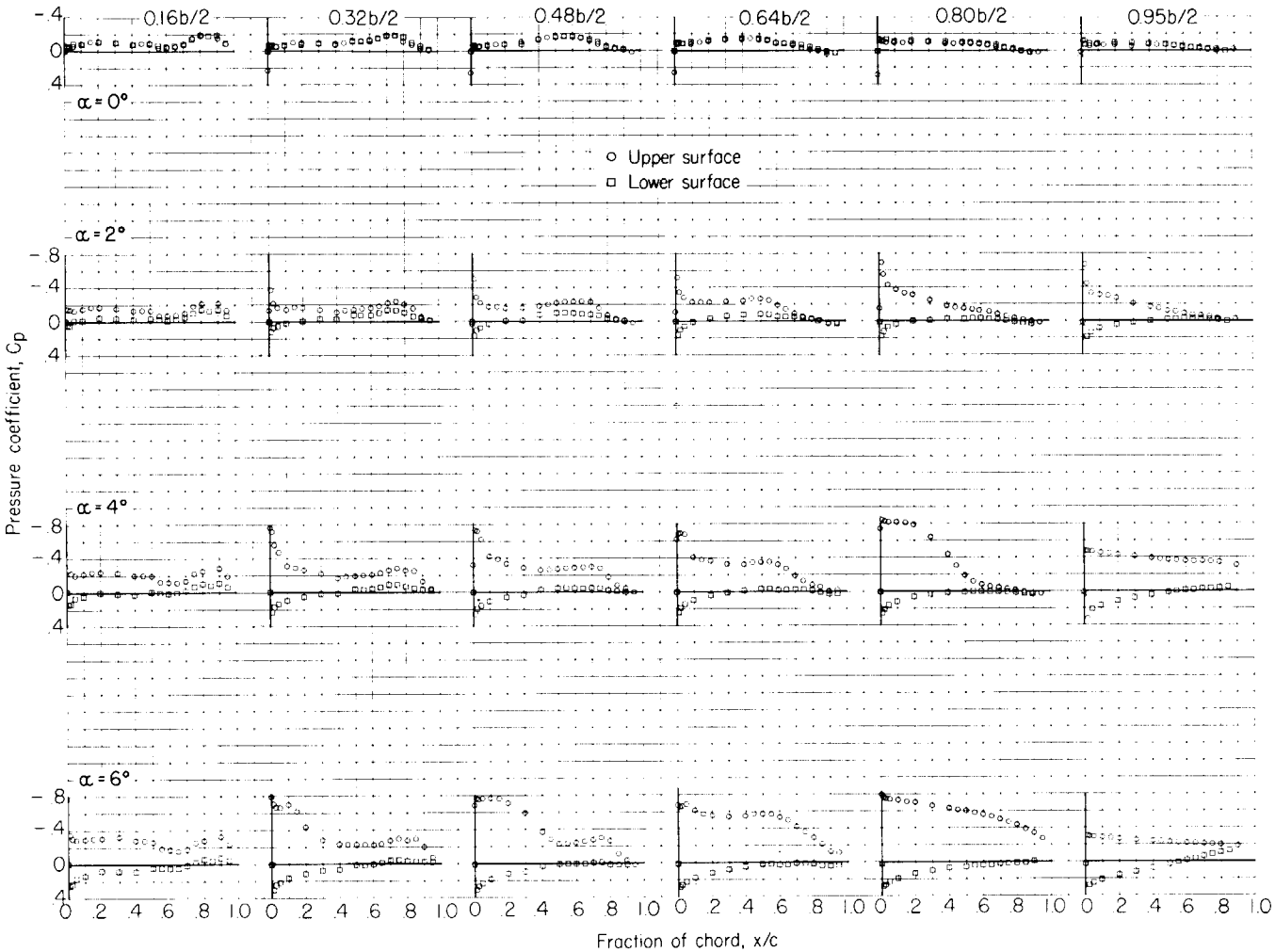

(e) M = 0.94.

Figure 5.- Continued.

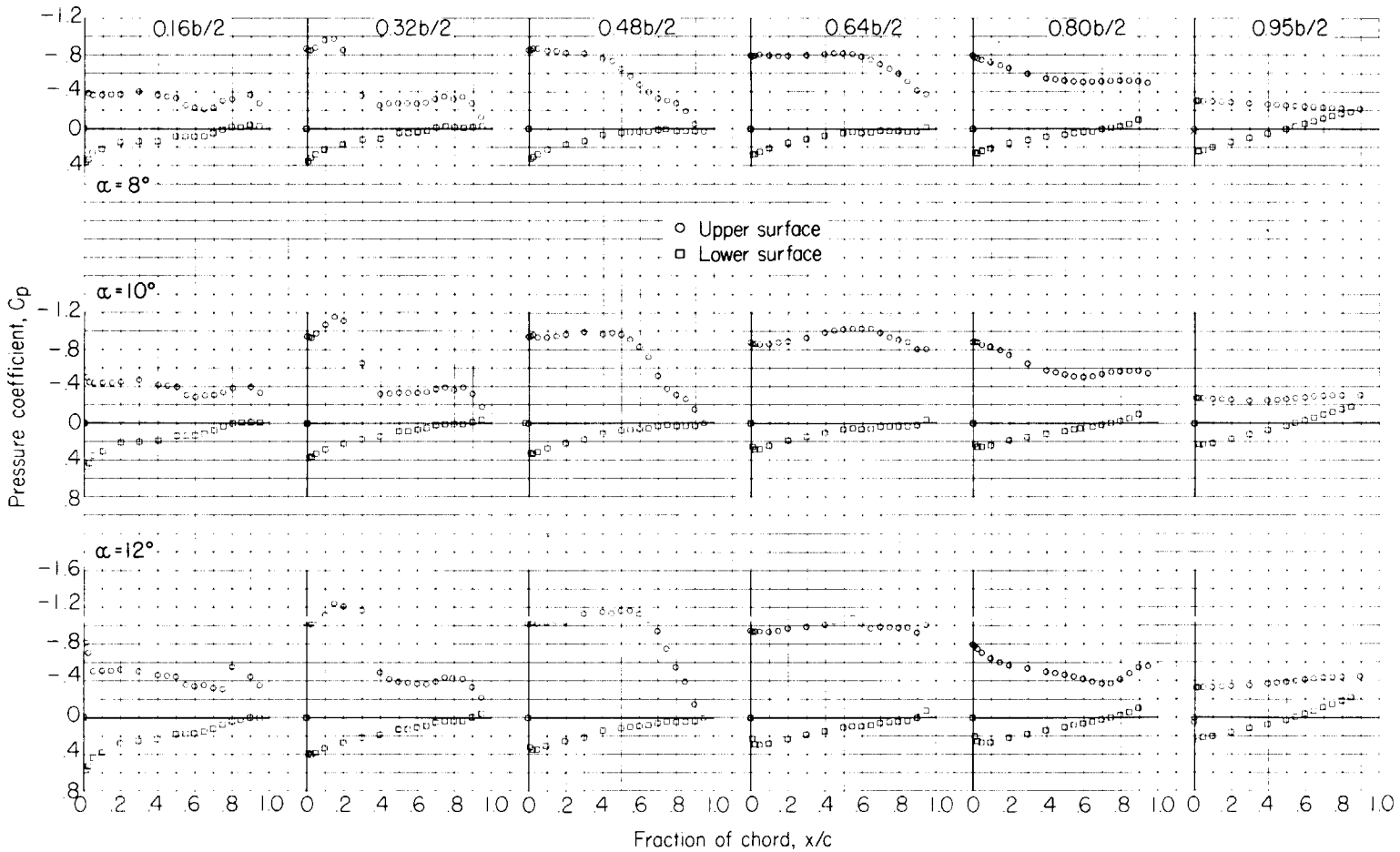

(e) Concluded.

Figure 5.- Continued.

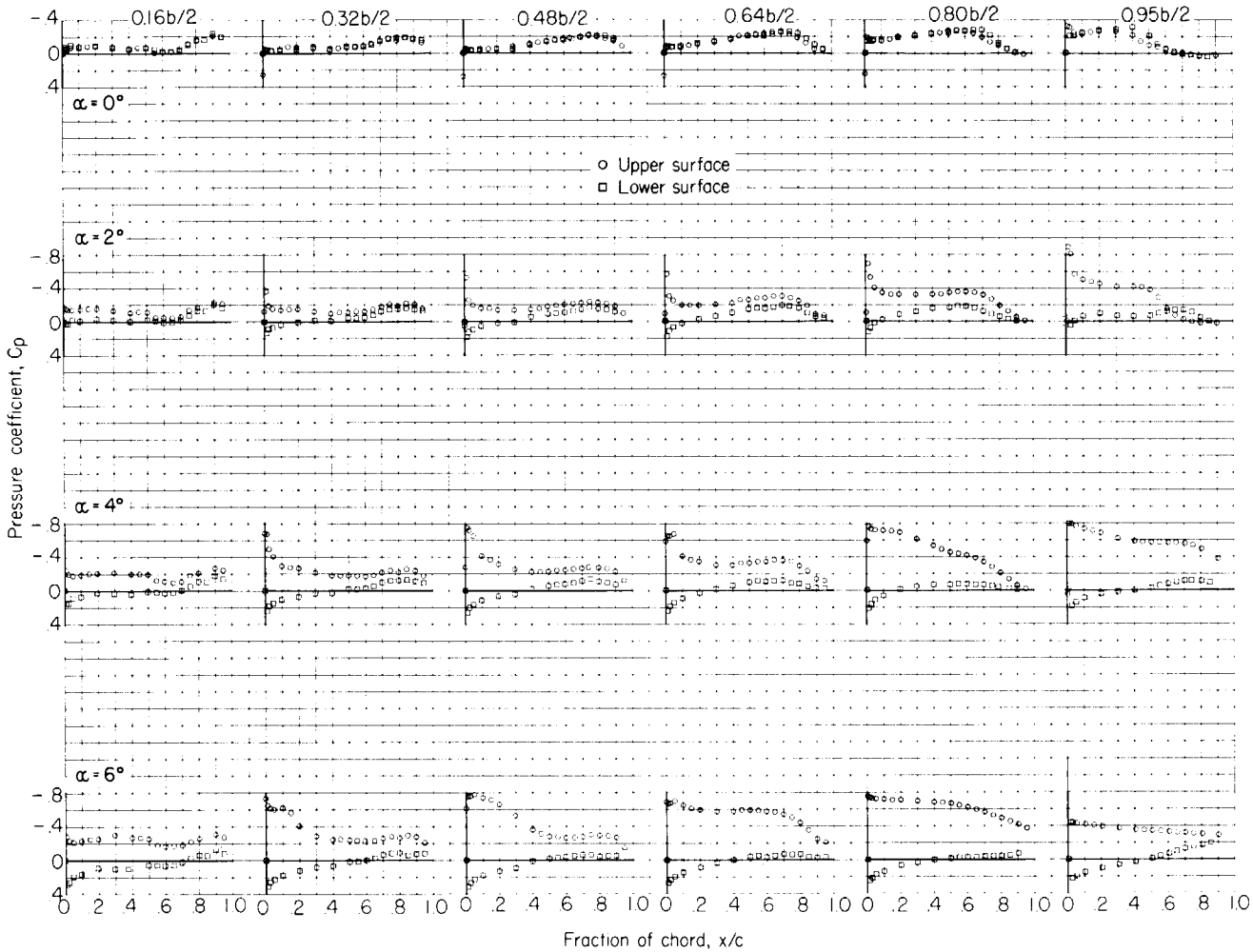

(f) M = 0.98.

Figure 5.- Continued.

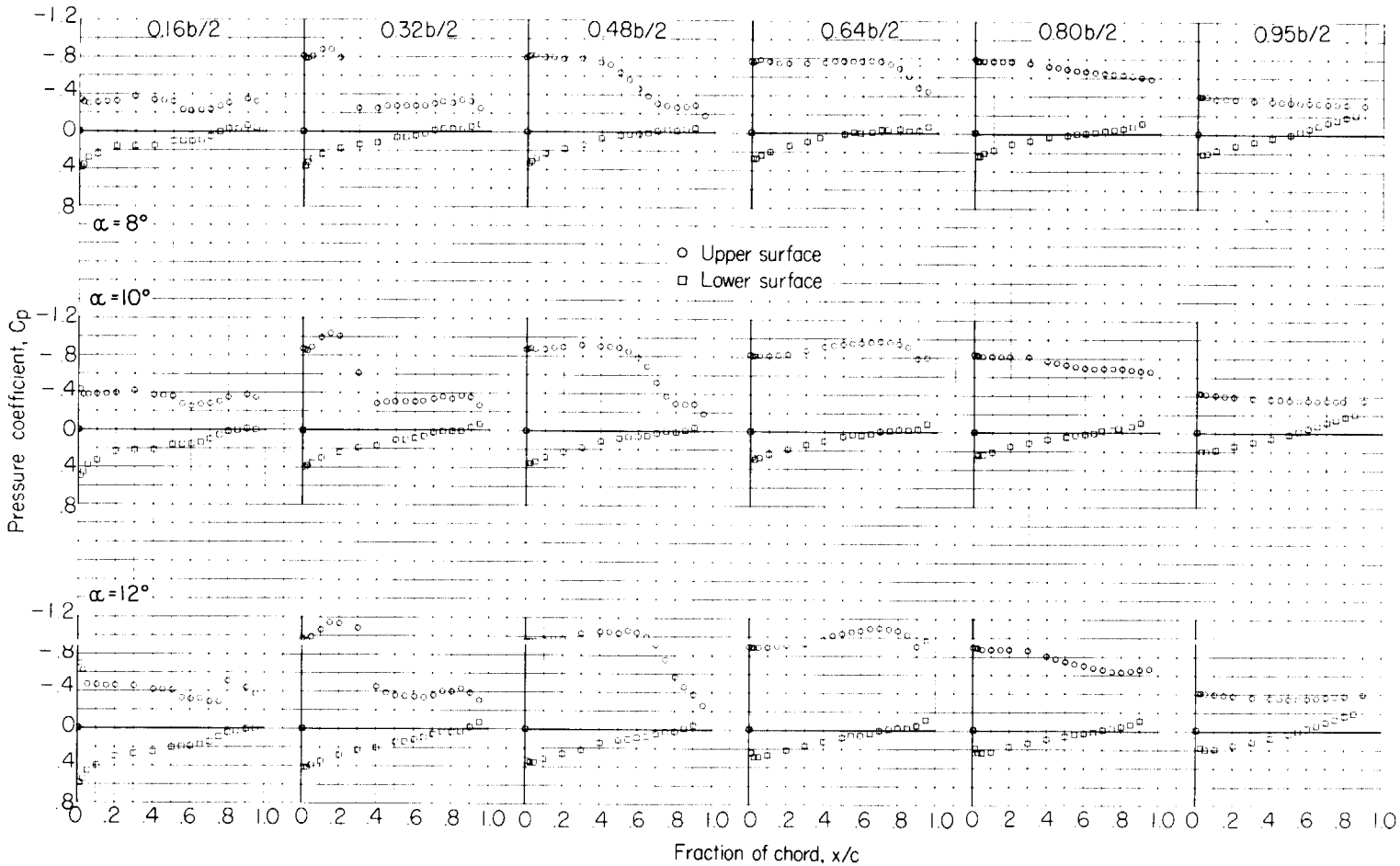

(f) Concluded.

Figure 5.- Continued.

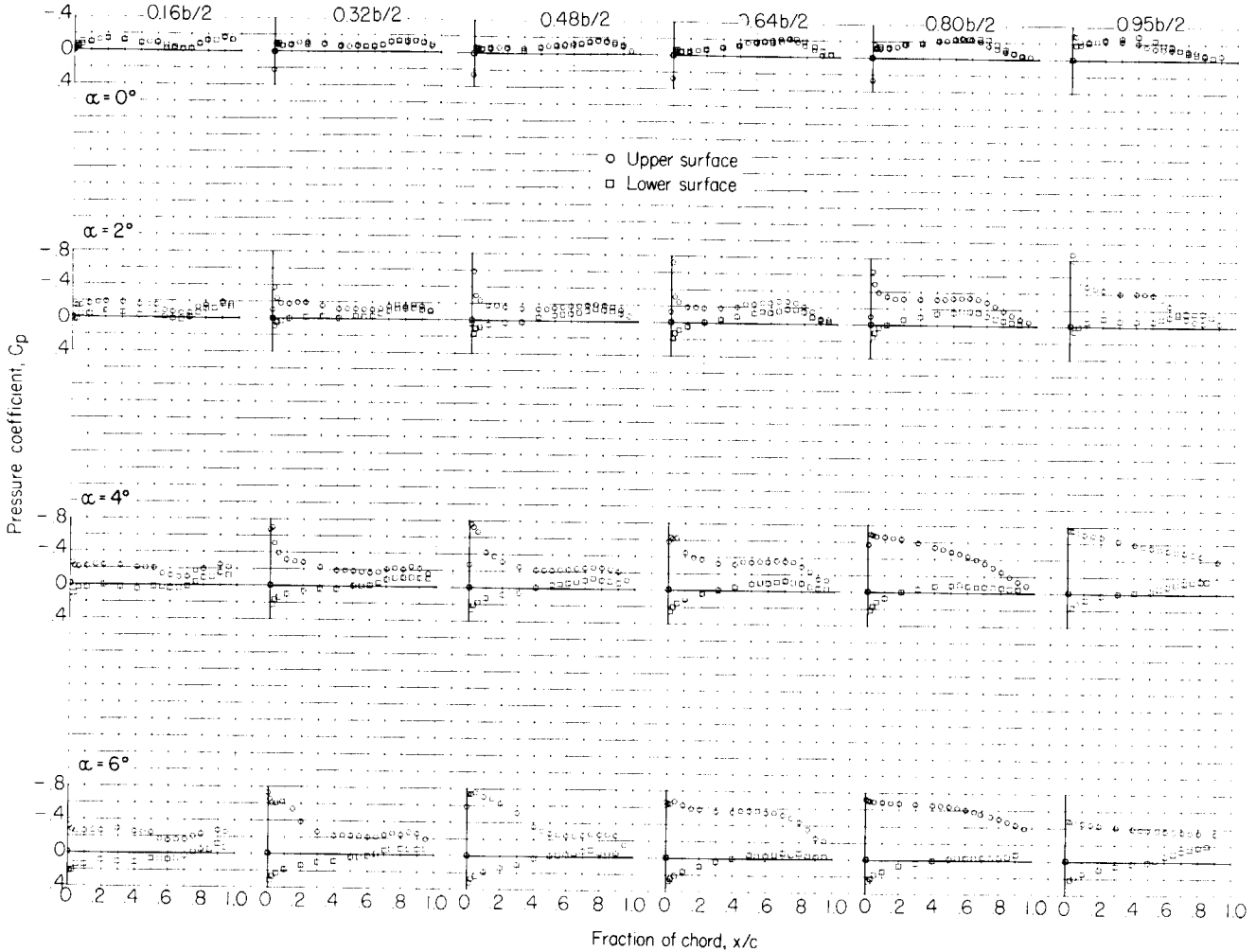

(g) M = 1.00.

Figure 5.- Continued.

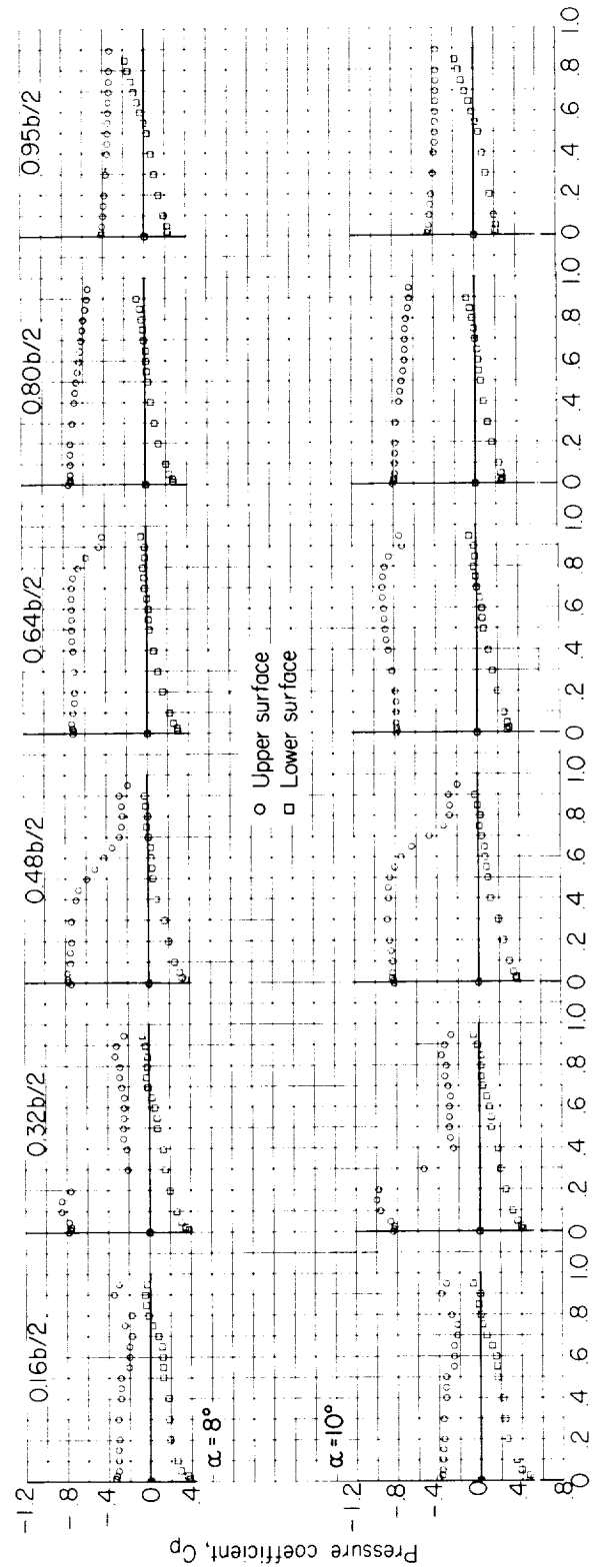

(g) Concluded.

Figure 5.- Continued.

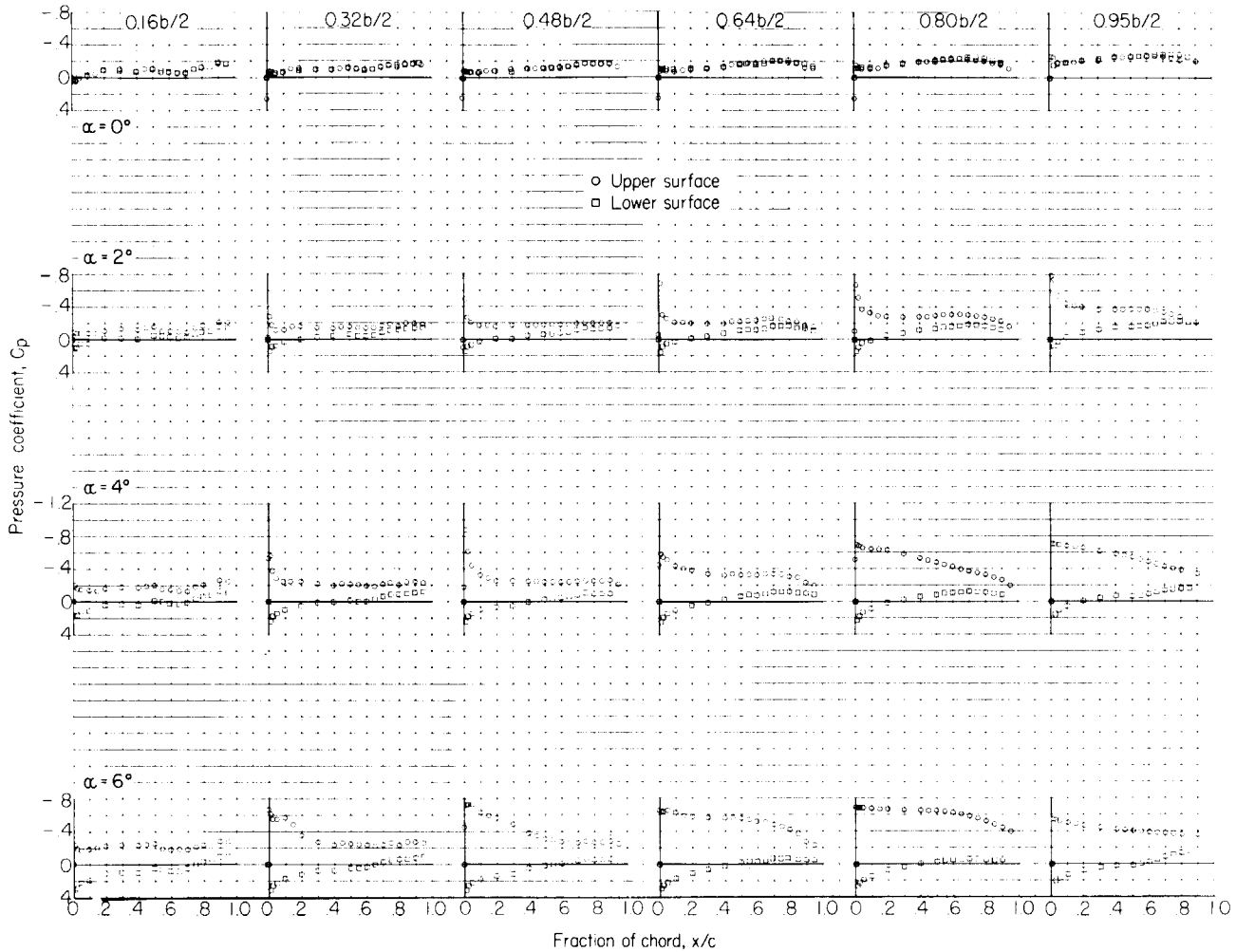

(h) M = 1.05.

Figure 5.- Continued.

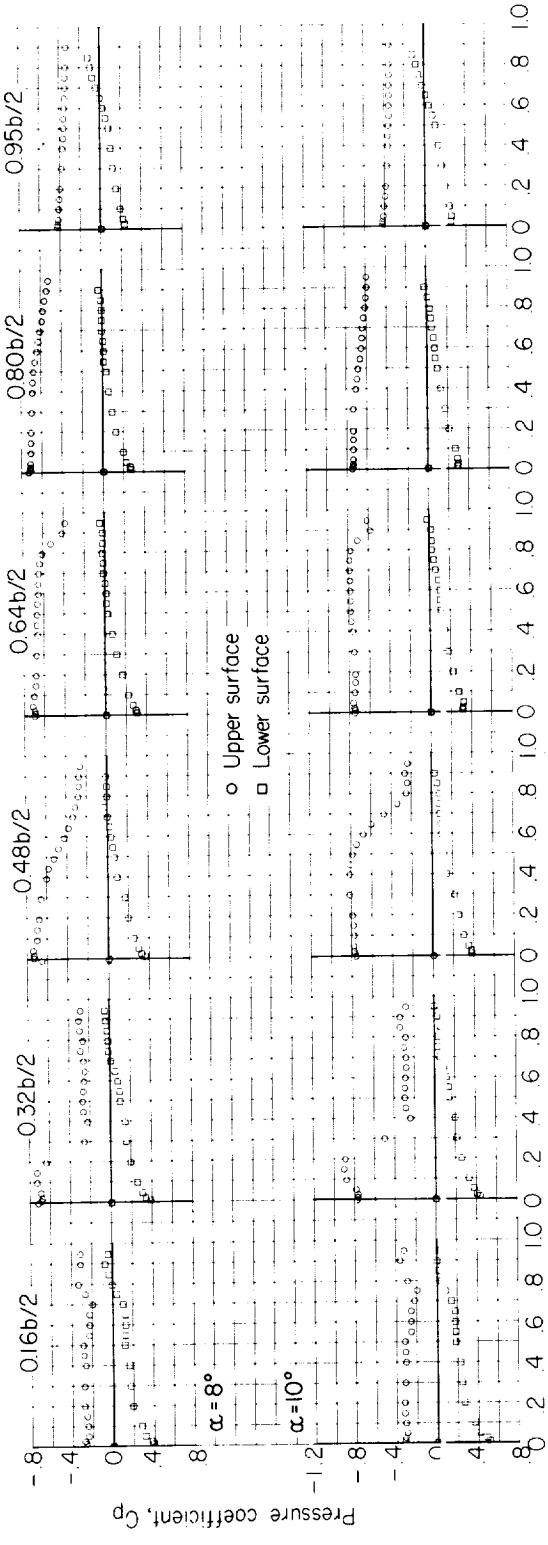

(h) Concluded.

Figure 5.- Concluded.

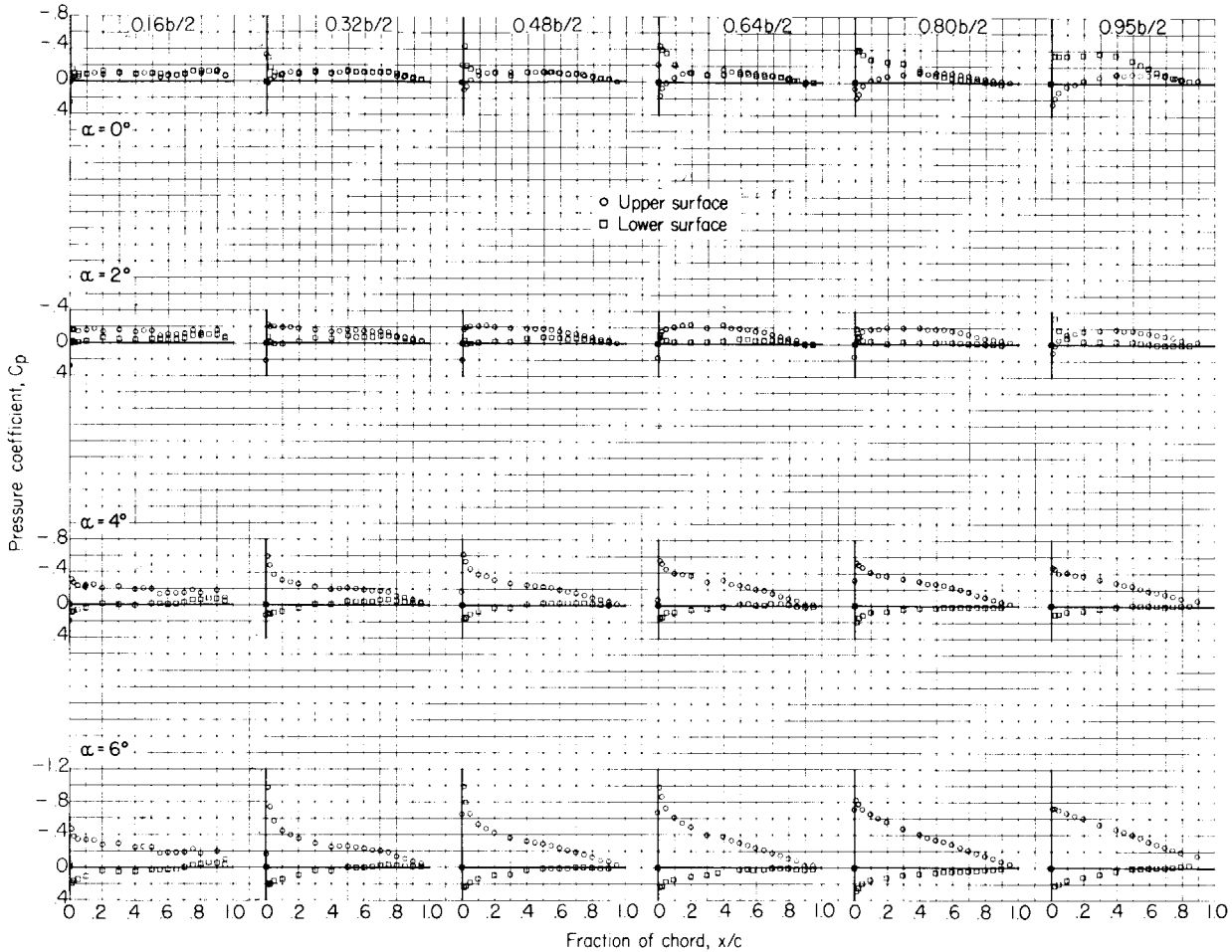

(a) M = 0.80.

Figure 6.- Chordwise pressure distributions for the cambered wing in combination with the indented body.

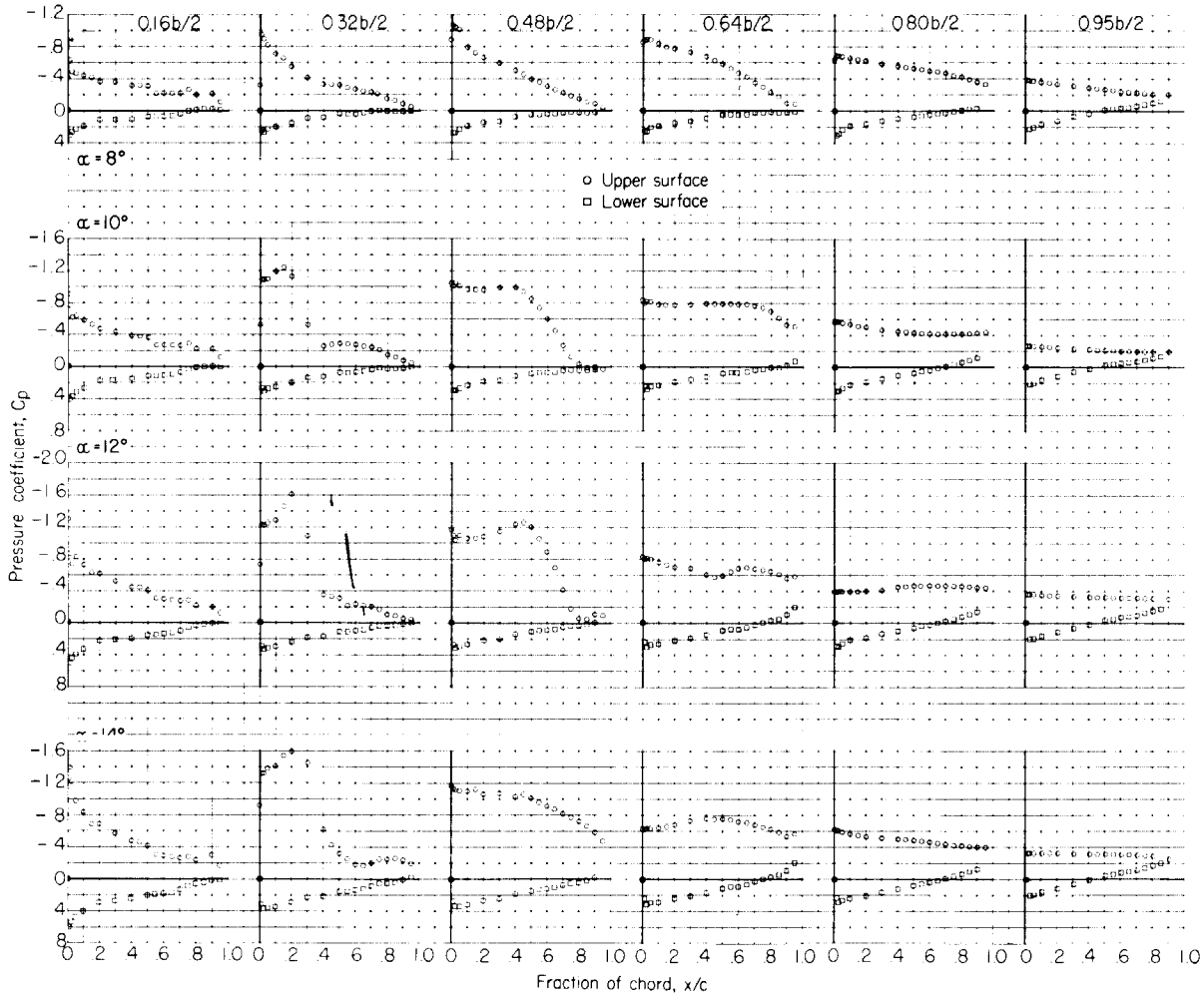

(a) Concluded.

Figure 6.- Continued.

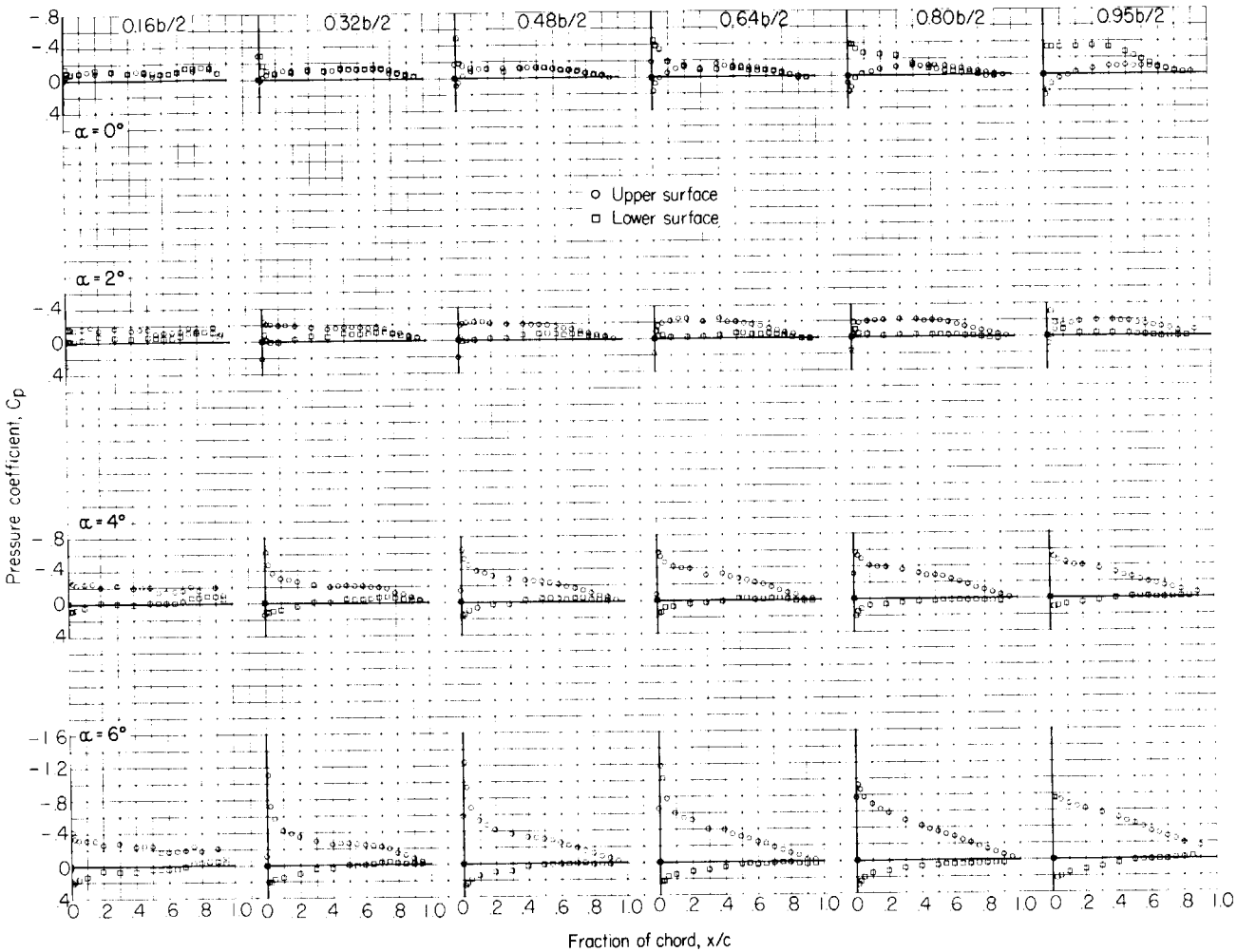

(b) M = 0.85.

Figure 6.- Continued.

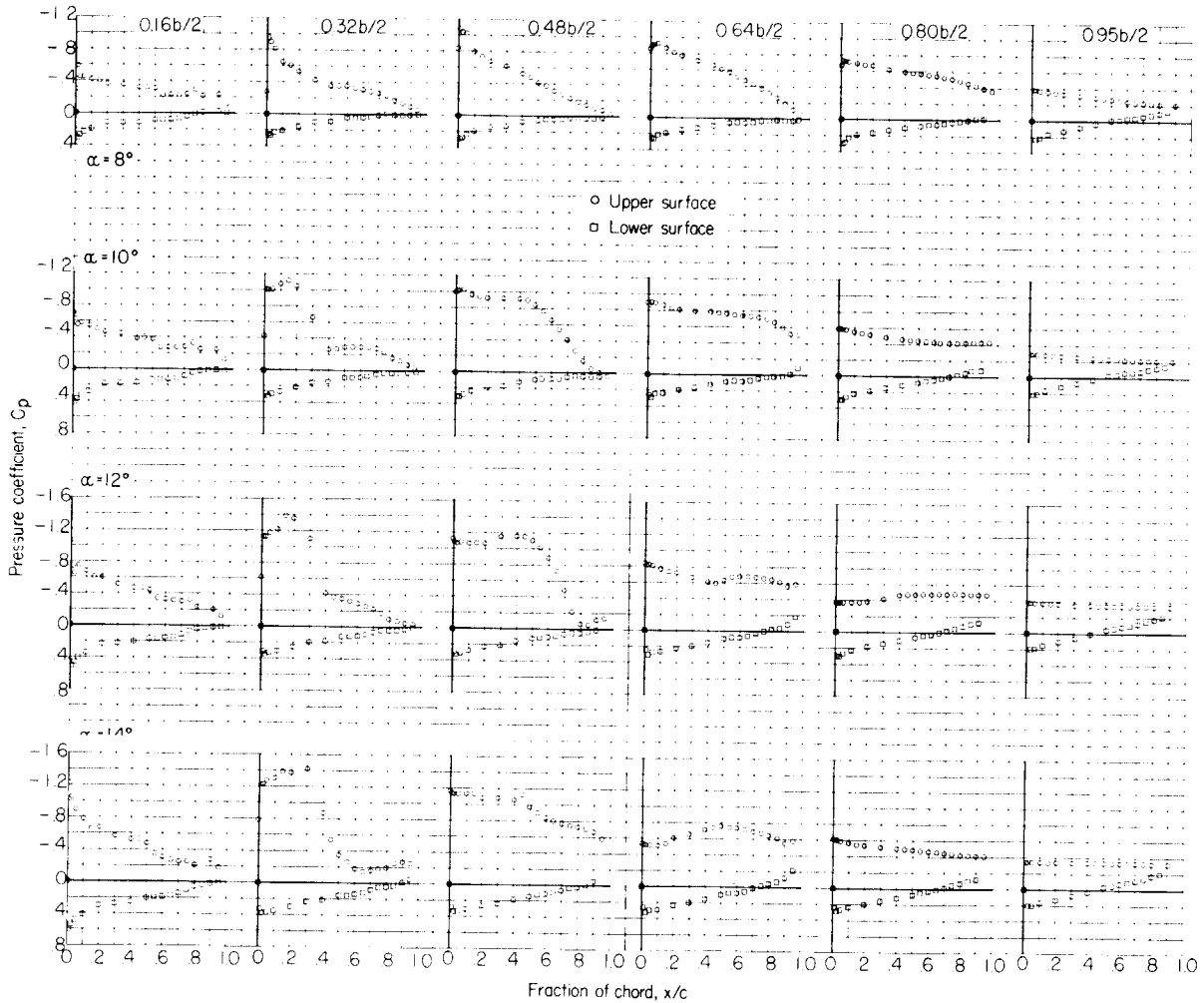

(b) Concluded.

Figure 6.- Continued.

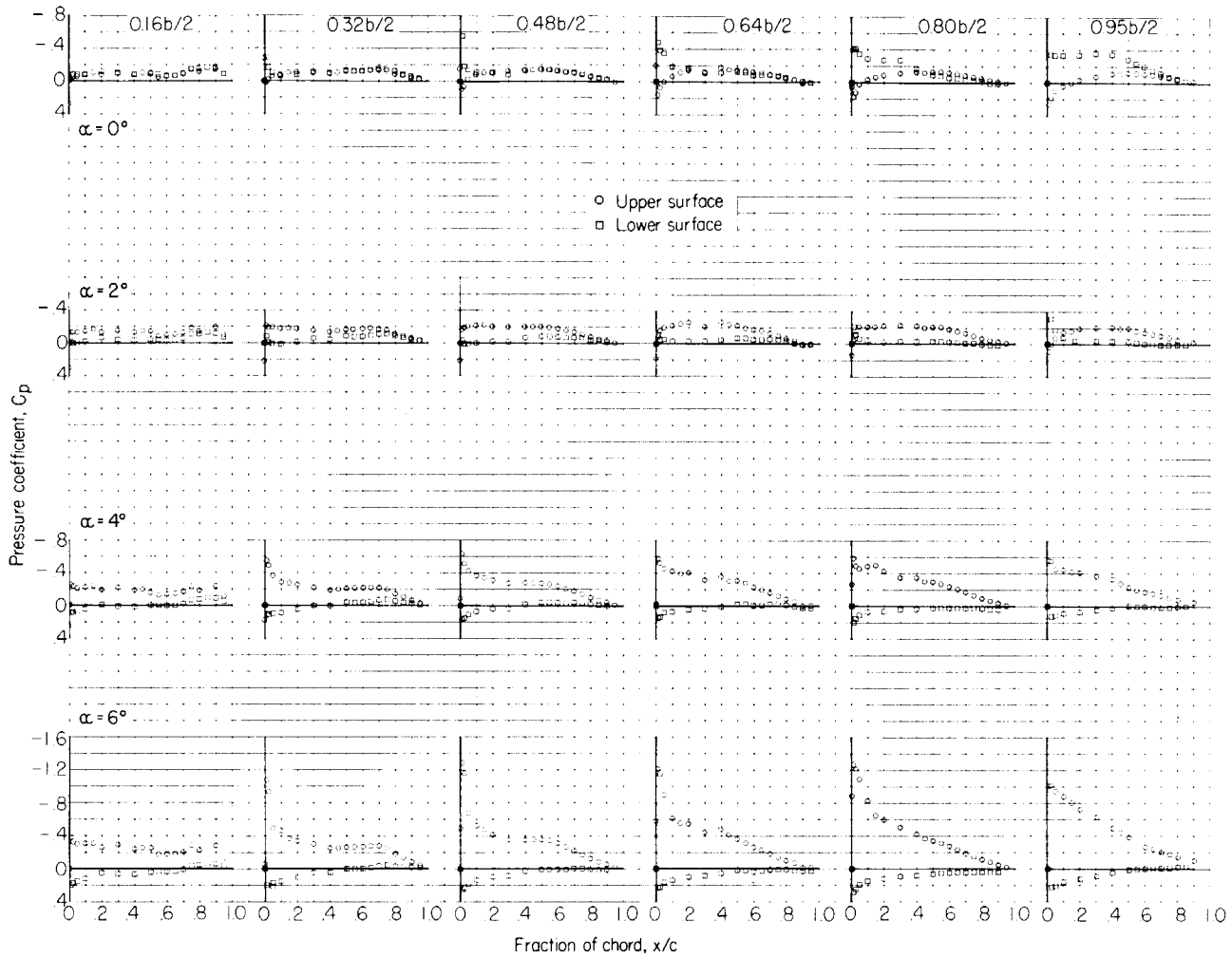

(c) M = 0.90.

Figure 6.- Continued.

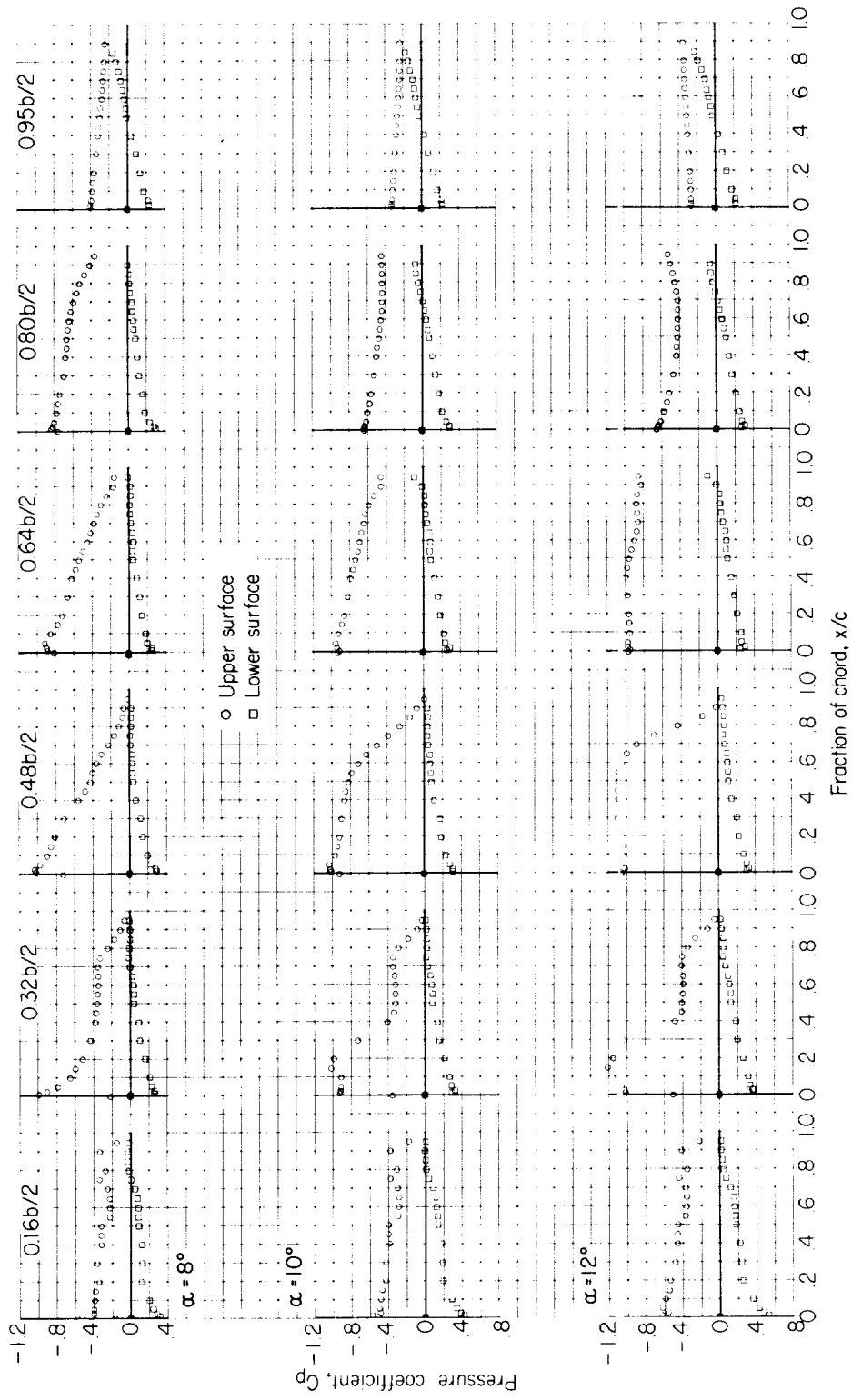

(c) Concluded.

Figure 6.- Continued.

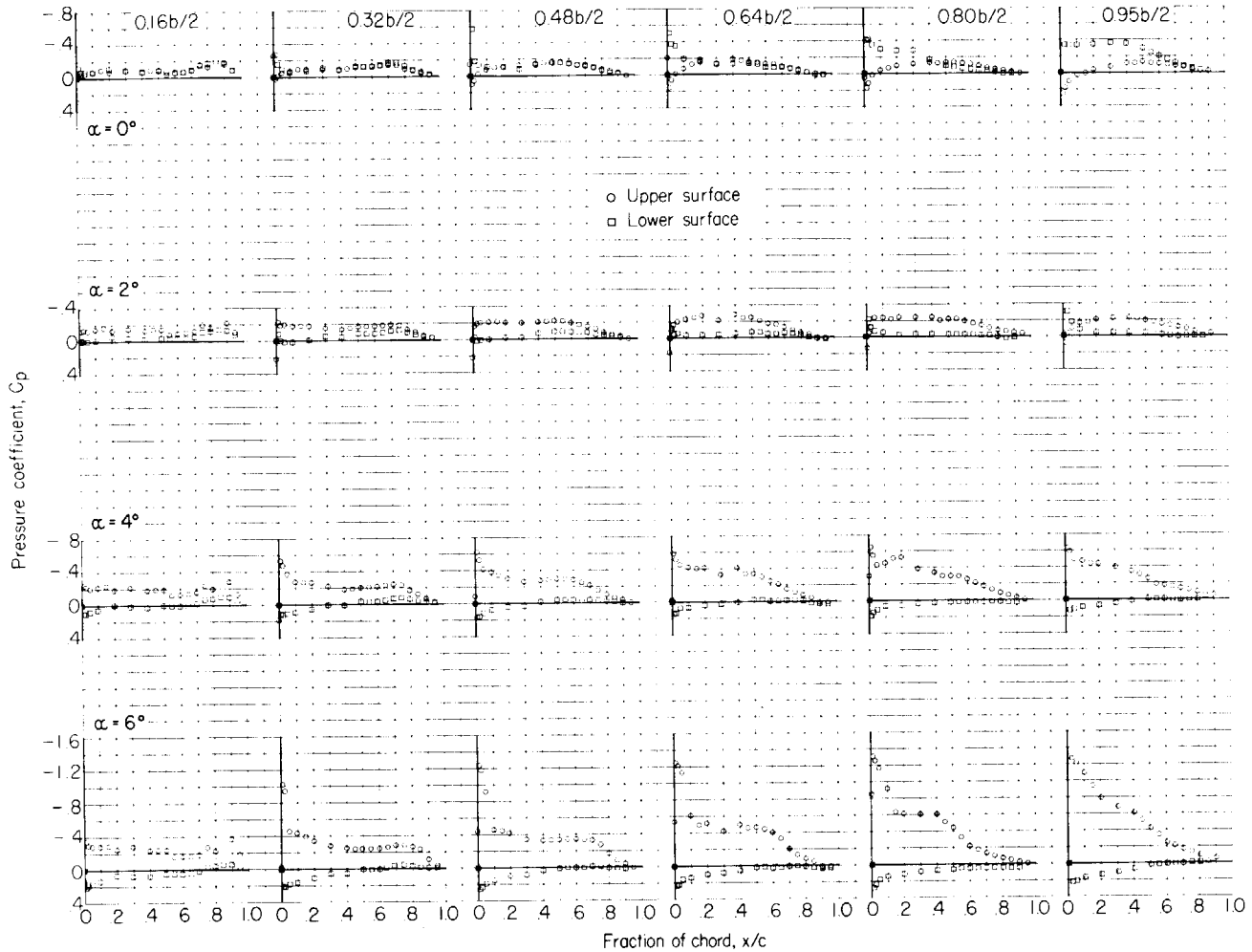

(d) M = 0.92.

Figure 6.- Continued.

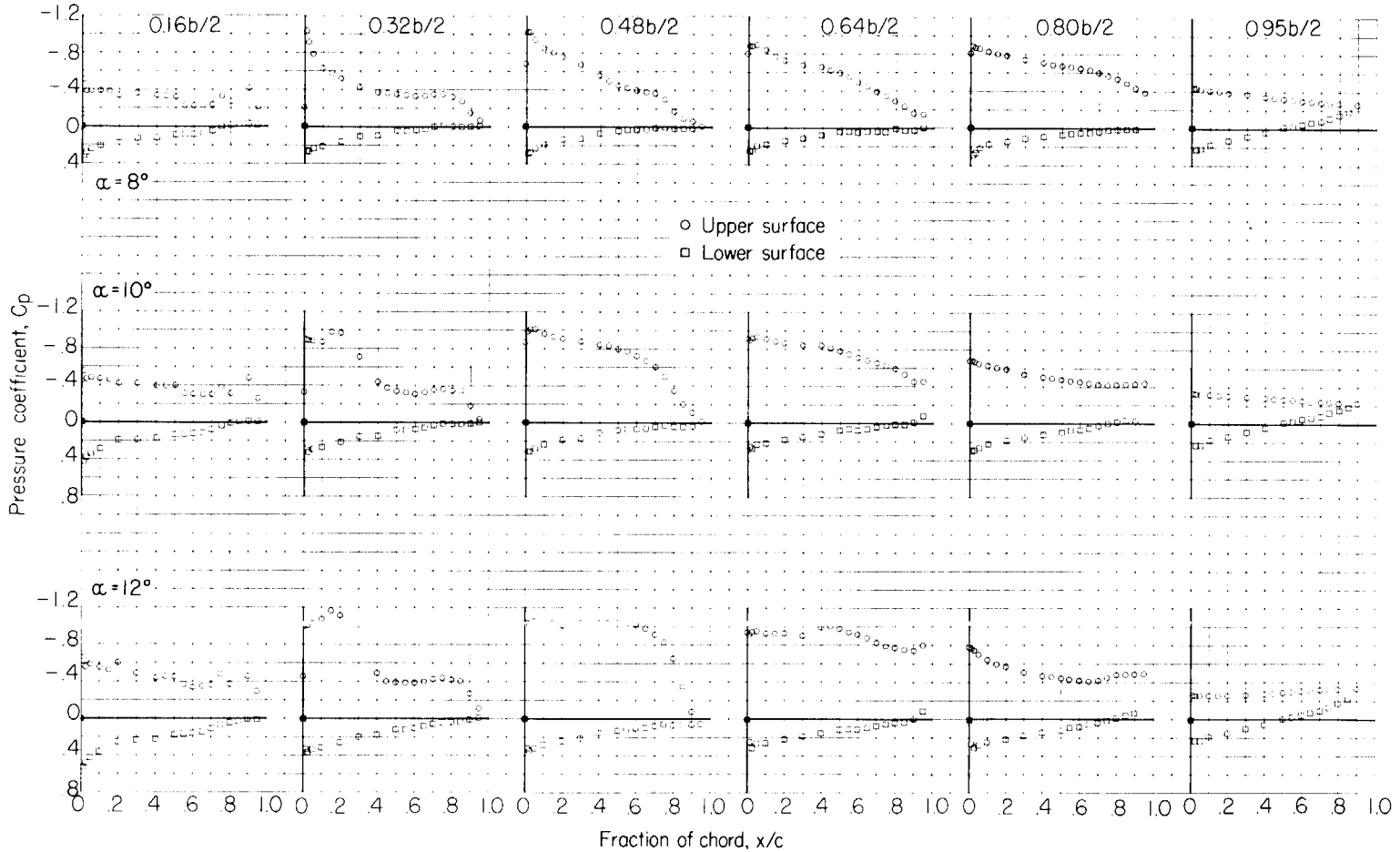

(d) Concluded.

Figure 6.- Continued.

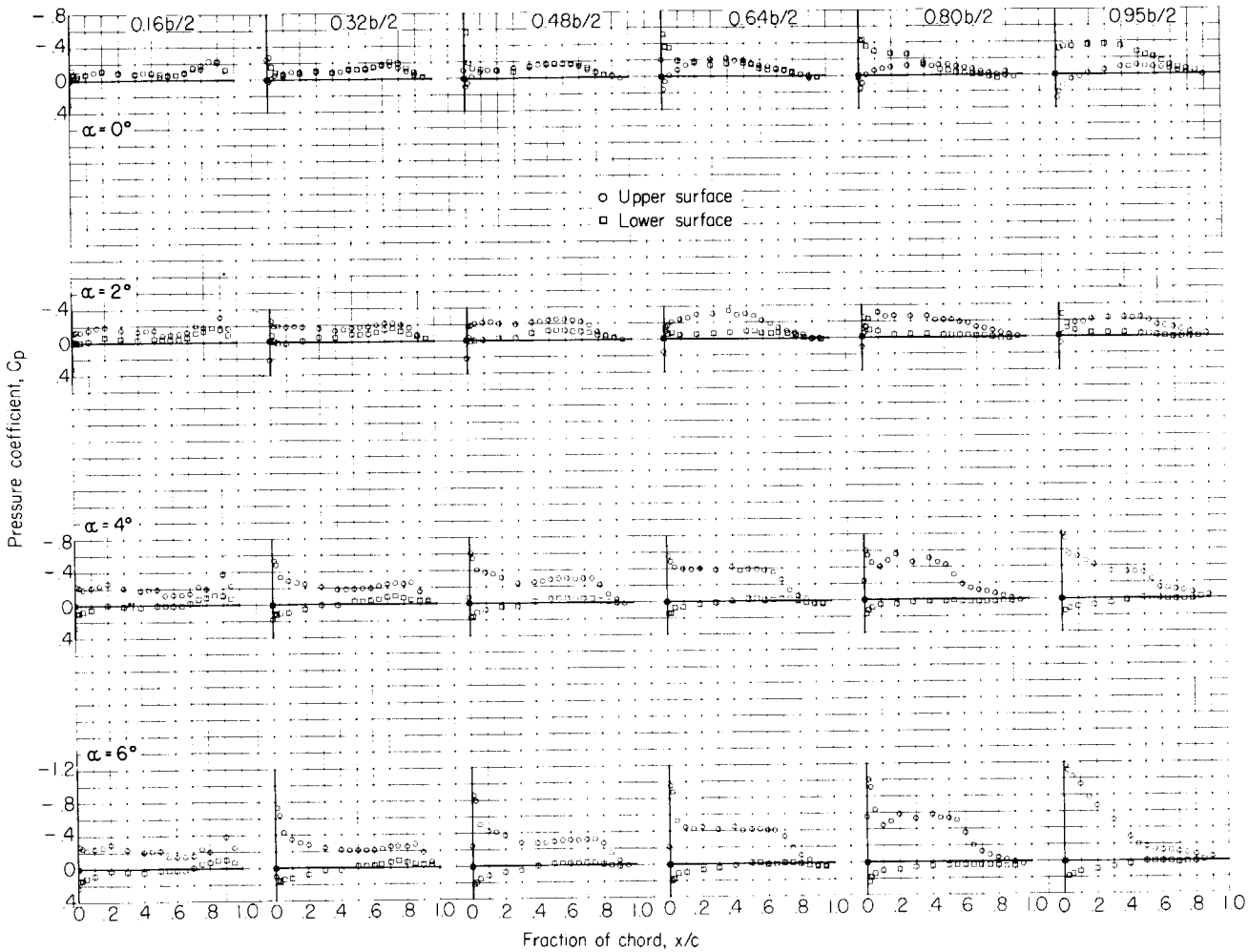

(e) M = 0.94.

Figure 6.- Continued.

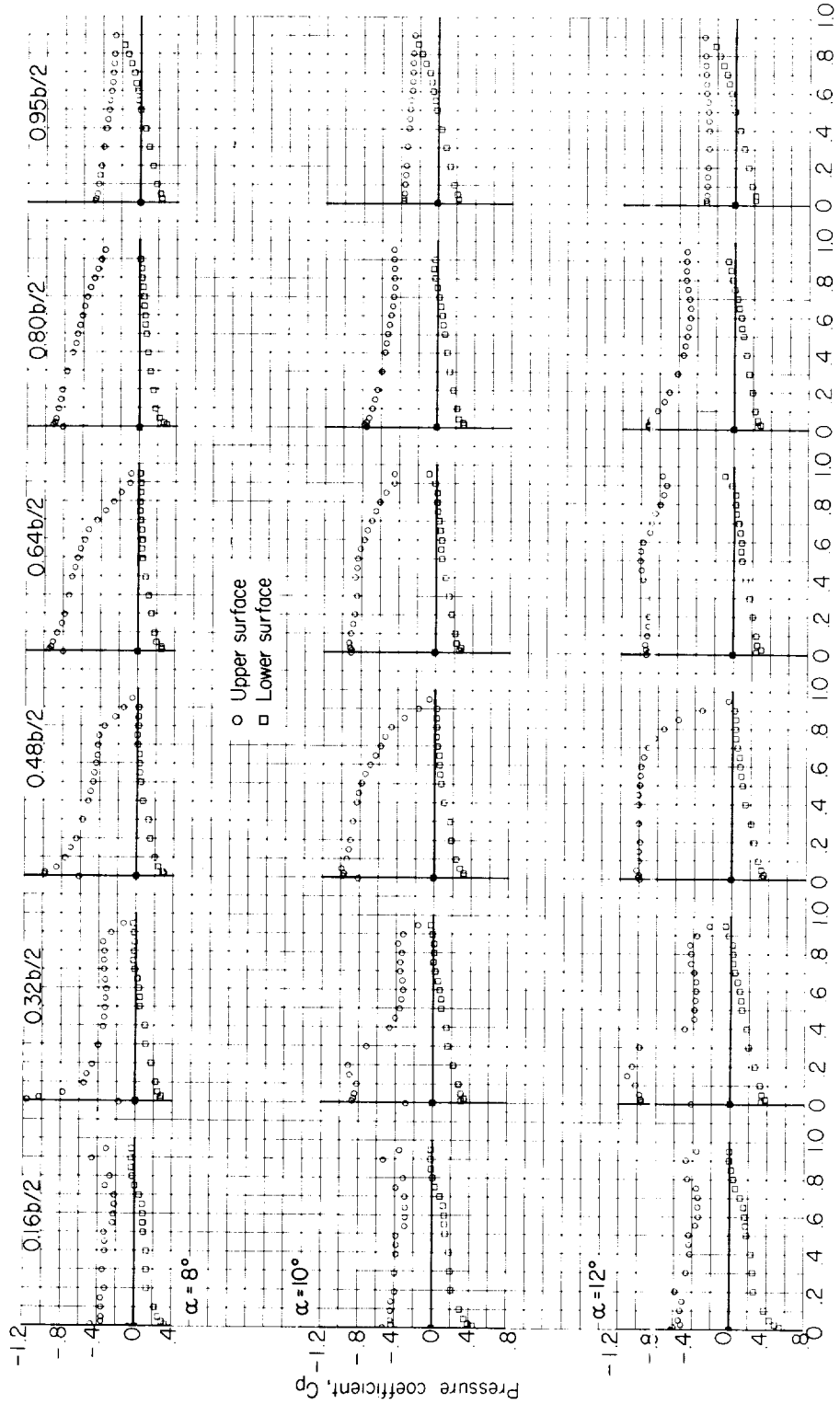

(e) Concluded.

Figure 6.- Continued.

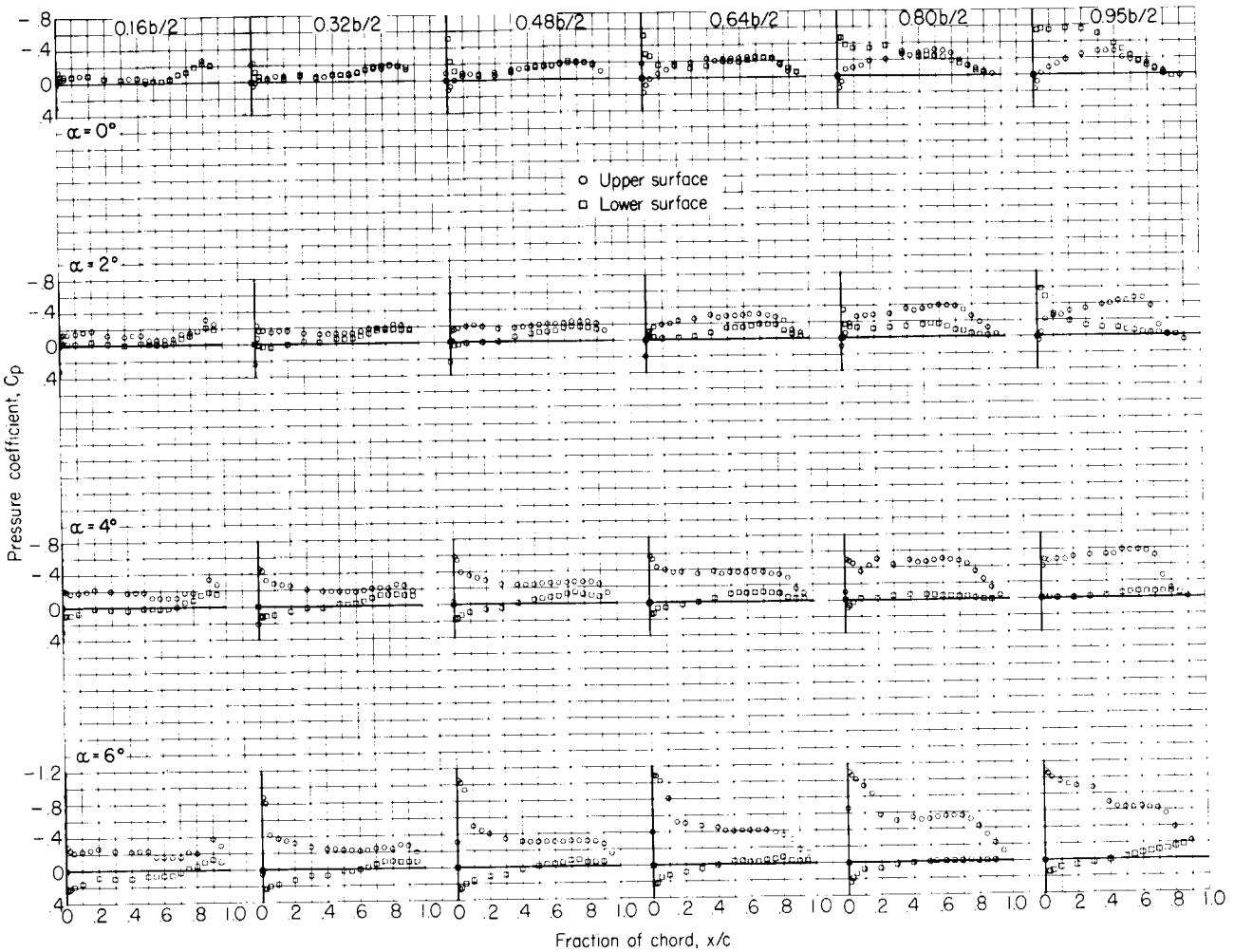

(f) M = 0.98.

Figure 6.- Continued.

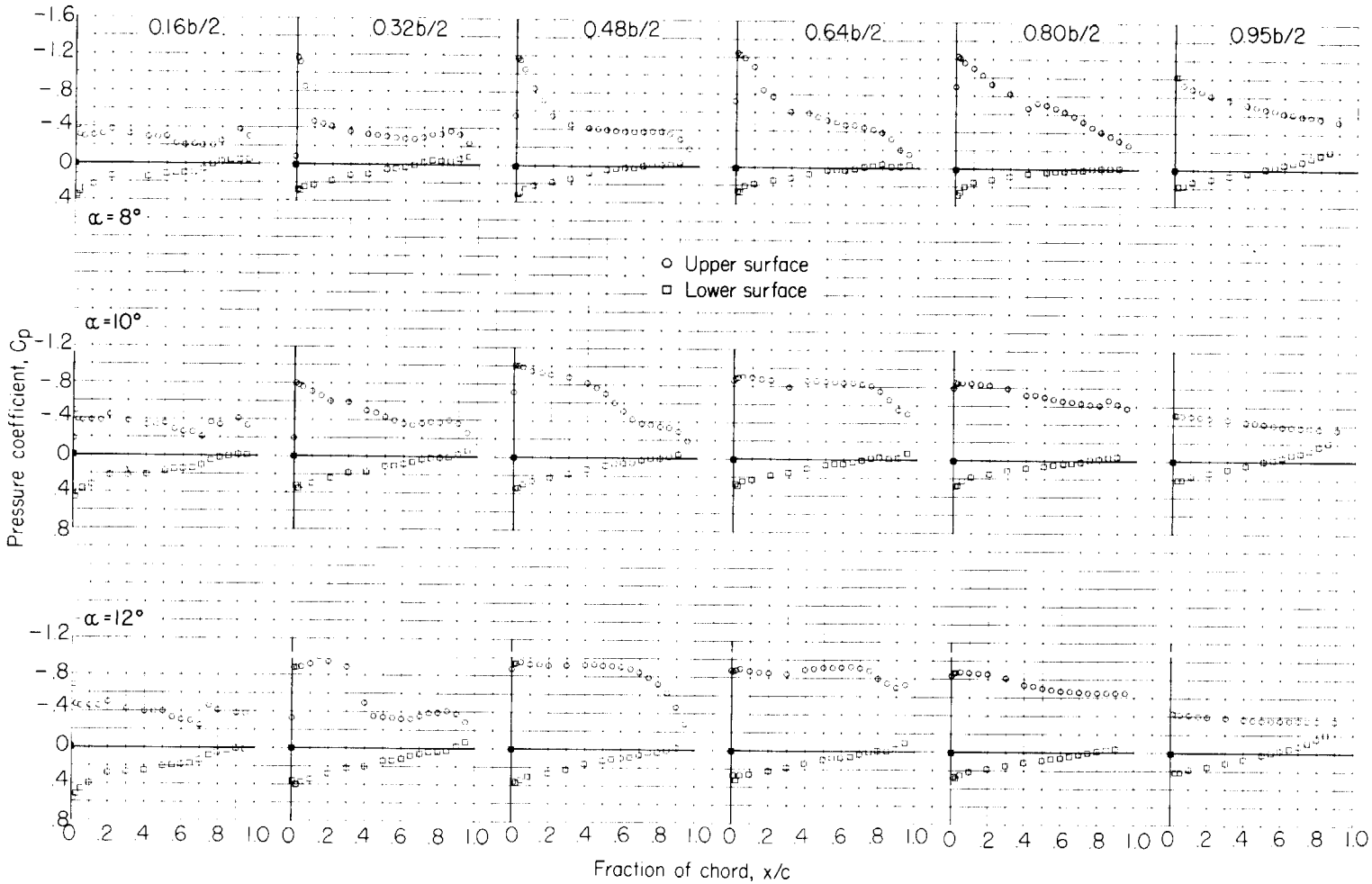

(f) Concluded.

Figure 6.- Continued.

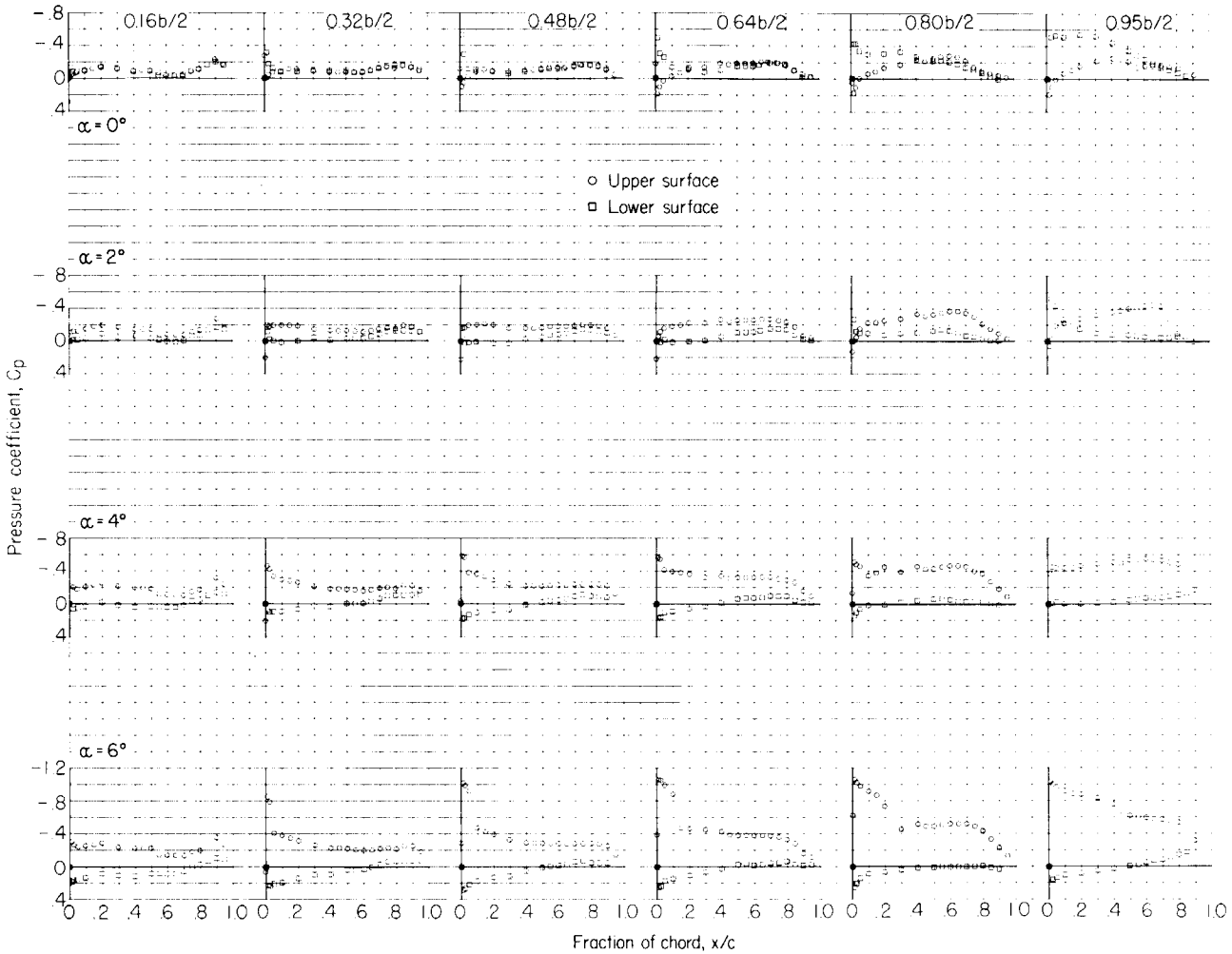

(g) M = 1.00.

Figure 6.- Continued.

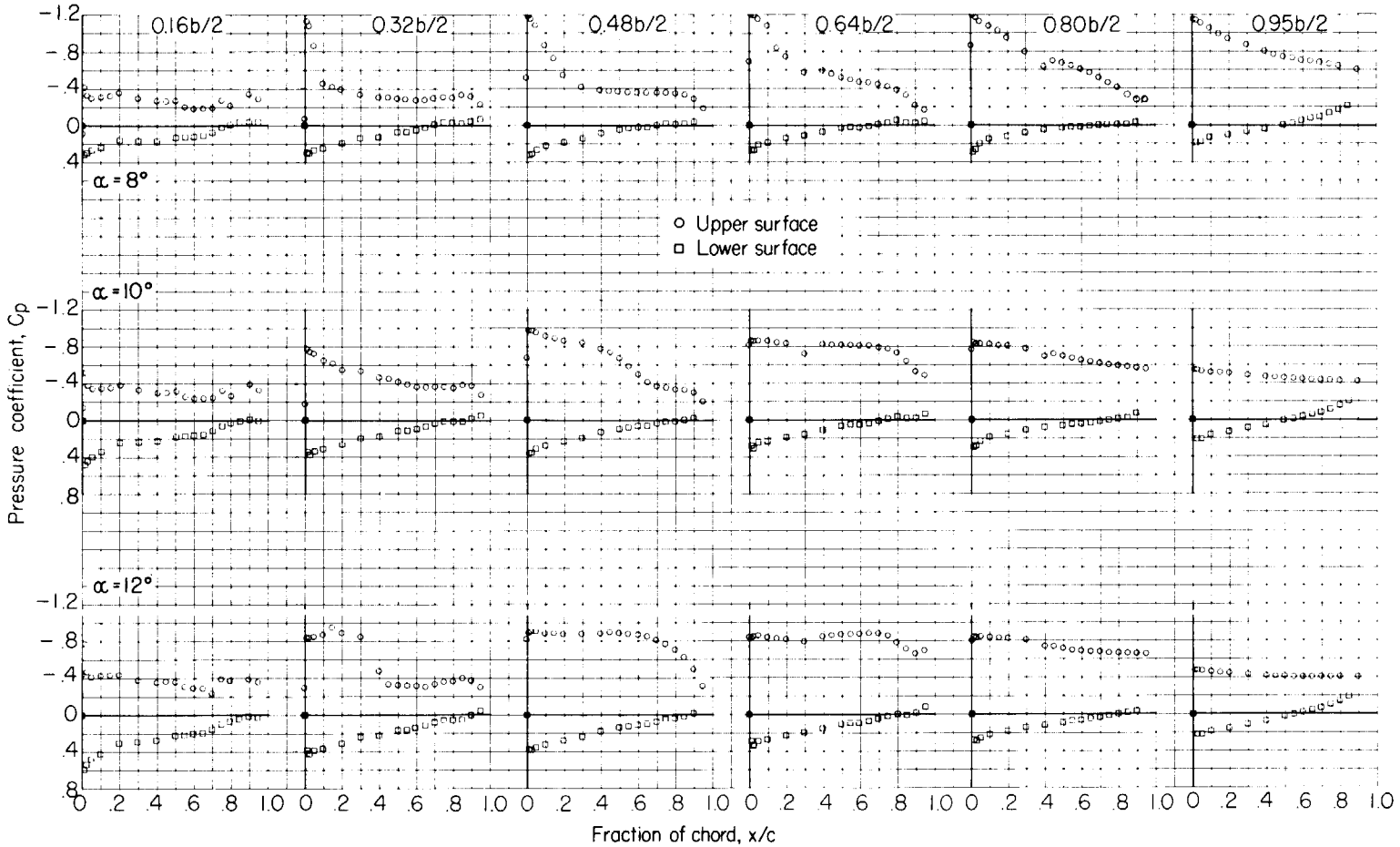

(g) Concluded.

Figure 6.- Continued.

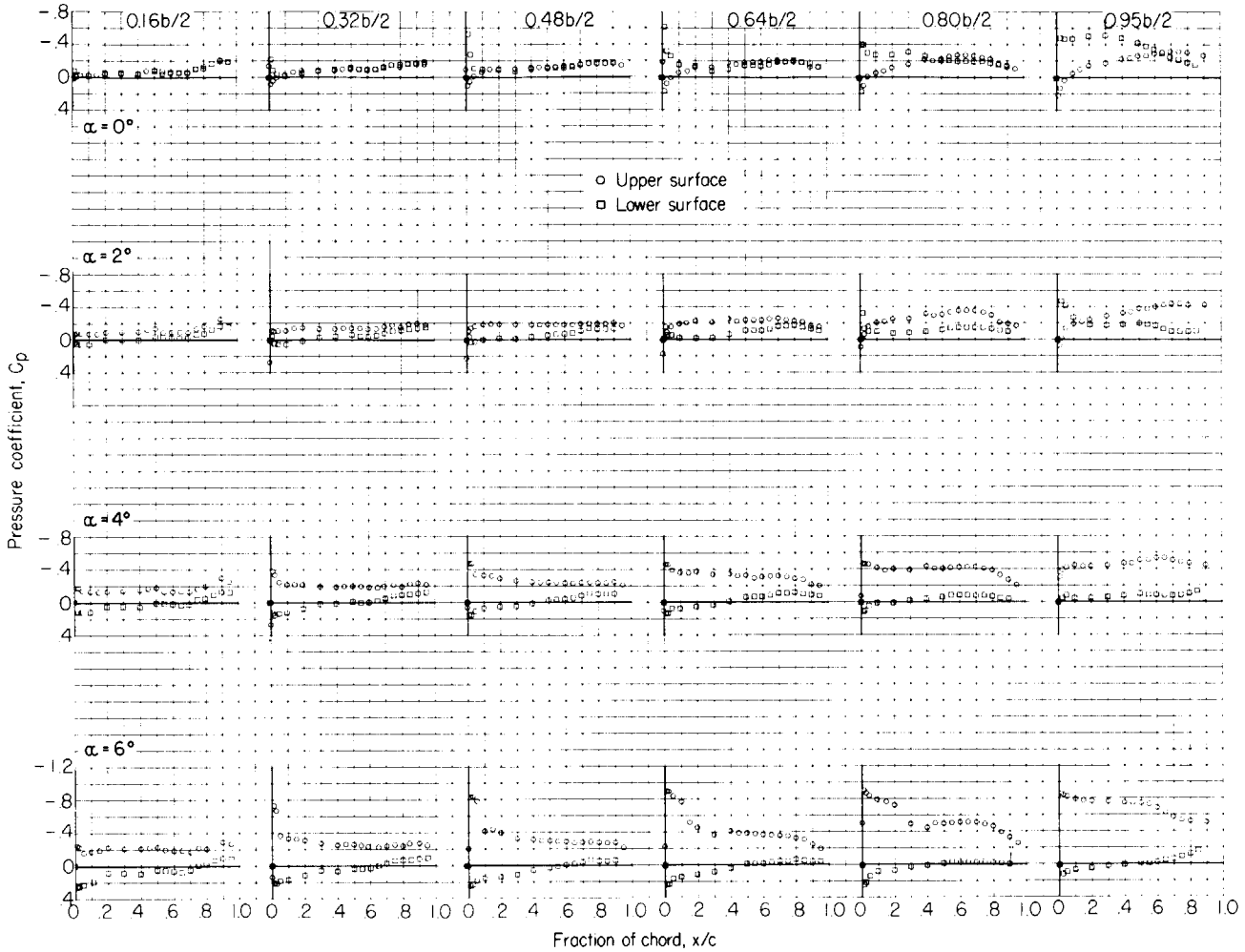

(h) M = 1.05.

Figure 6.- Continued.

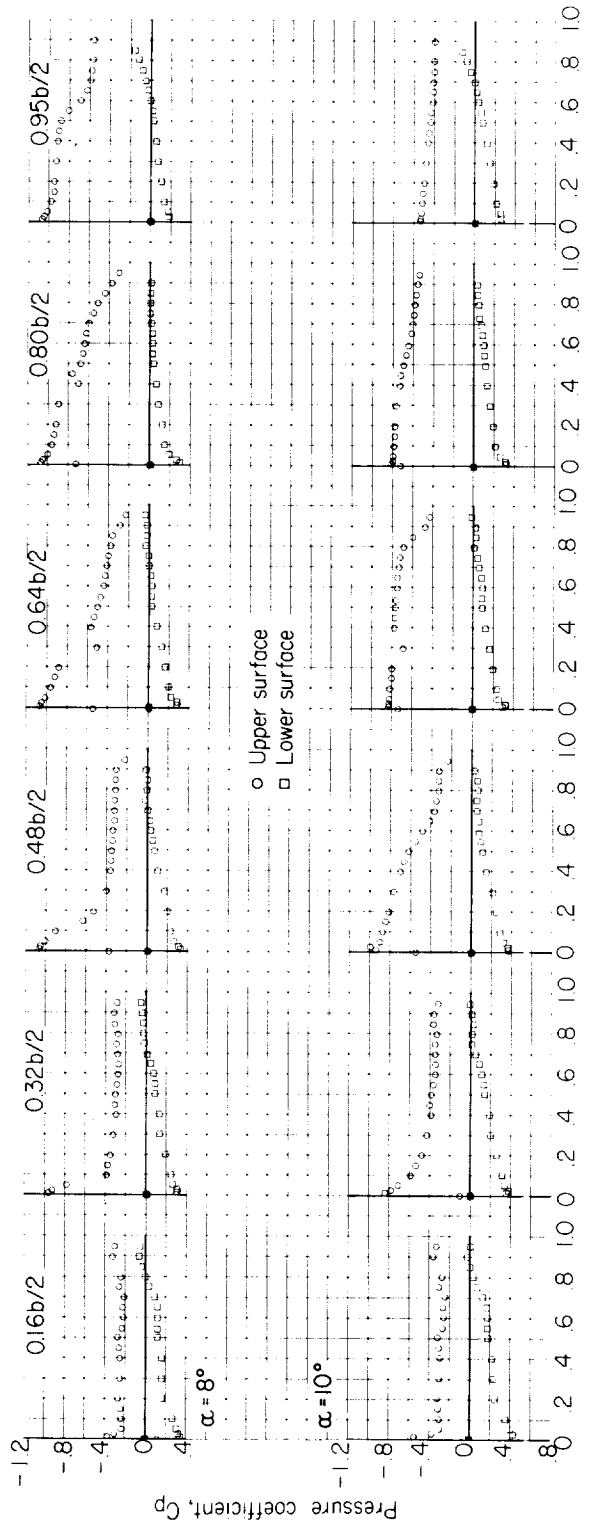

(h) Concluded.

Figure 6.- Concluded.

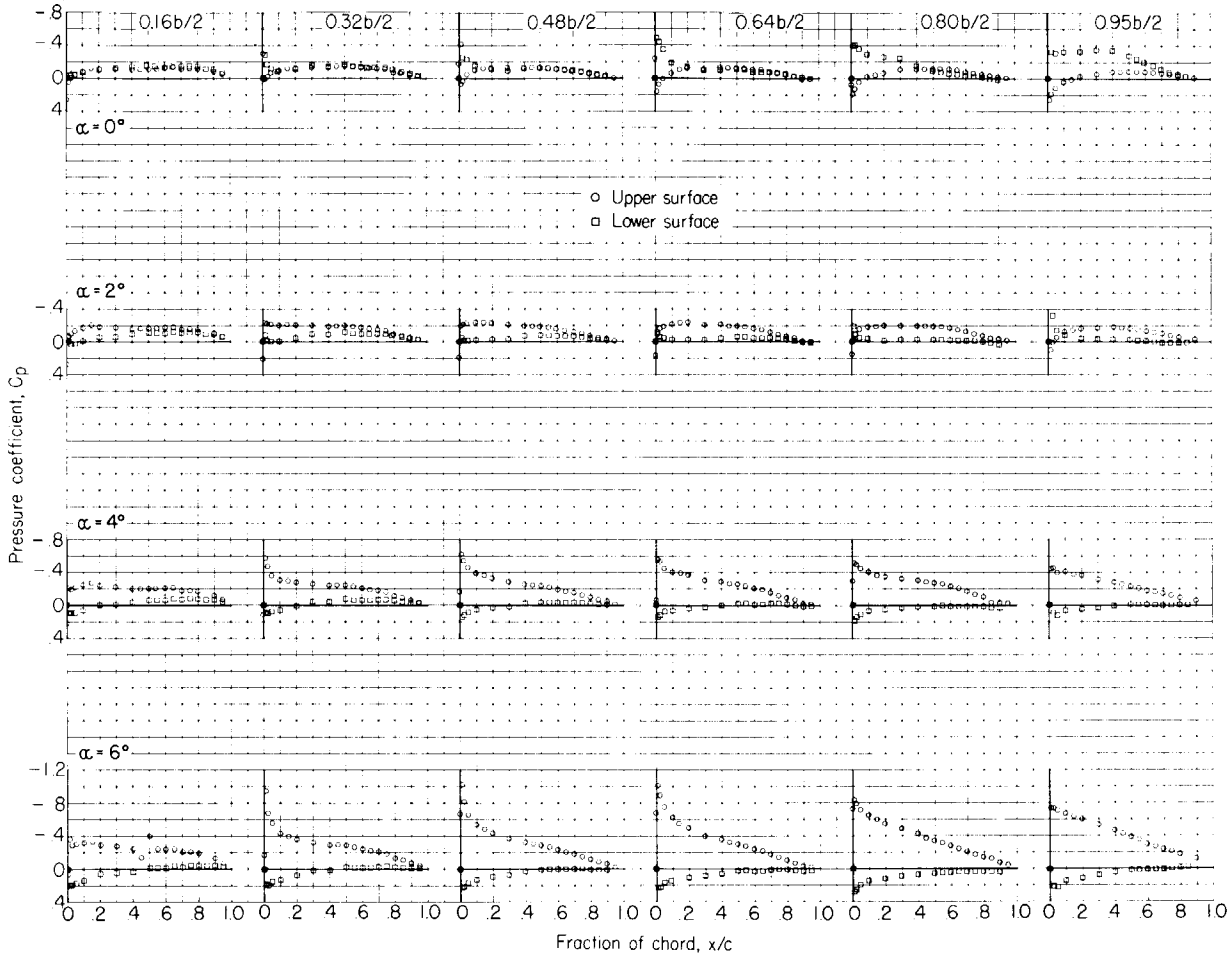

(a) M = 0.80.

Figure 7.- Chordwise pressure distributions for the cambered wing in combination with the non-indented body.

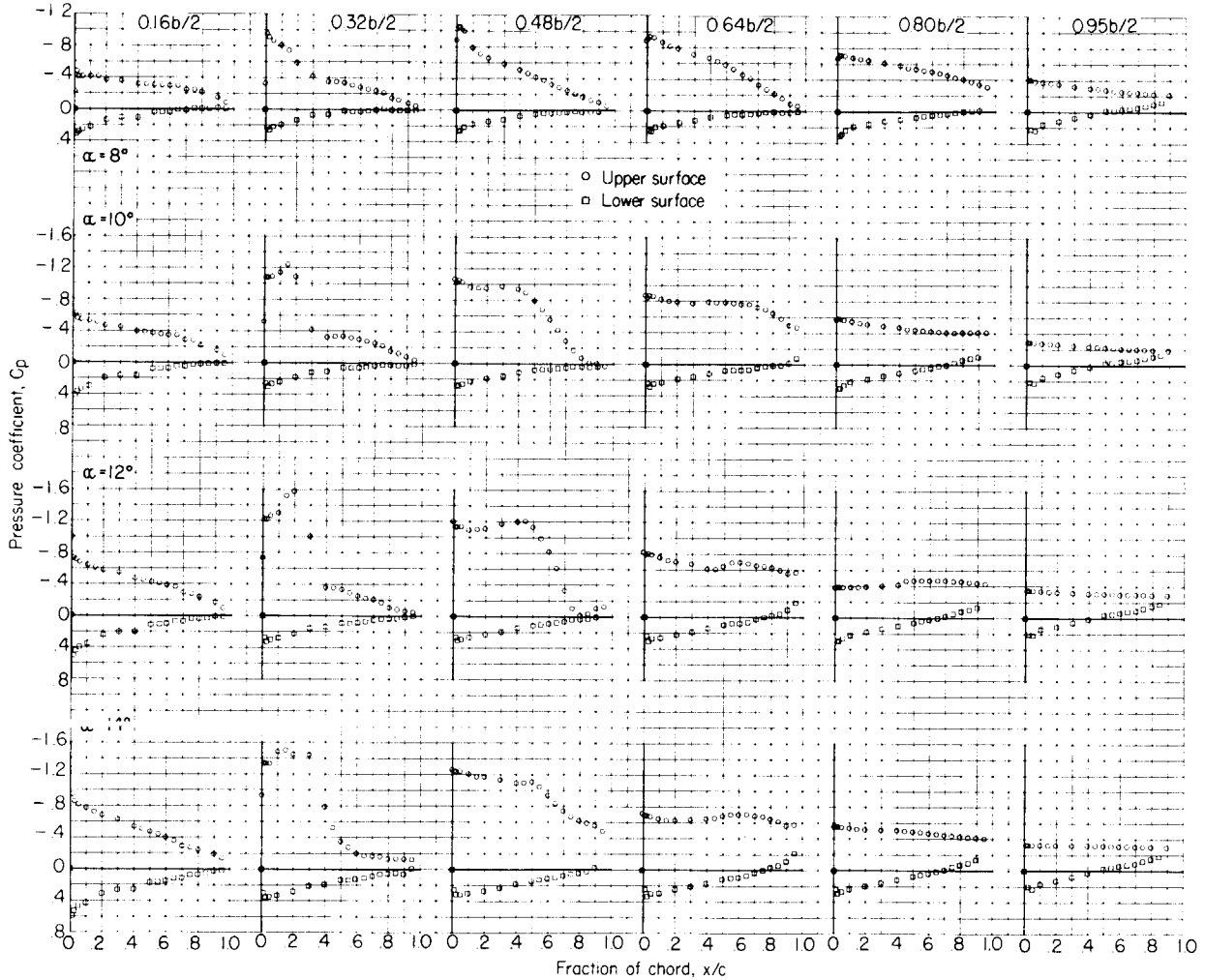

(a) Concluded.

Figure 7.- Continued.

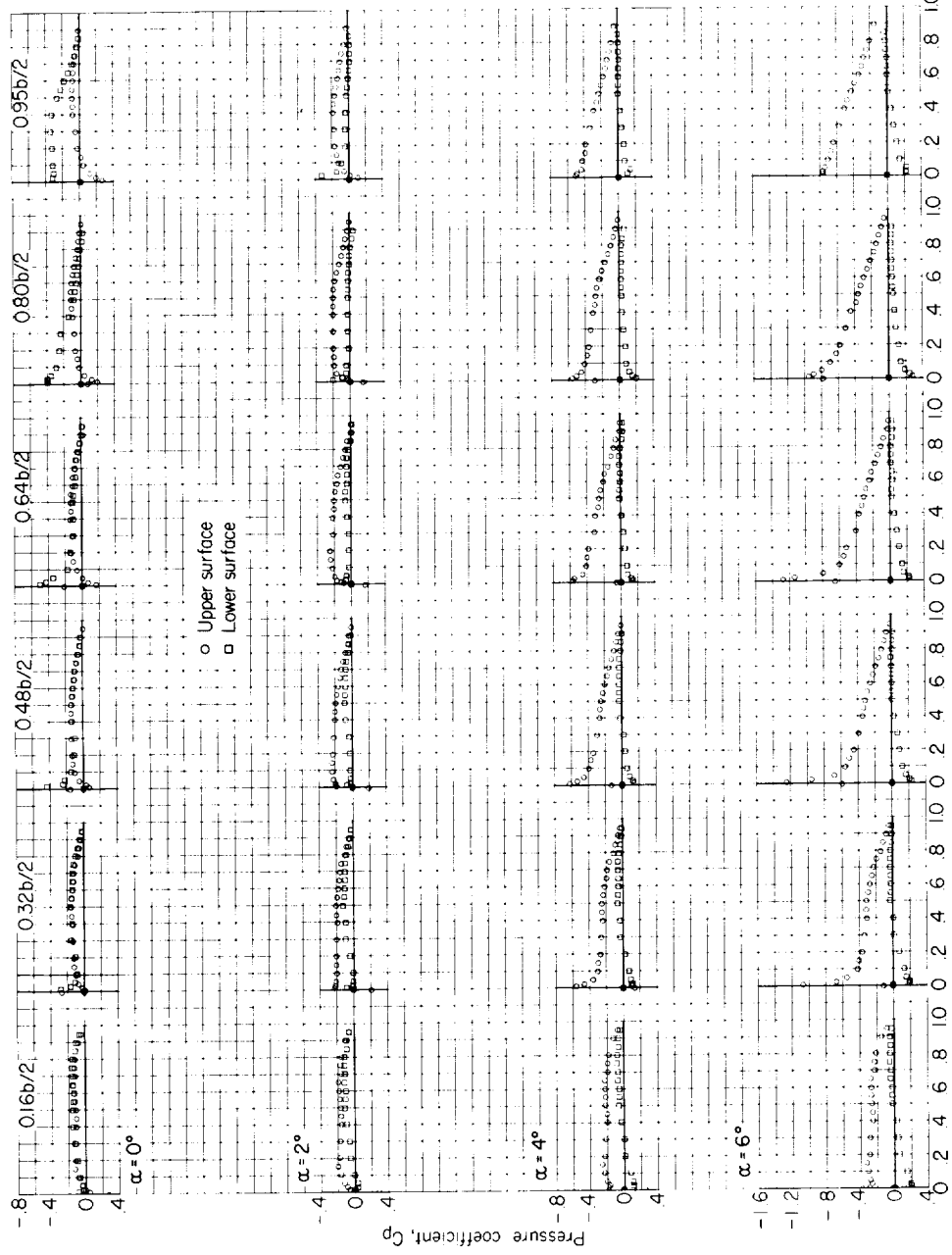

(b) M = 0.85.

Figure 7.- Continued.

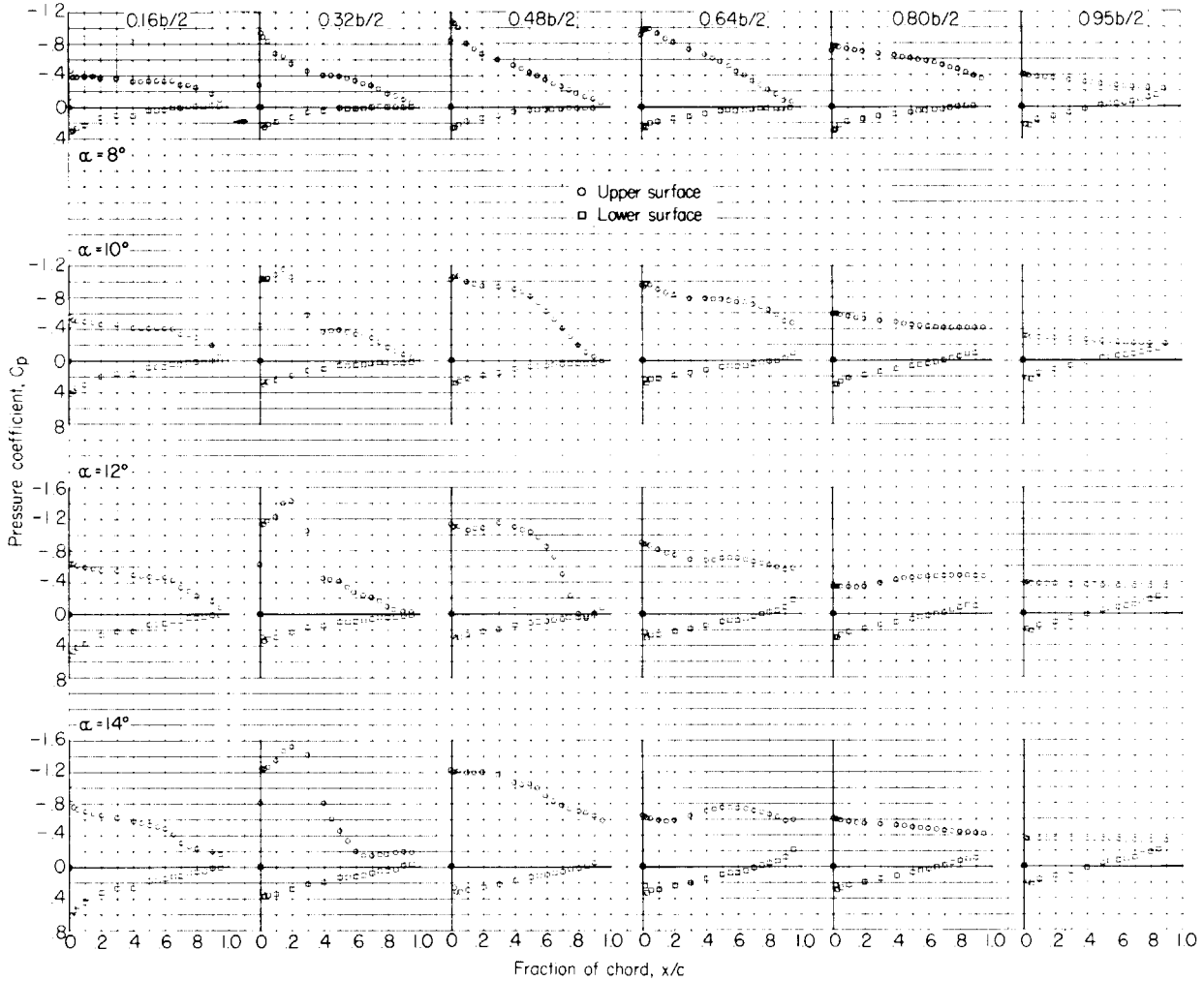

(b) Concluded.

Figure 7.- Continued.

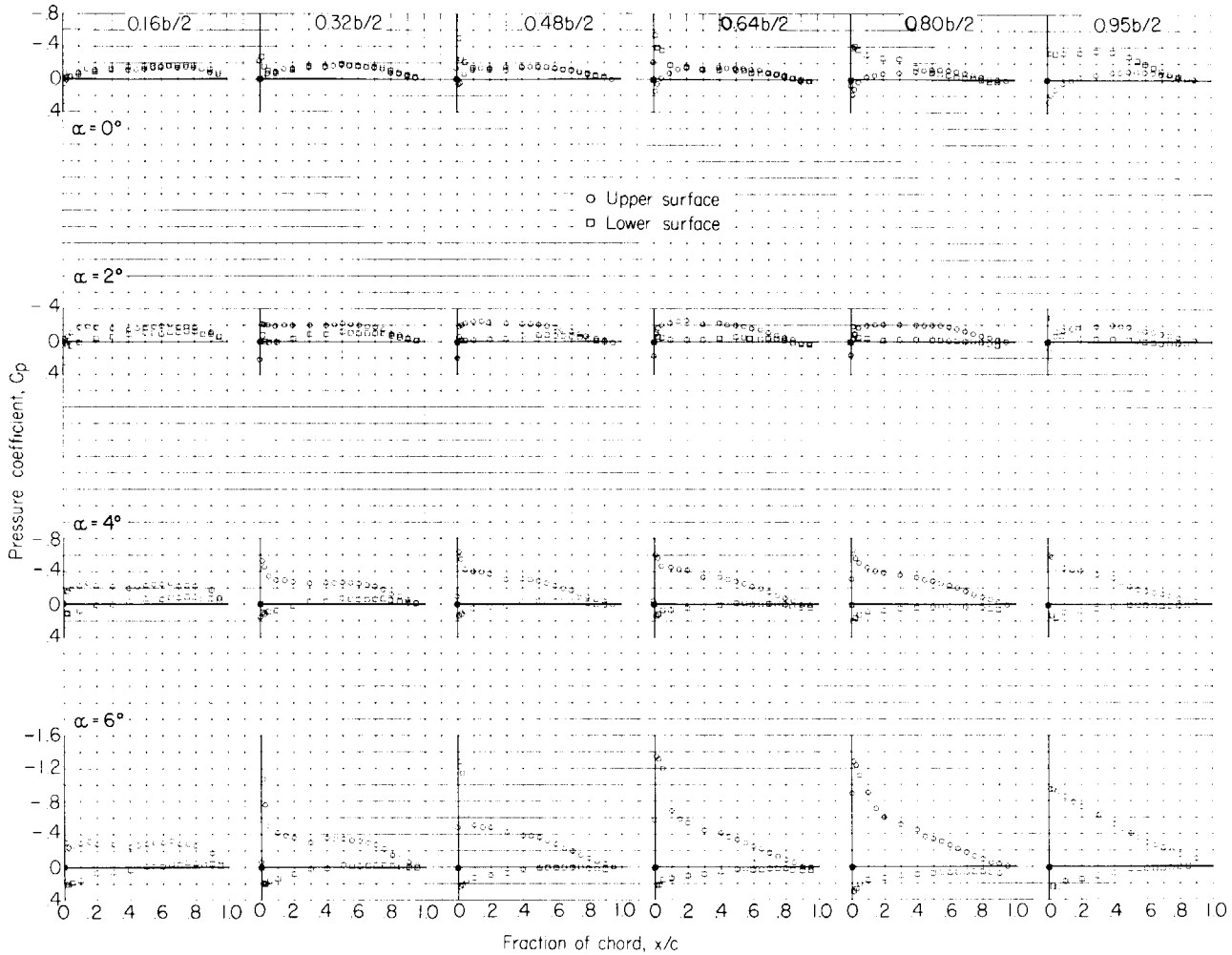

(c) M = 0.90.

Figure 7.- Continued.

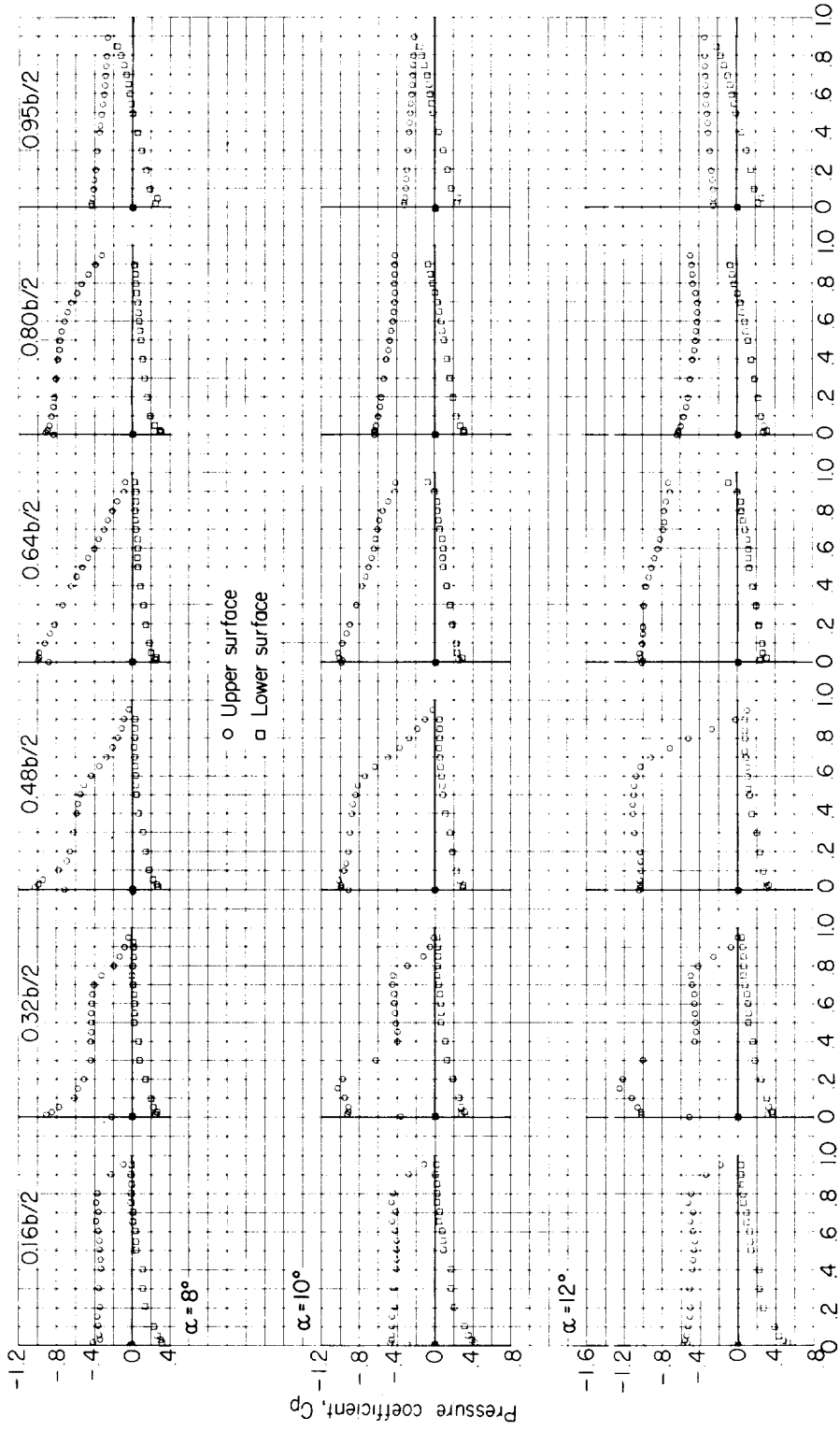

(c) Concluded.

Figure 7.- Continued.

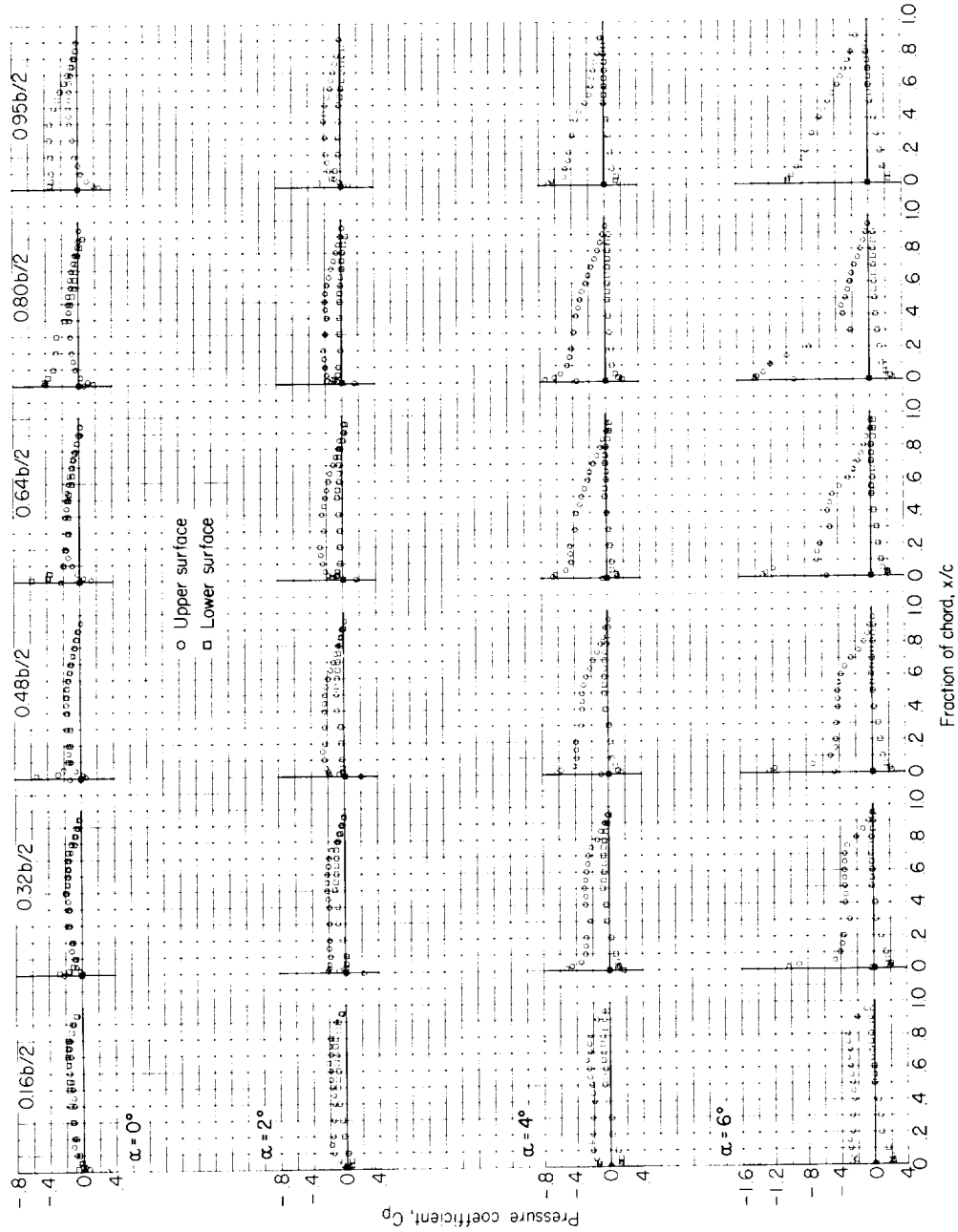

(d) M = 0.92.

Figure 7.- Continued.

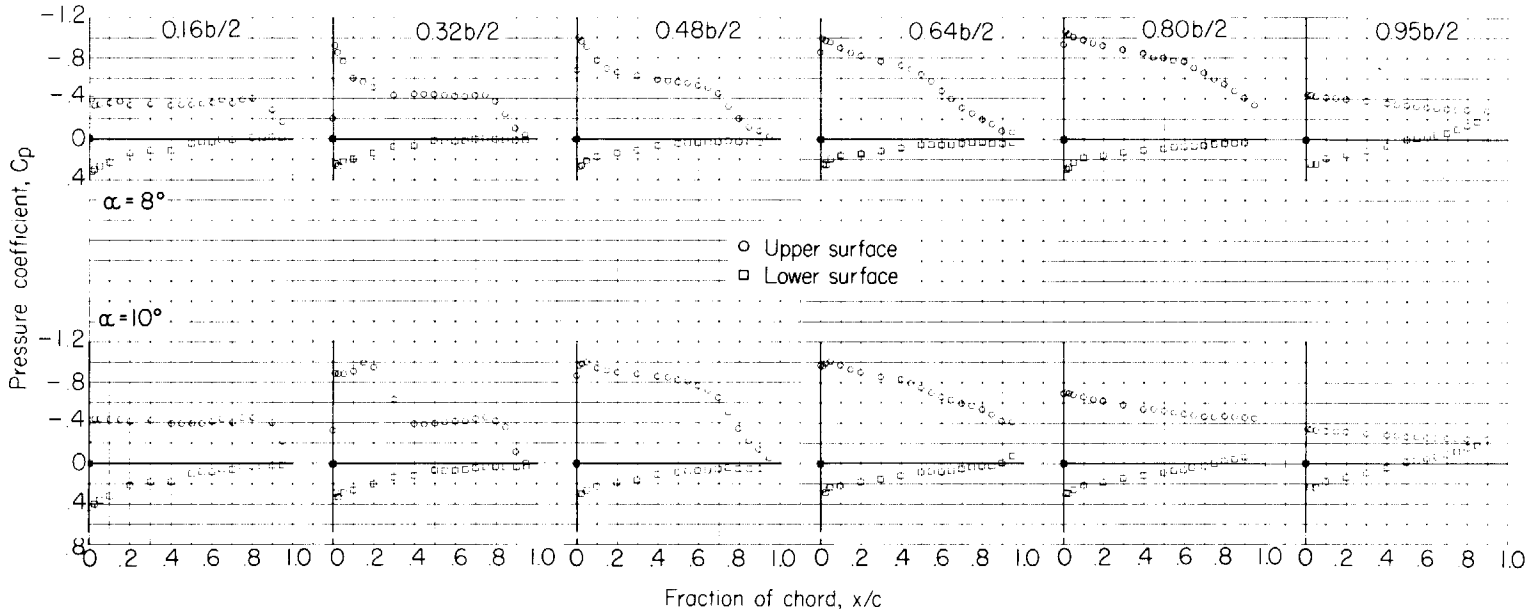

(d) Concluded.

Figure 7.- Continued.

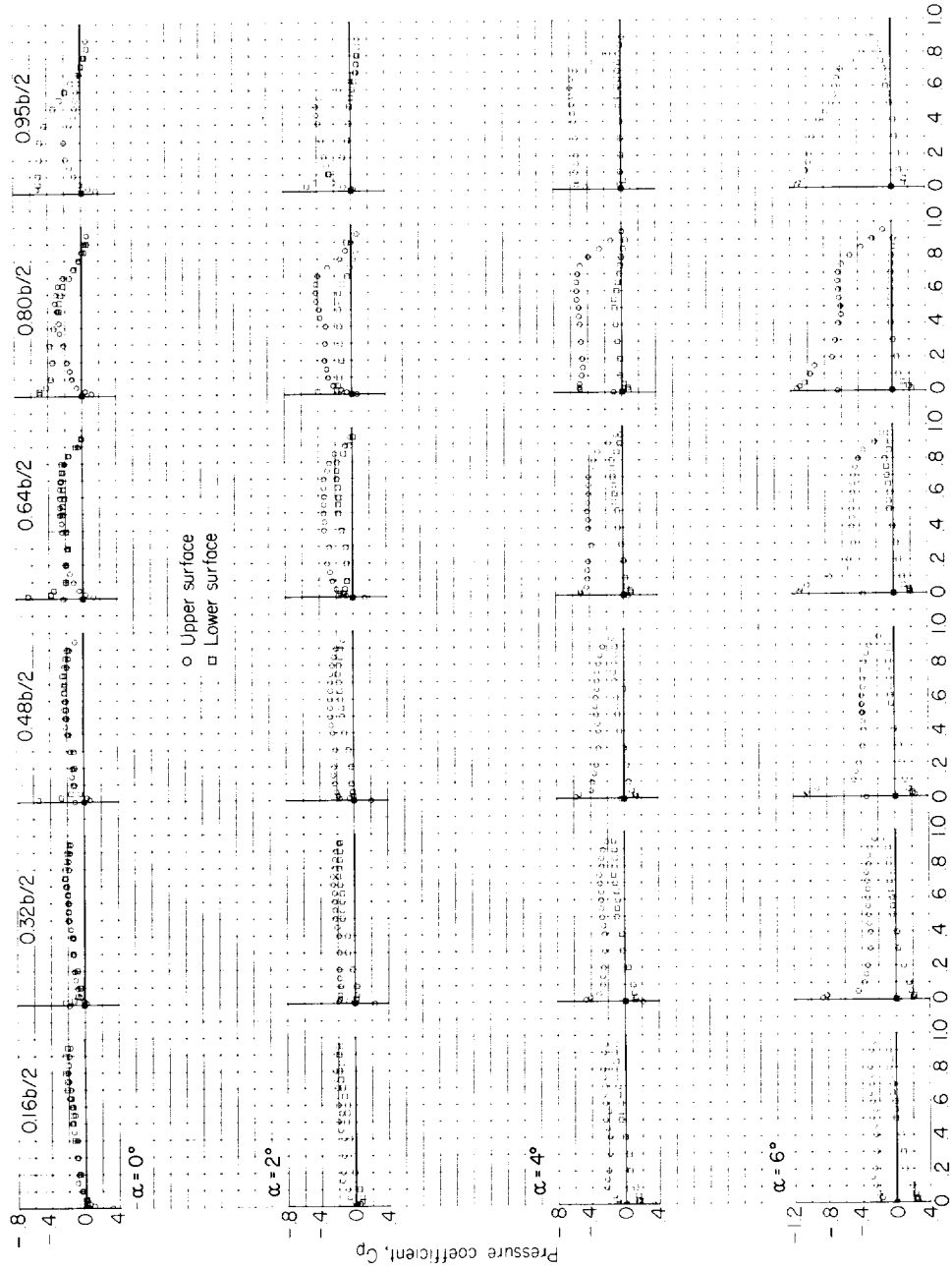

(e) M = 0.98.

Figure 7.- Continued.

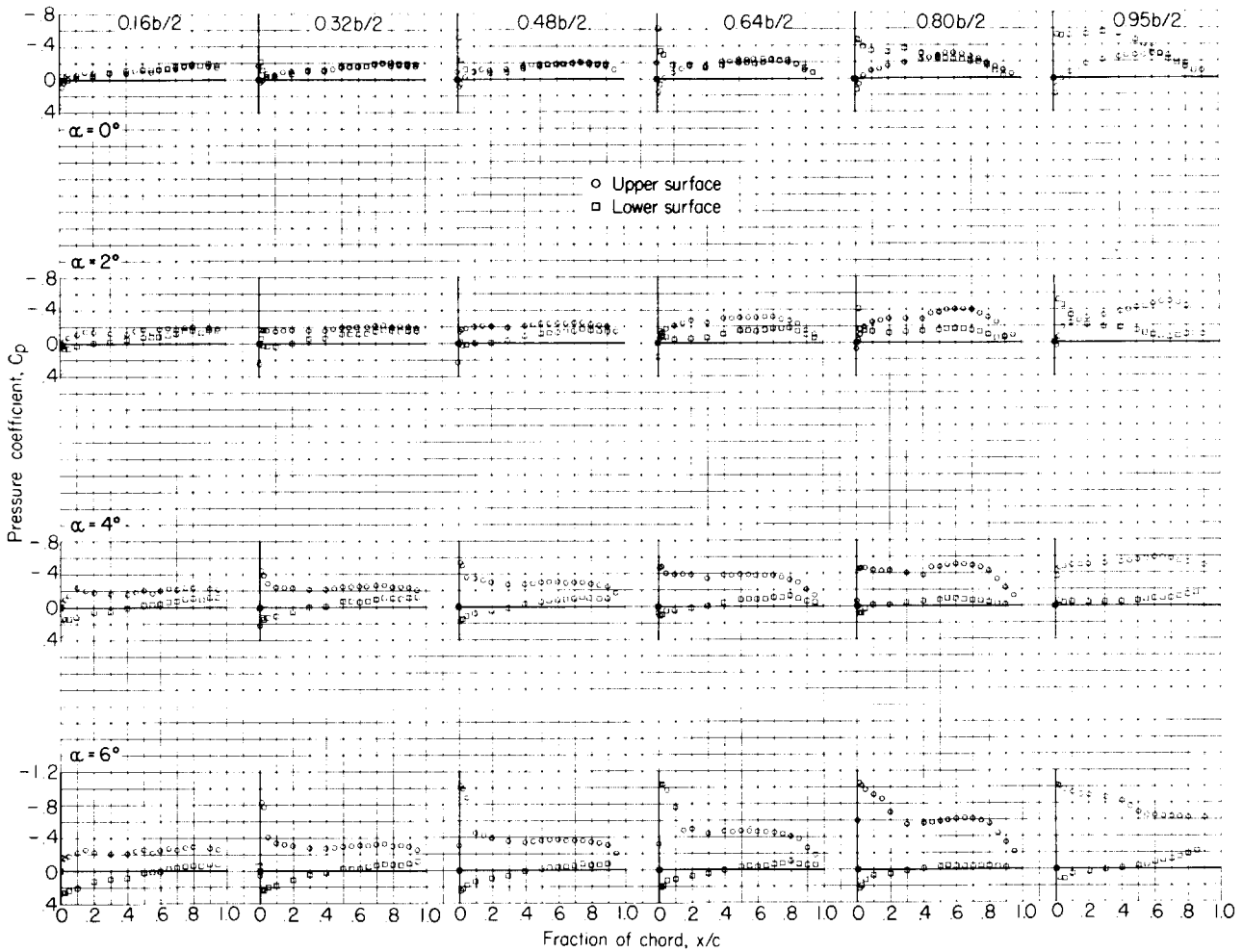

(f) M = 1.00.

Figure 7.- Continued.

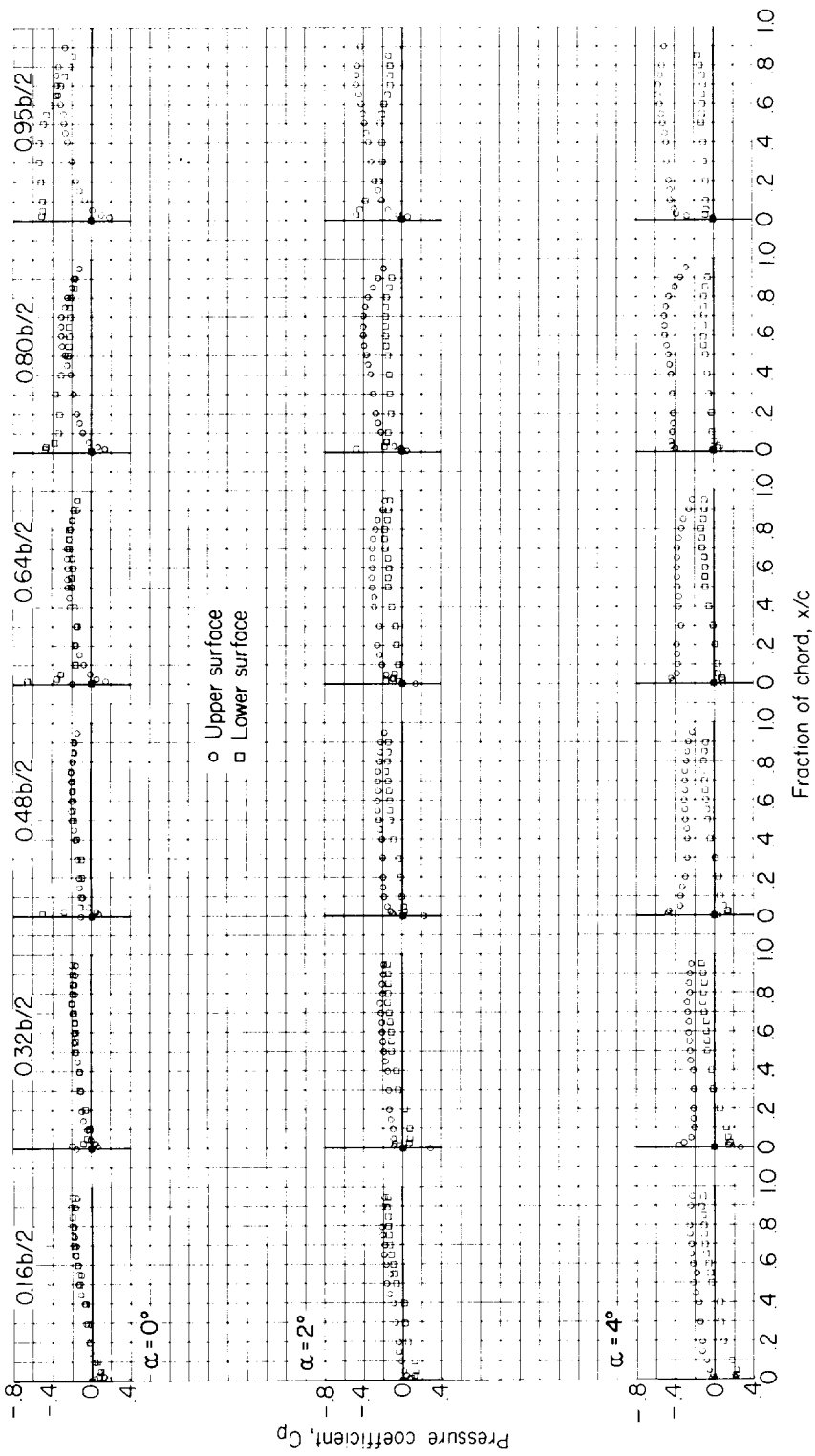

(g) M = 1.05.

Figure 7.- Concluded.

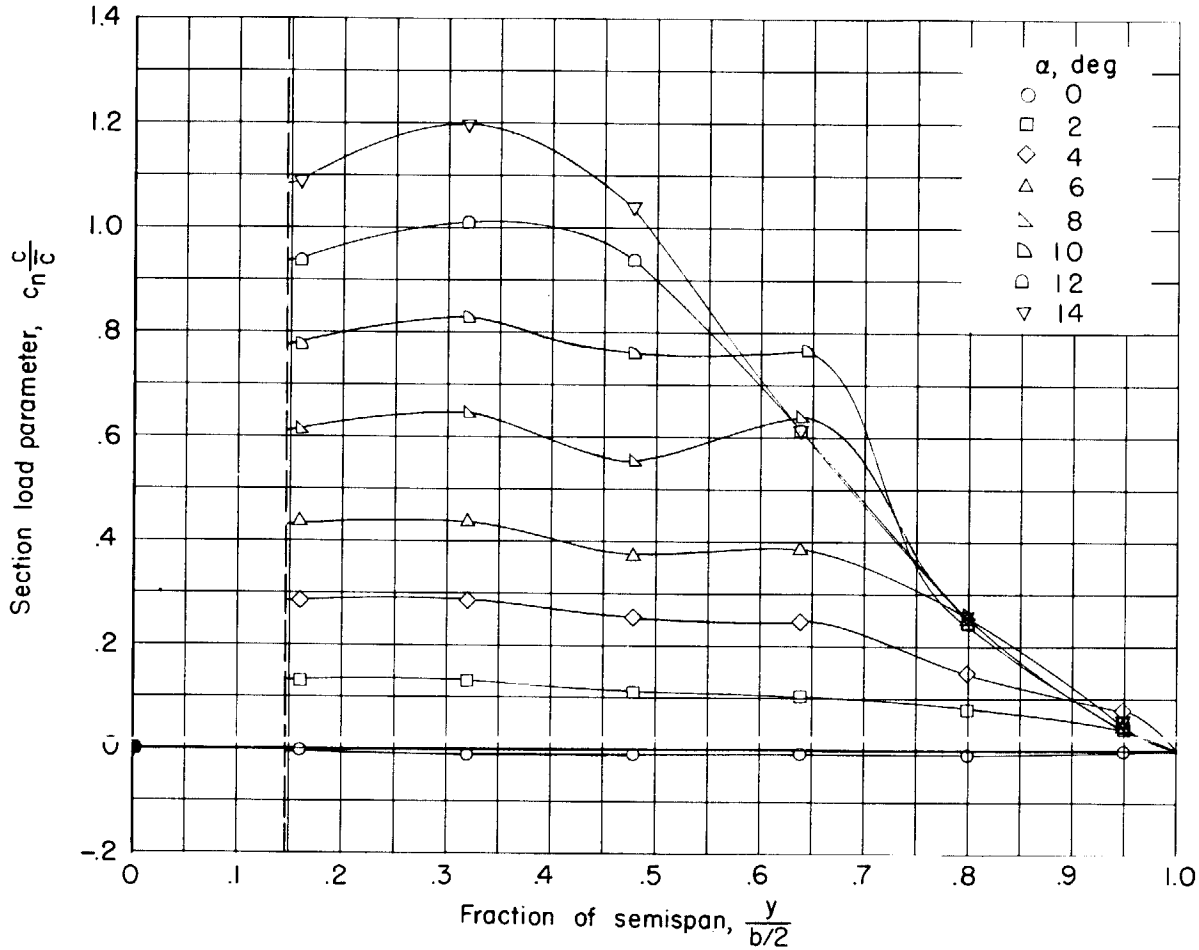

(a) M = 0.80.

Figure 8.- Spanwise variation of section normal-load parameter for the plane wing in combination with the indented body at various angles of attack and Mach numbers.

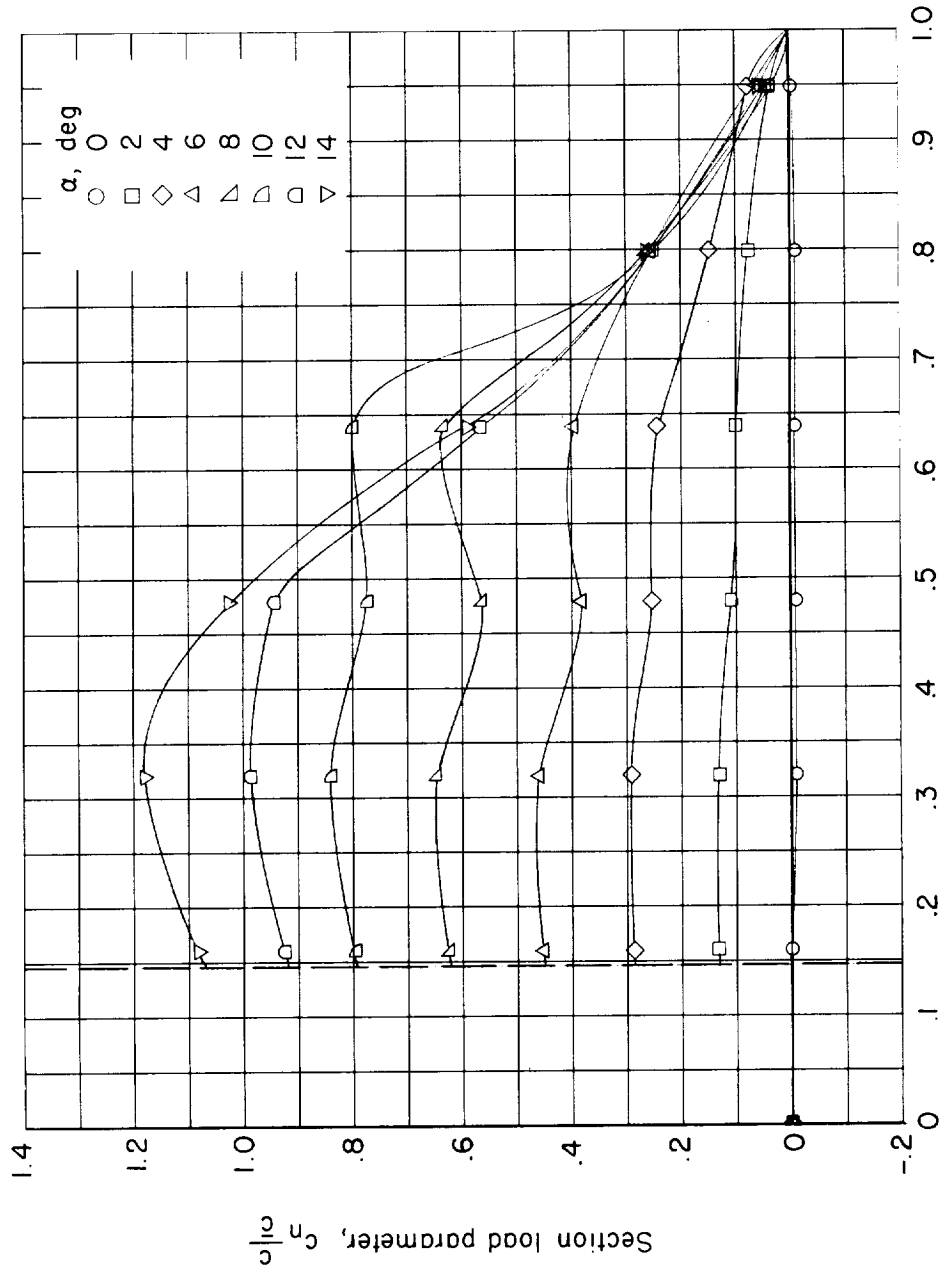

(b) M = 0.85.

Figure 8.- Continued.

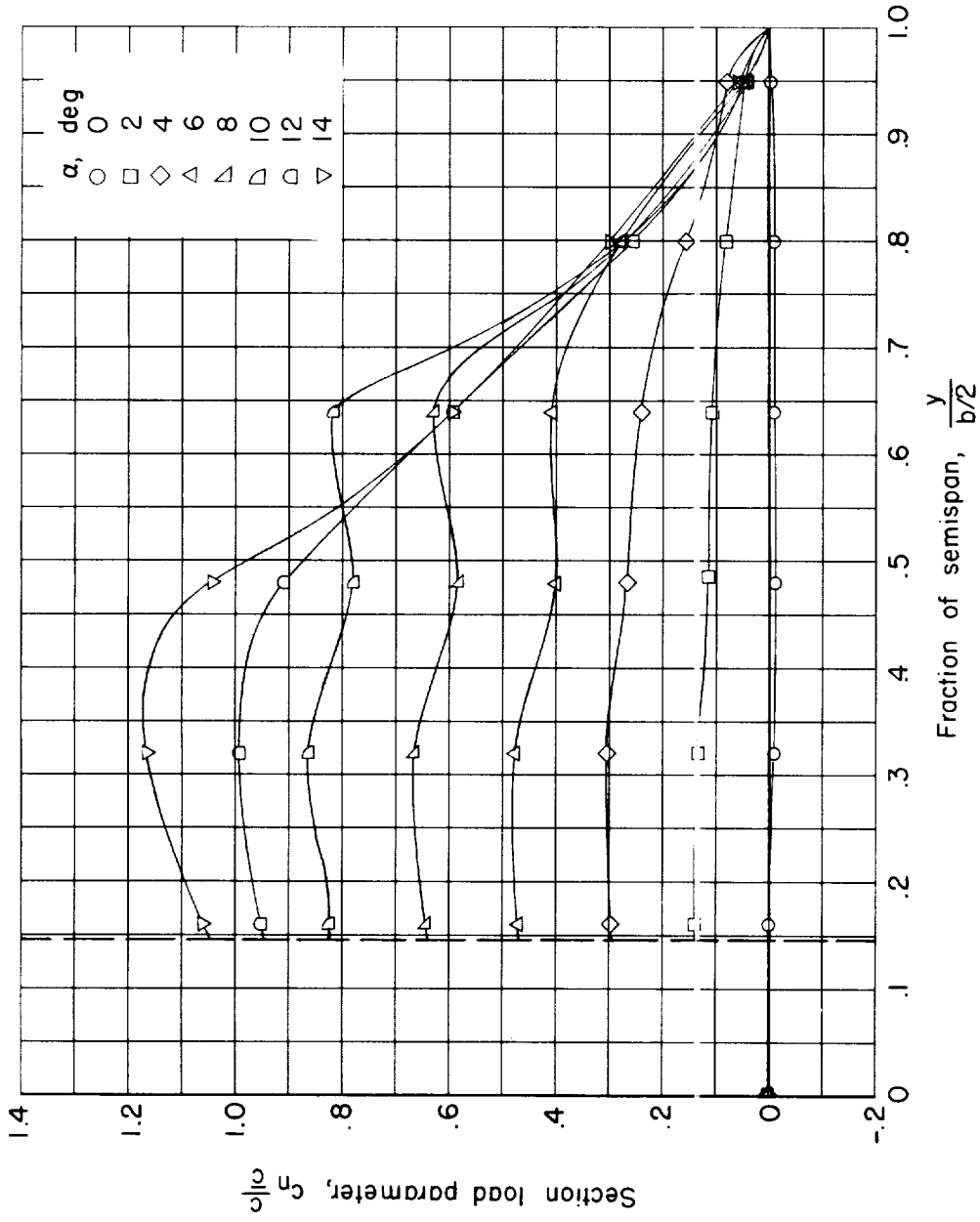

(c) M = 0.90.

Figure 8.- Continued.

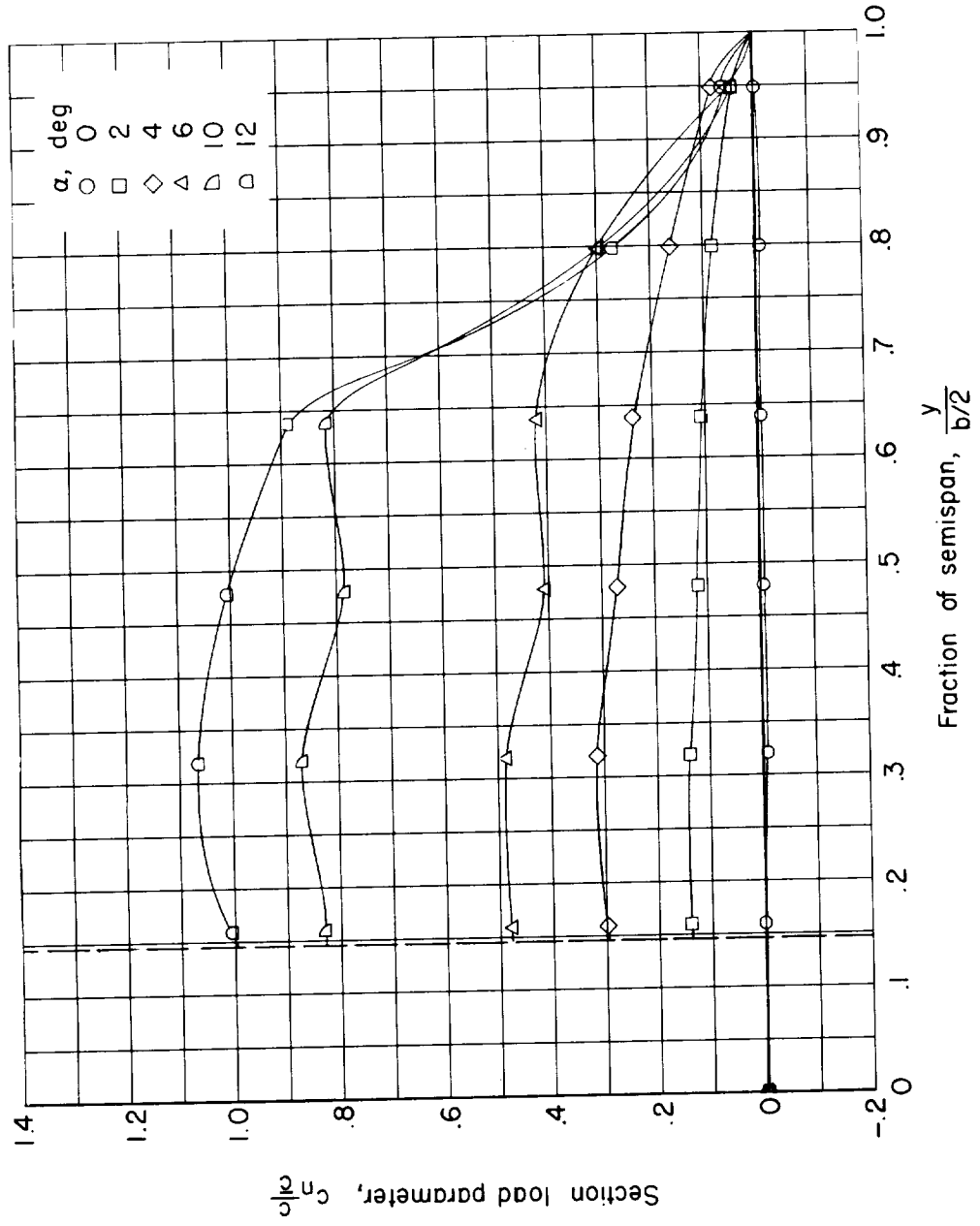

(d) M = 0.92.

Figure 8.- Continued.

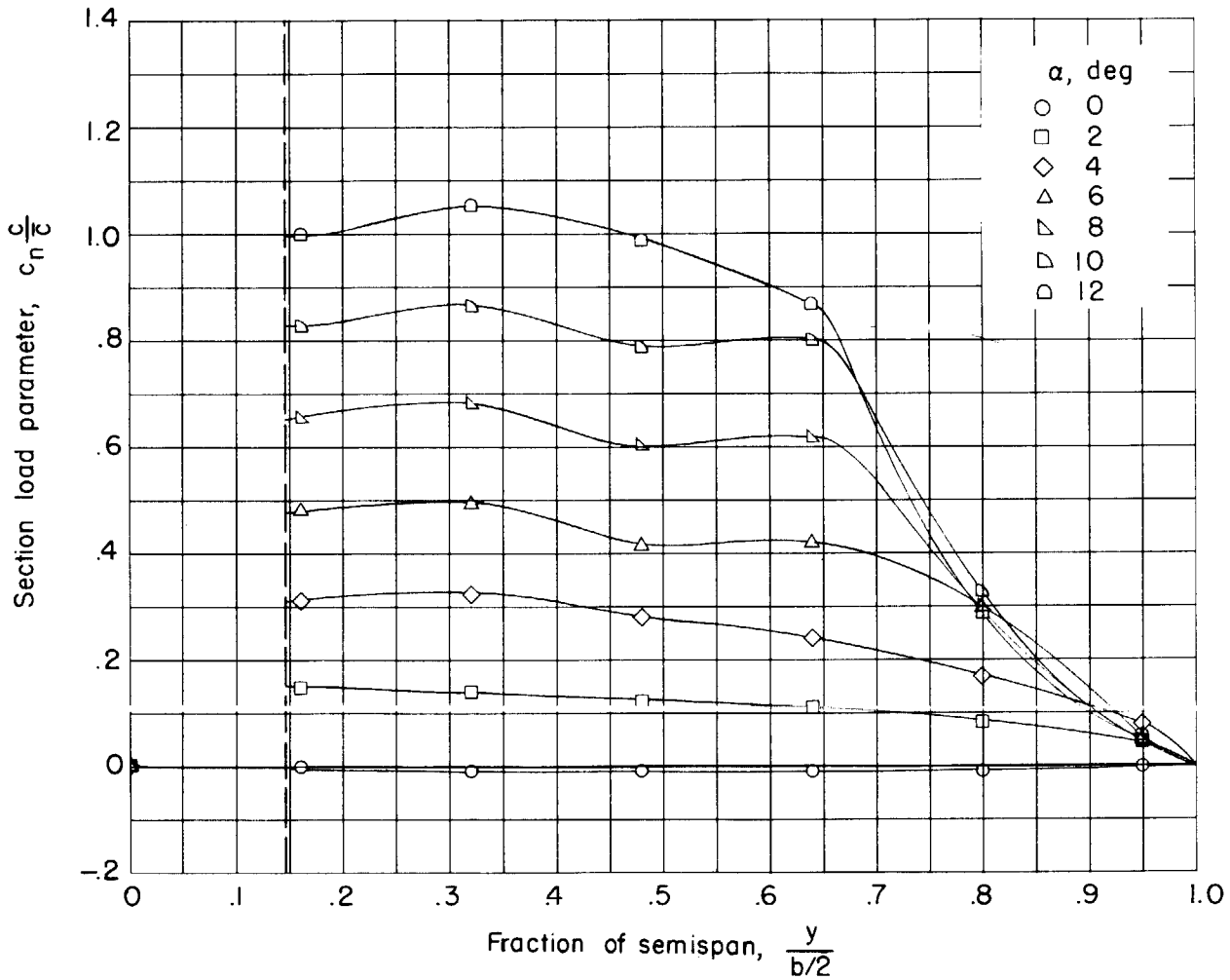

(e) M = 0.94.

Figure 8.- Continued.

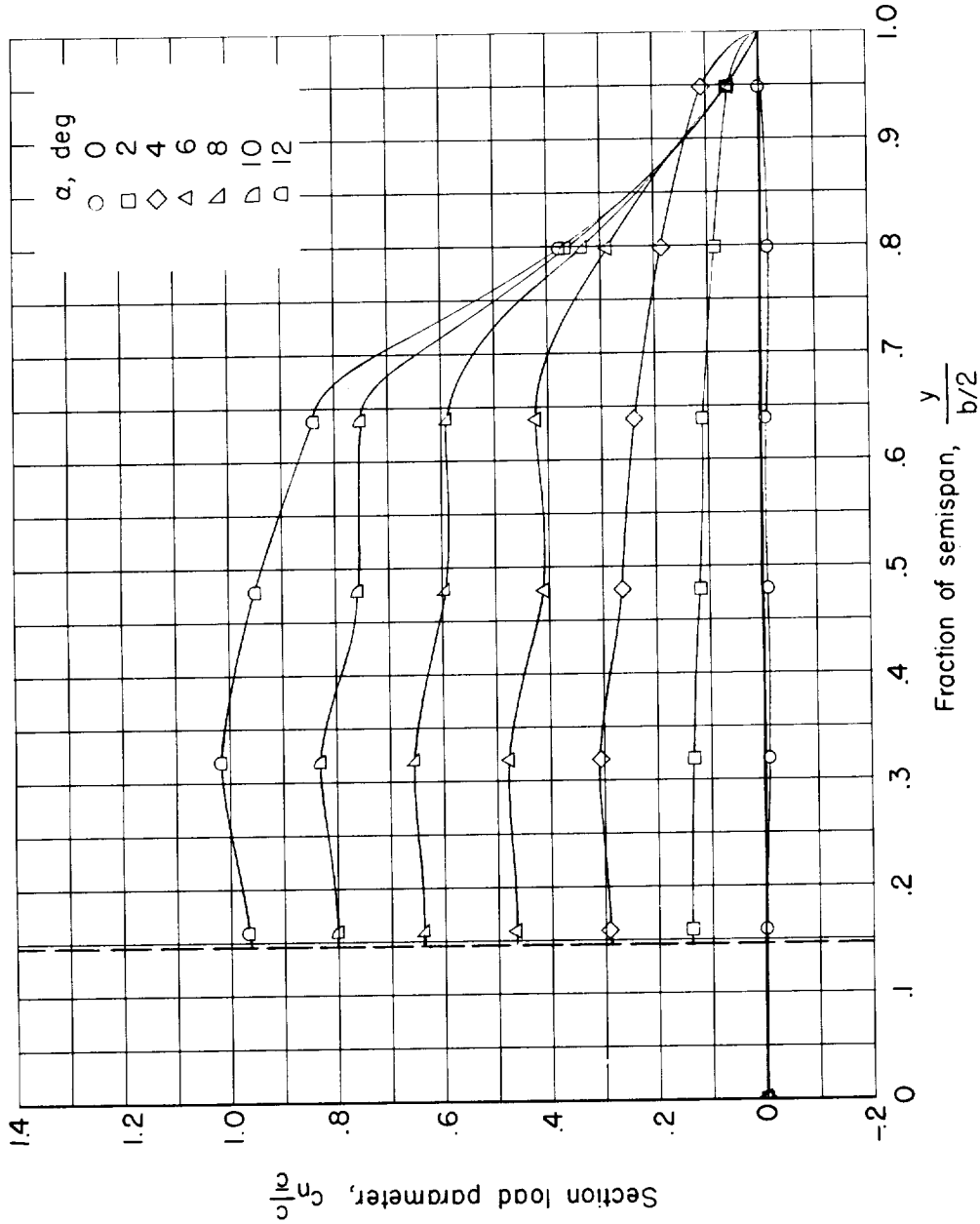

(f) M = 0.98.

Figure 8.- Continued.

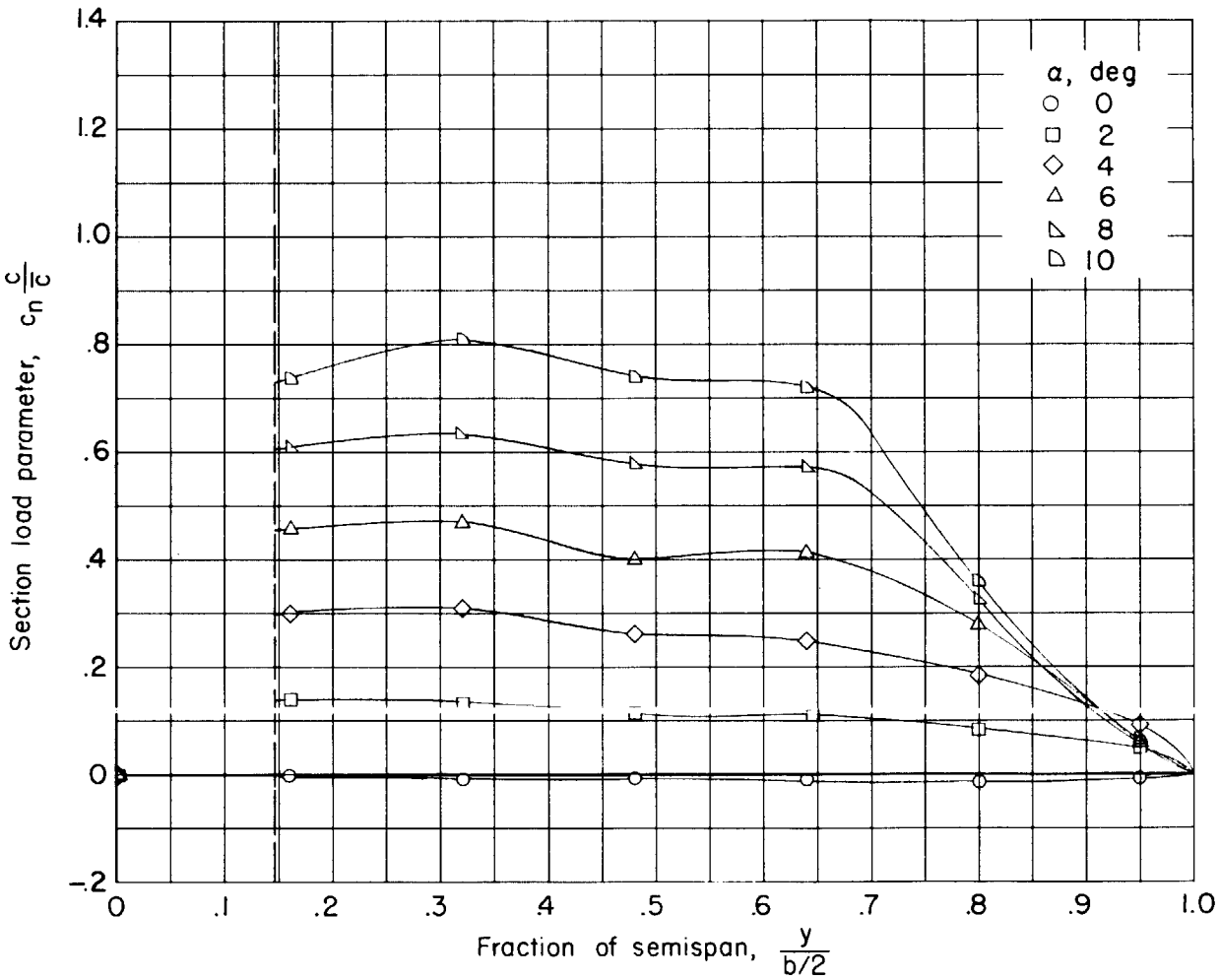

(g) M = 1.00.

Figure 8.- Continued.

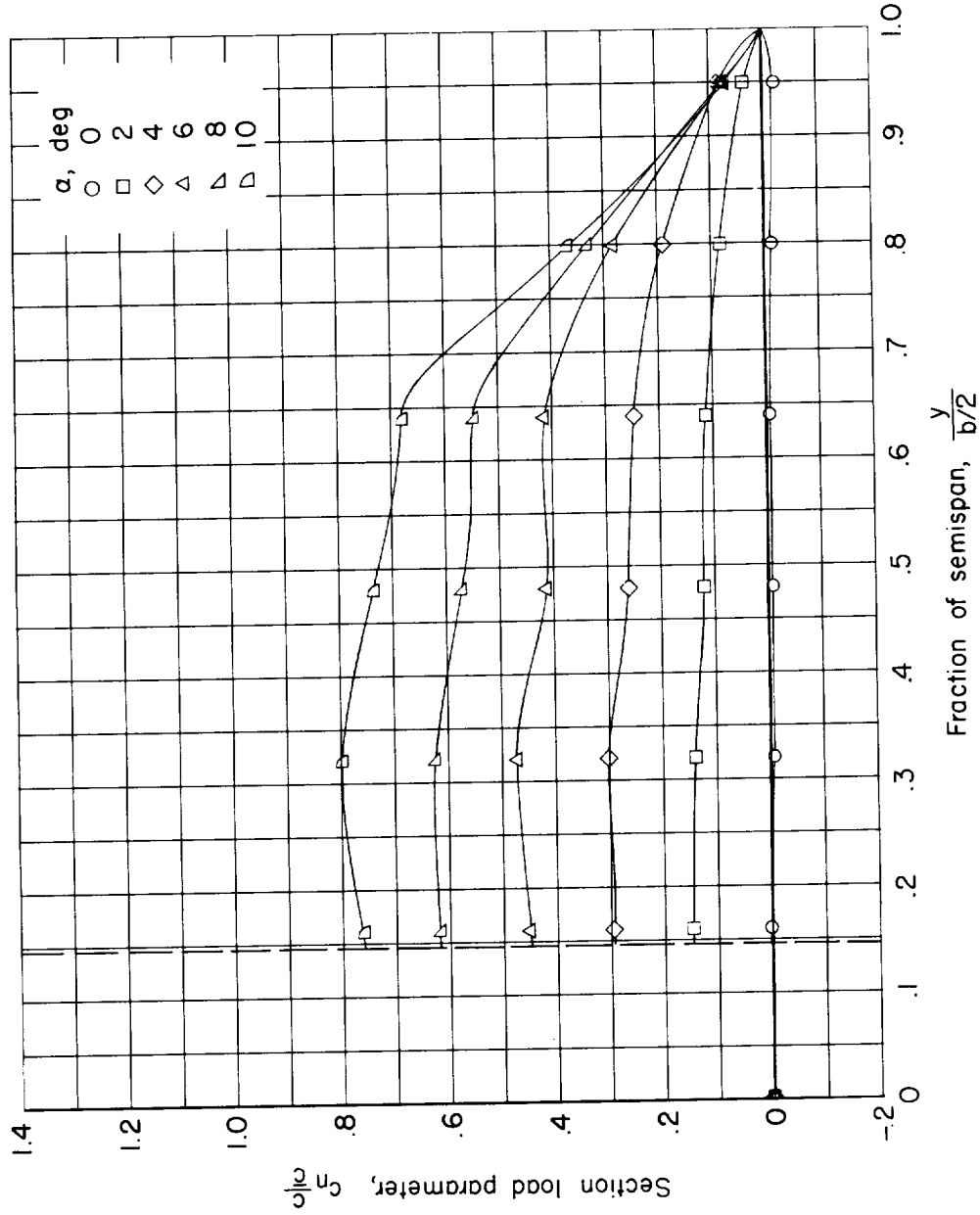

(h) M = 1.05.

Figure 8.- Concluded.

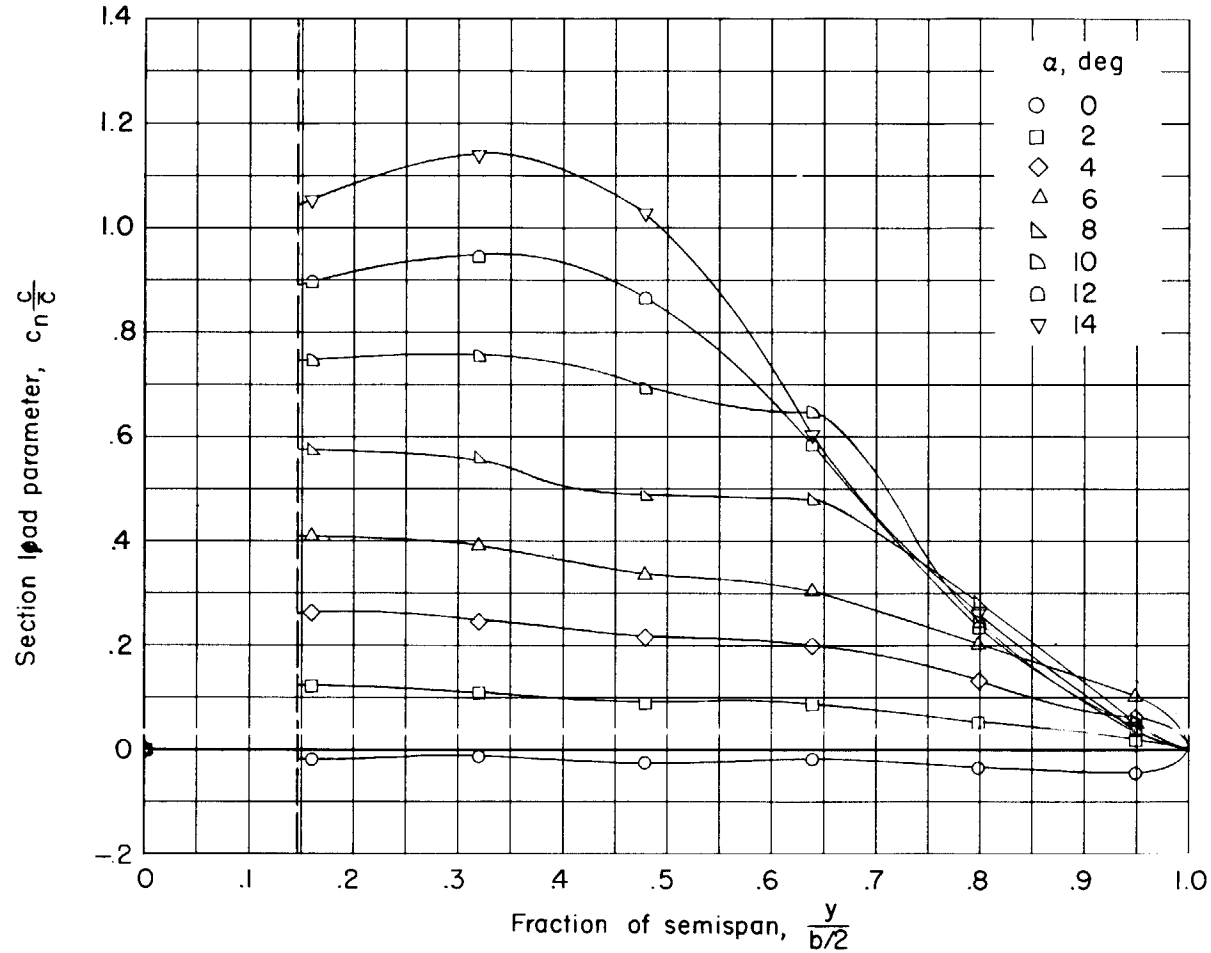

(a) M = 0.80.

Figure 9.- Spanwise variation of section normal-load parameter for the cambered wing in combination with the indented body at various angles of attack and Mach numbers.

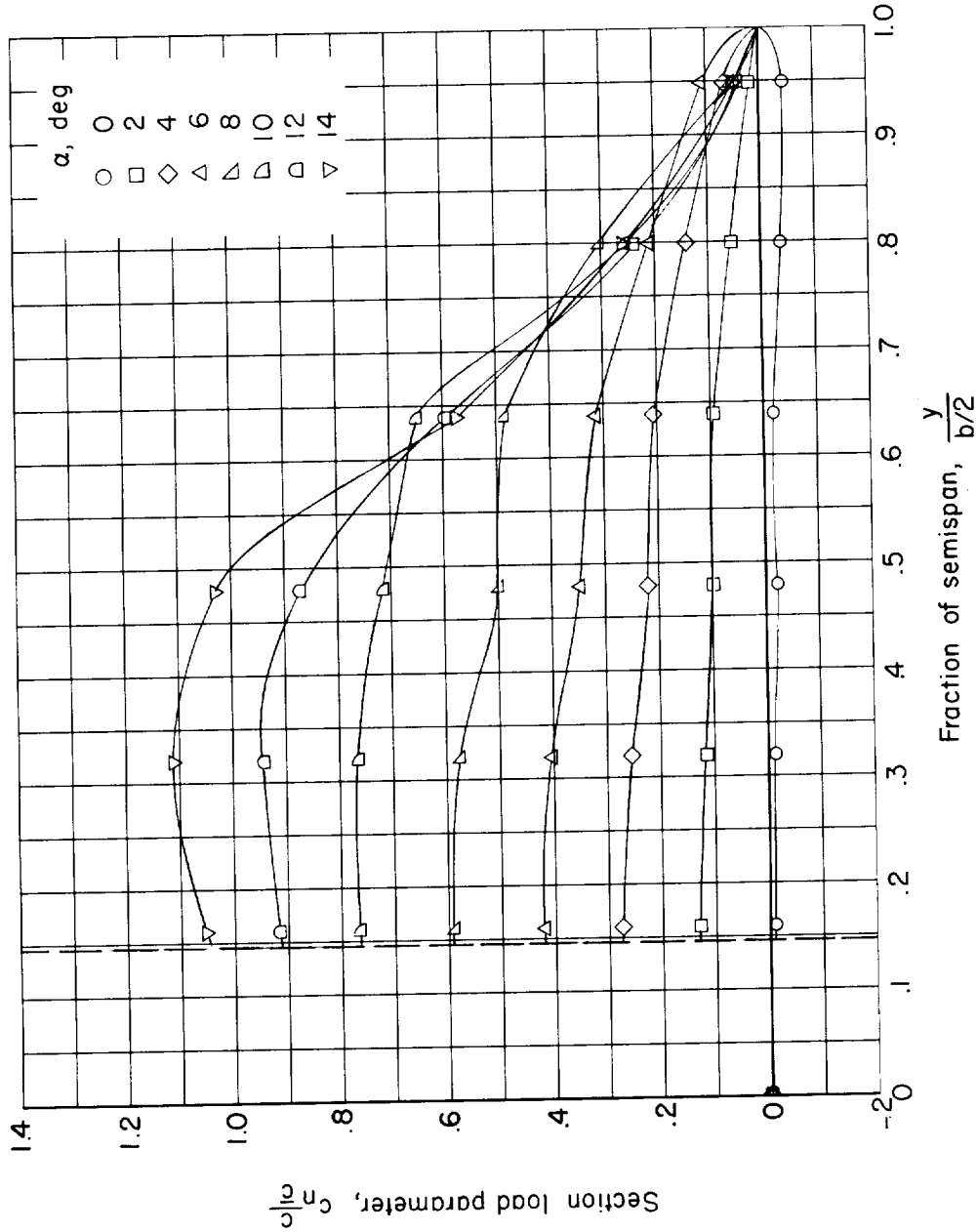

(b) M = 0.85.

Figure 9.- Continued.

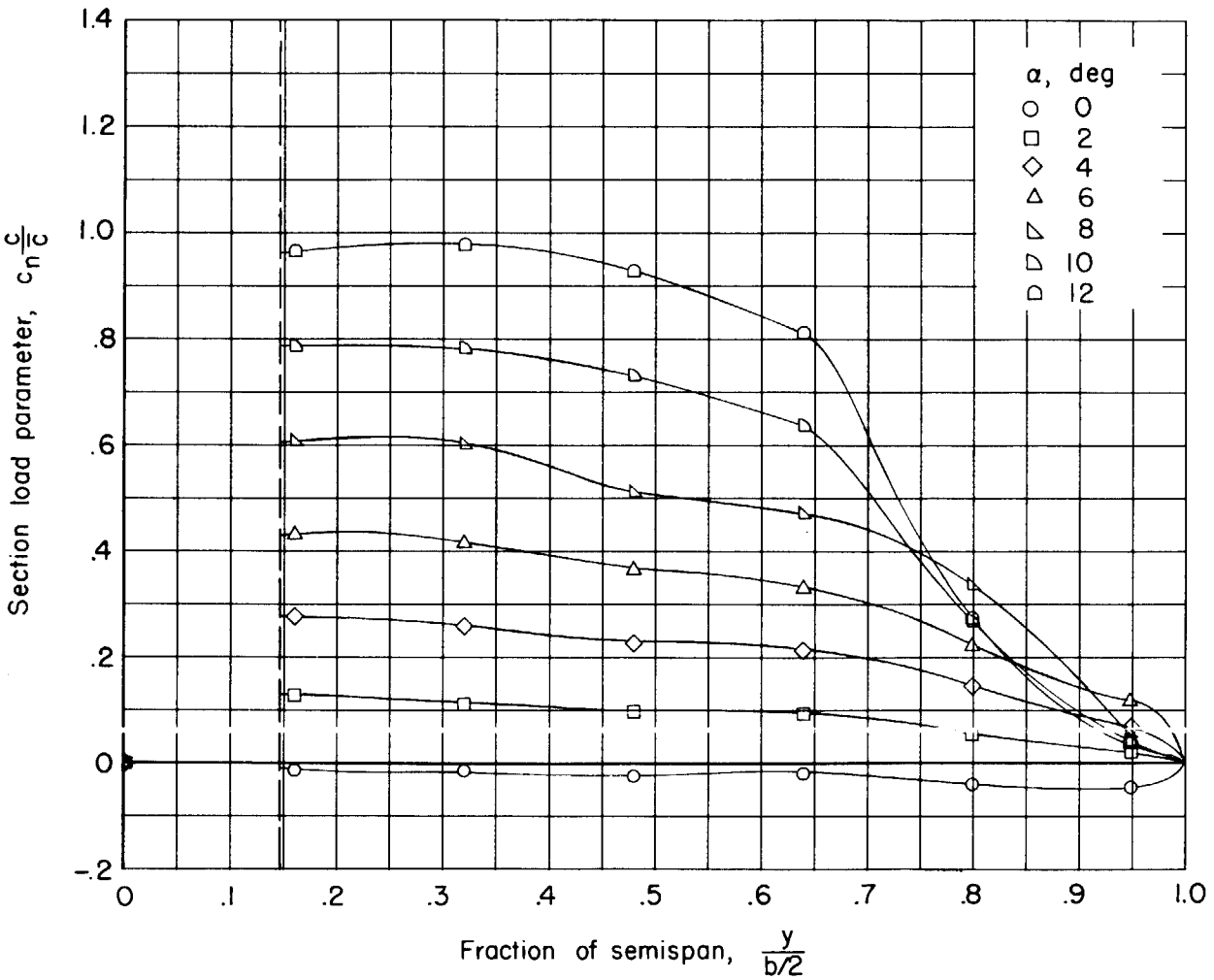

(c) M = 0.90.

Figure 9.- Continued.

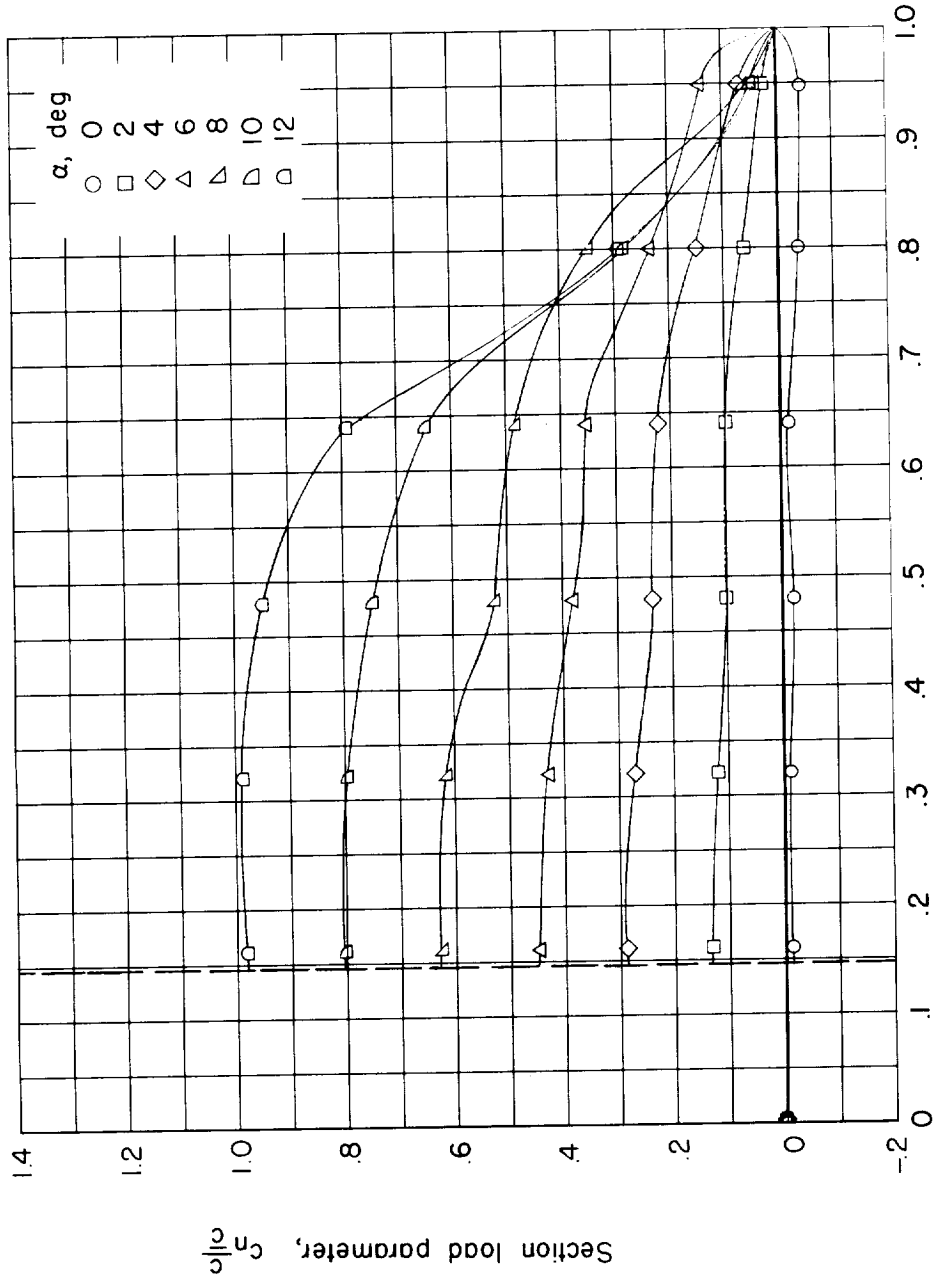

(d) M = 0.92.

Figure 9.- Continued.

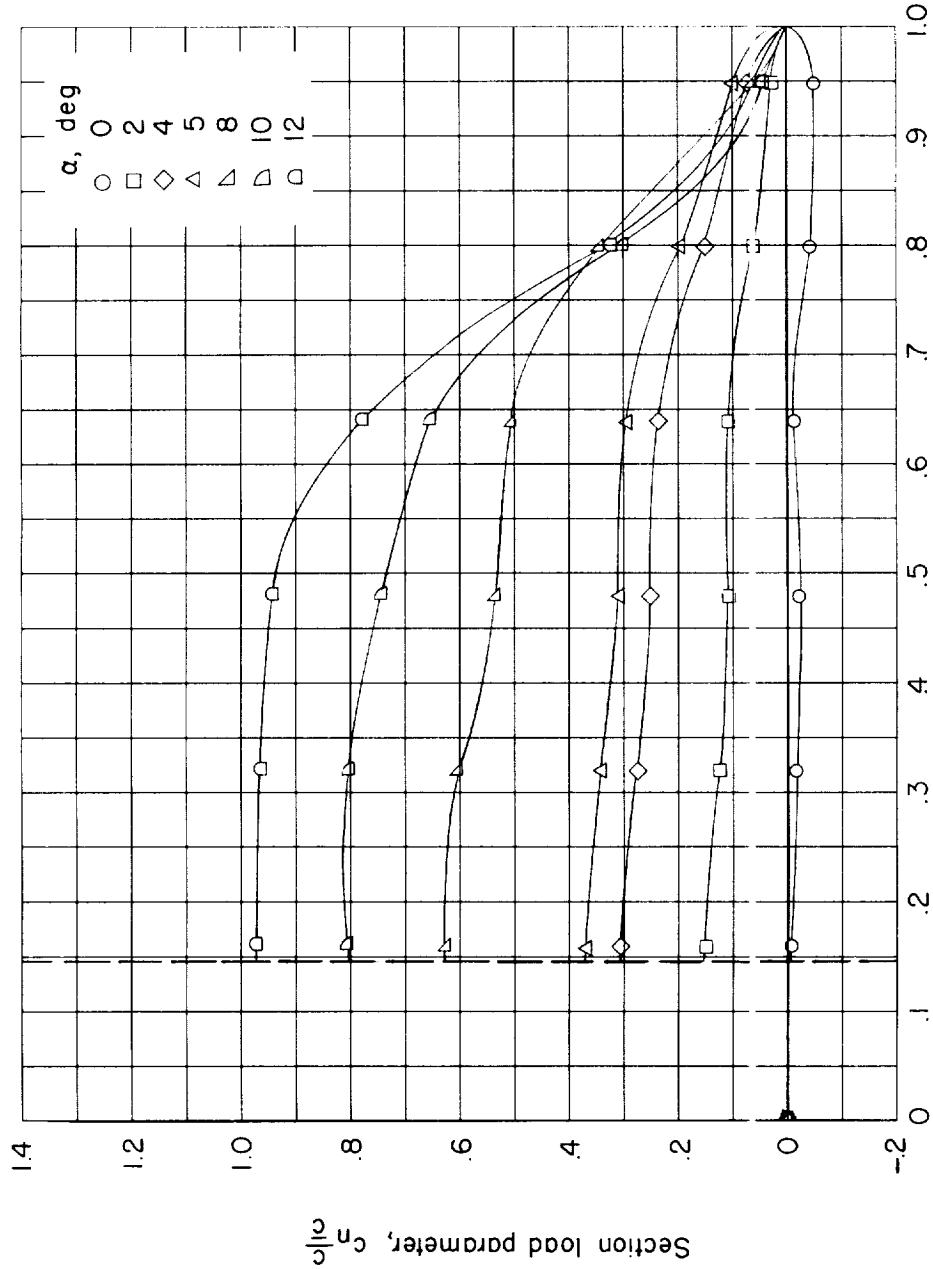

(e) M = 0.94.

Figure 9.- Continued.

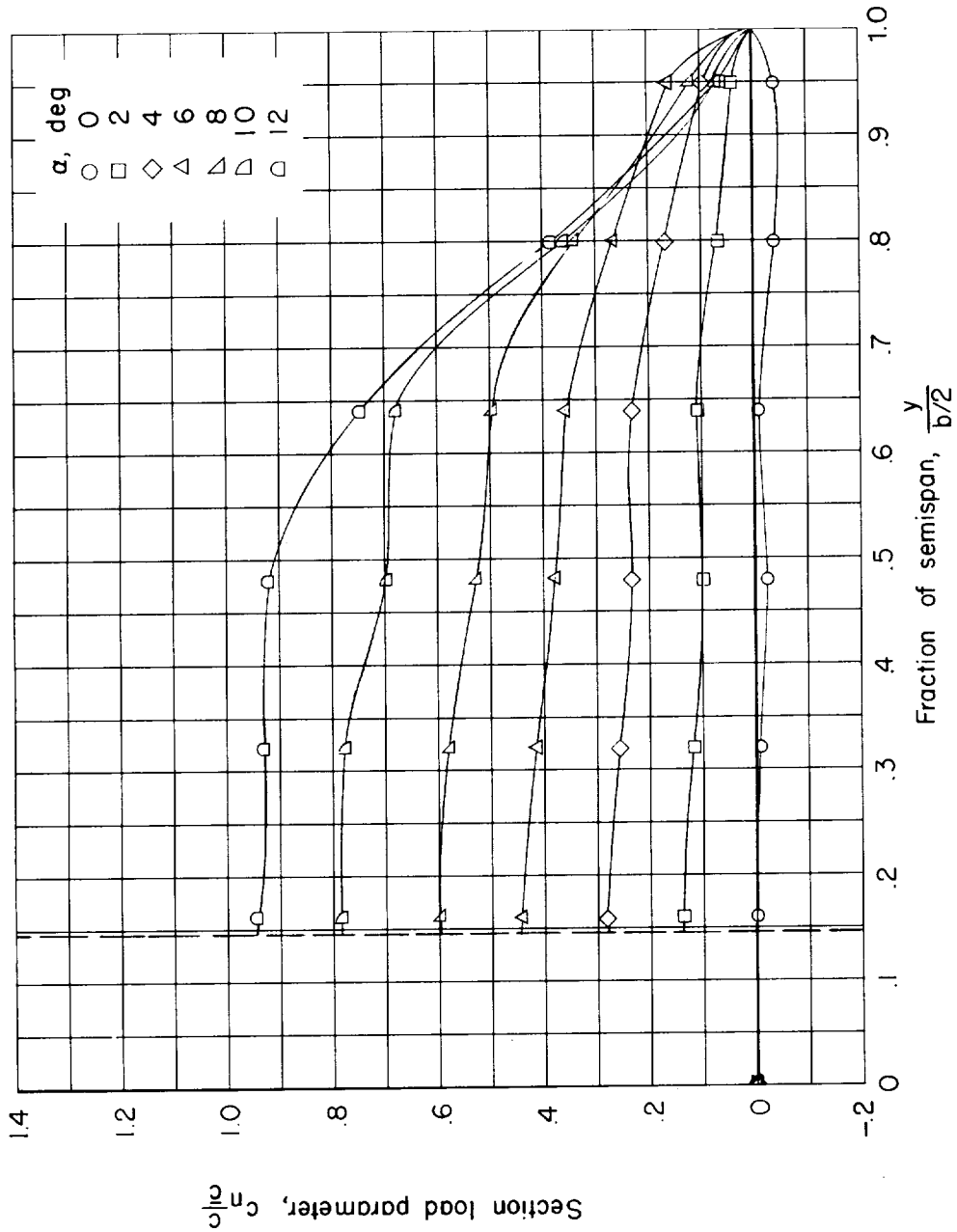

(f) M = 0.98.

Figure 9.- Continued.

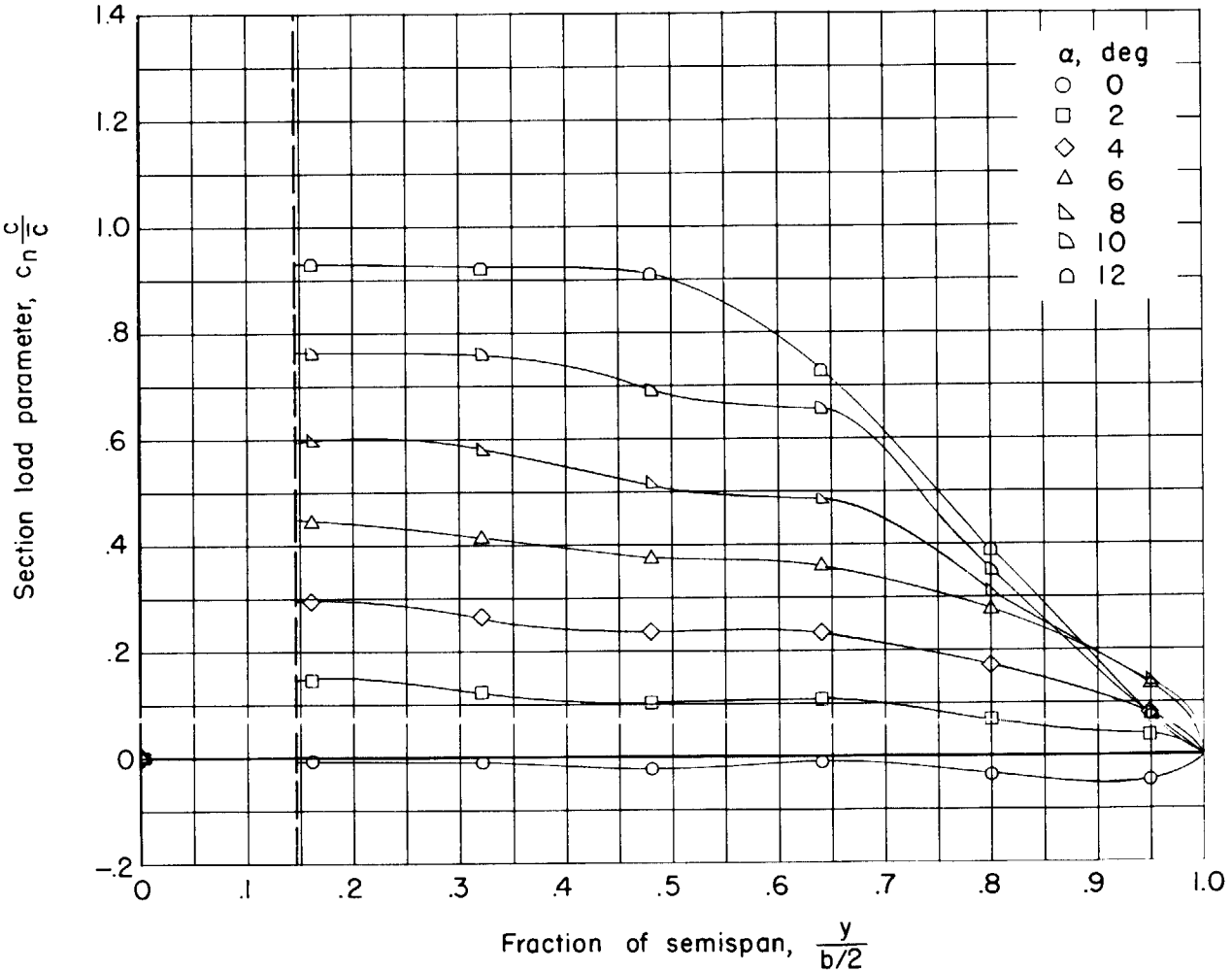

(g) M = 1.00.

Figure 9.- Continued.

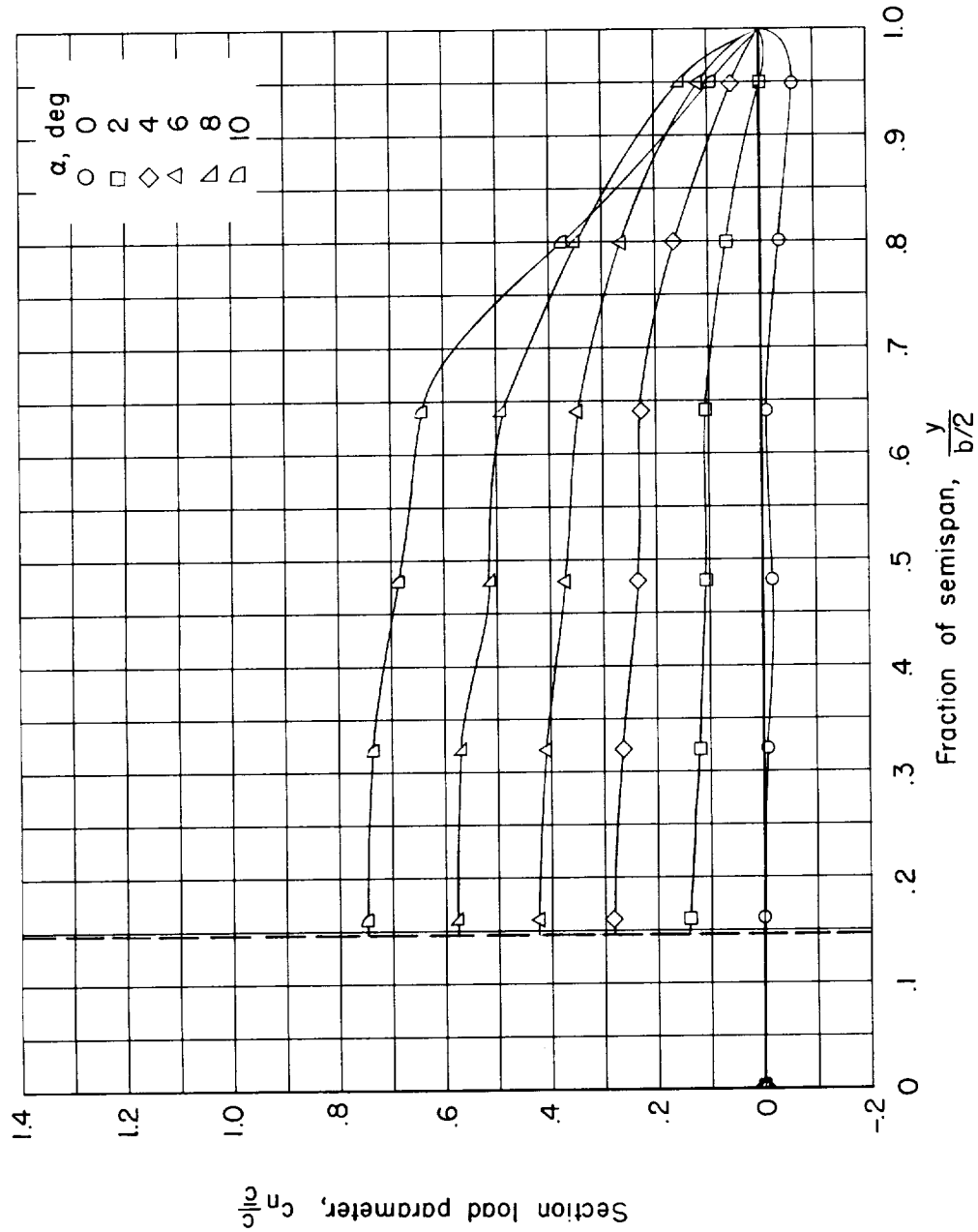

(h) M = 1.05.

Figure 9.- Concluded.

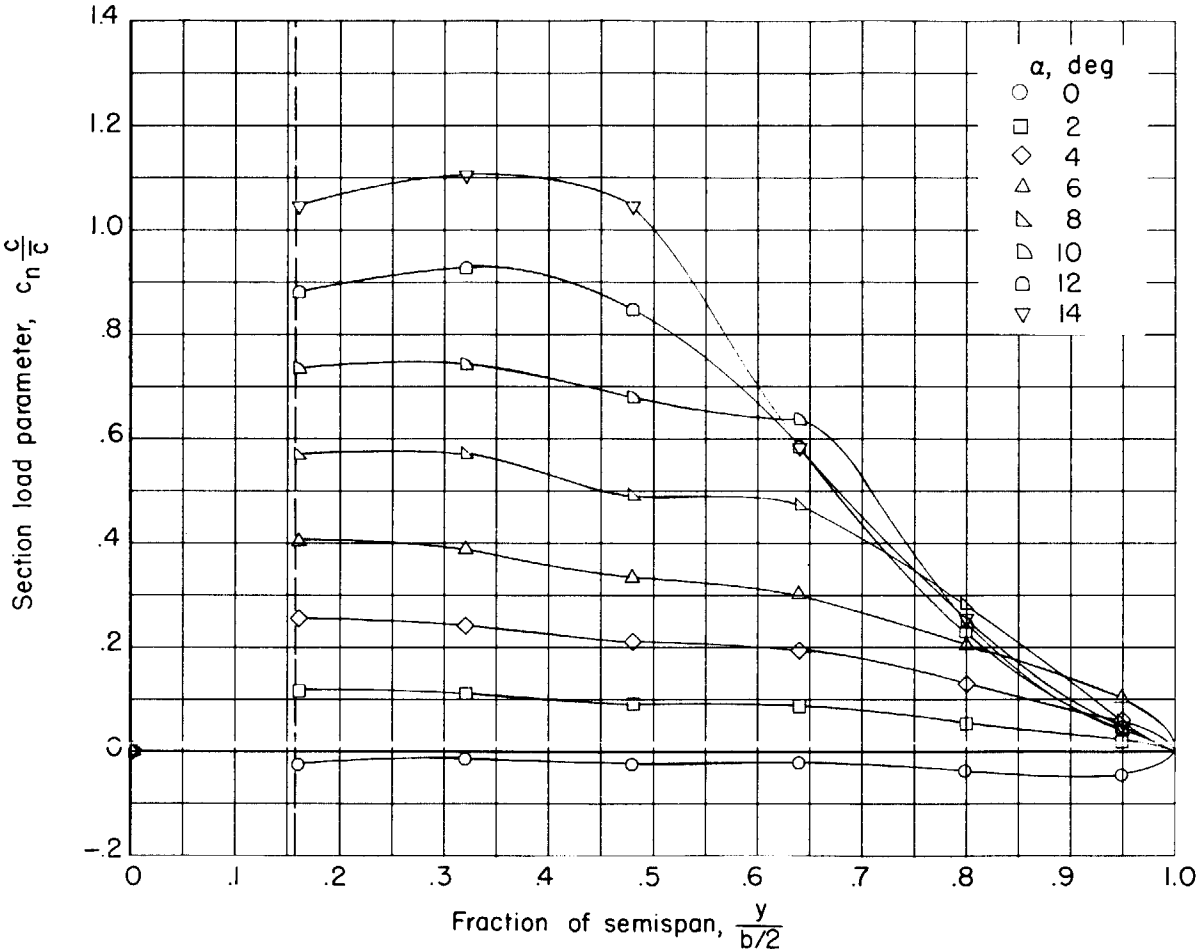

(a) M = 0.80.

Figure 10.- Spanwise variation of section normal-load parameter for the cambered wing in combination with the nonindented body at various angles of attack and Mach numbers.

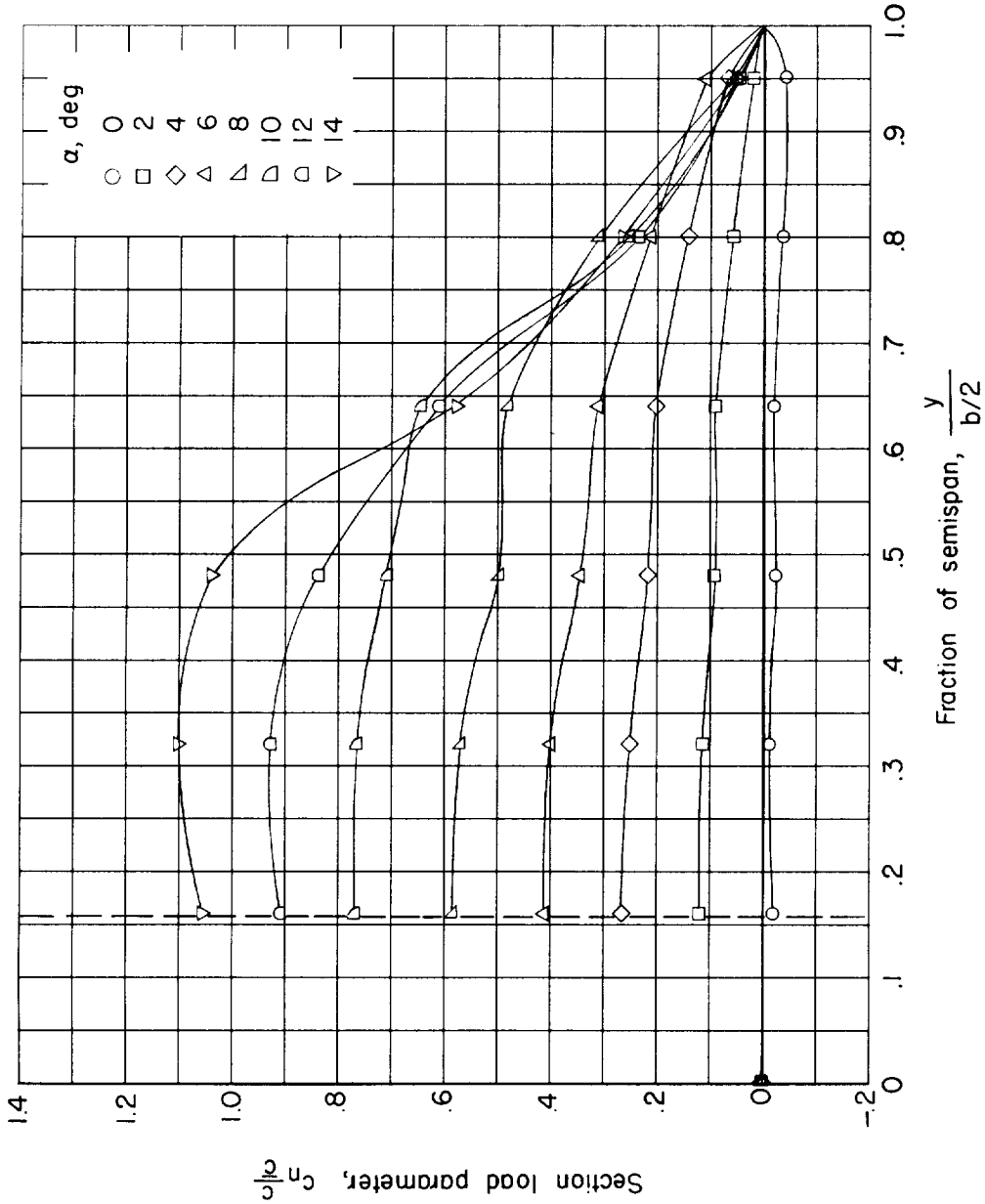

(b) M = 0.85.

Figure 10.- Continued.

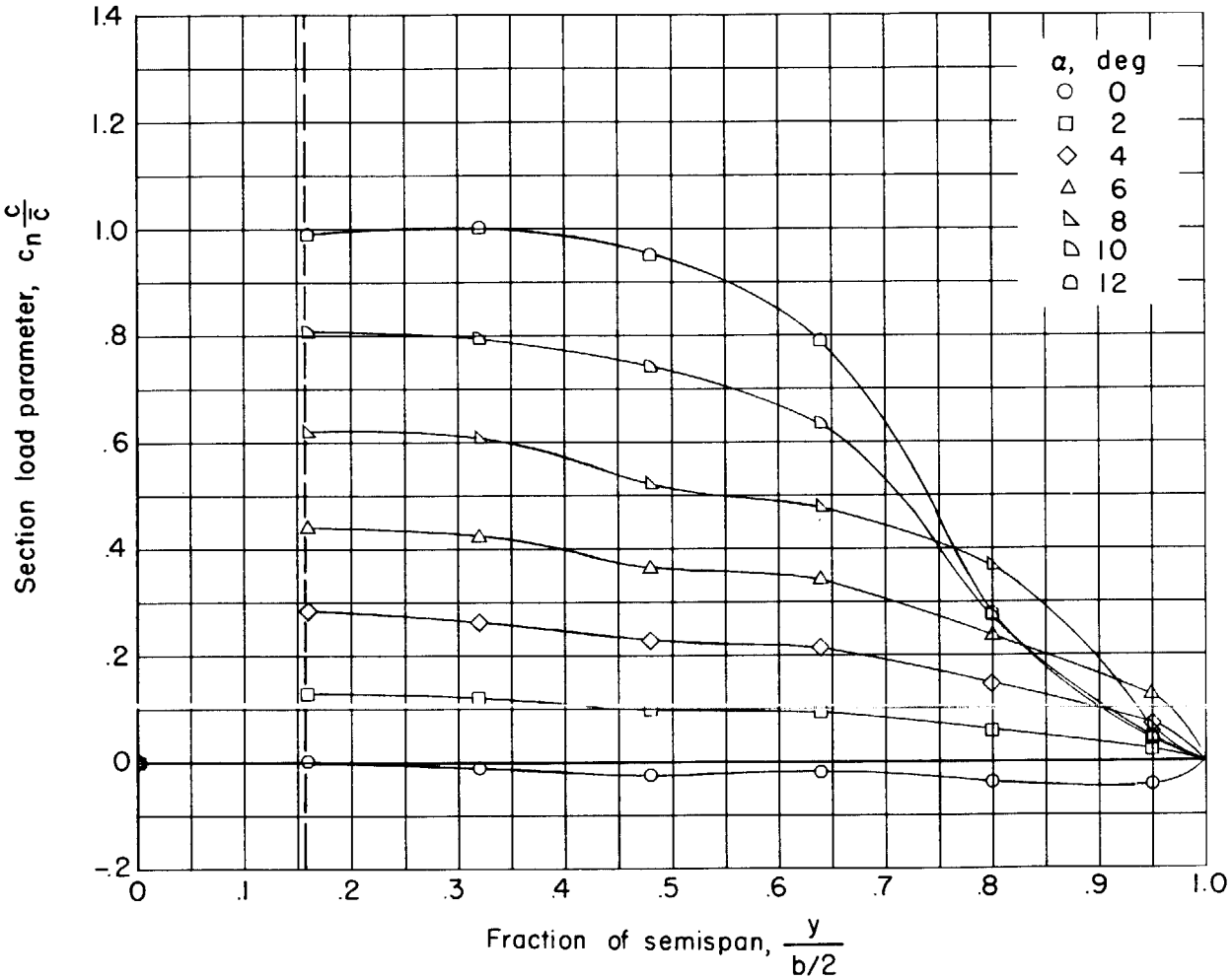

(c) M = 0.90.

Figure 10.- Continued.

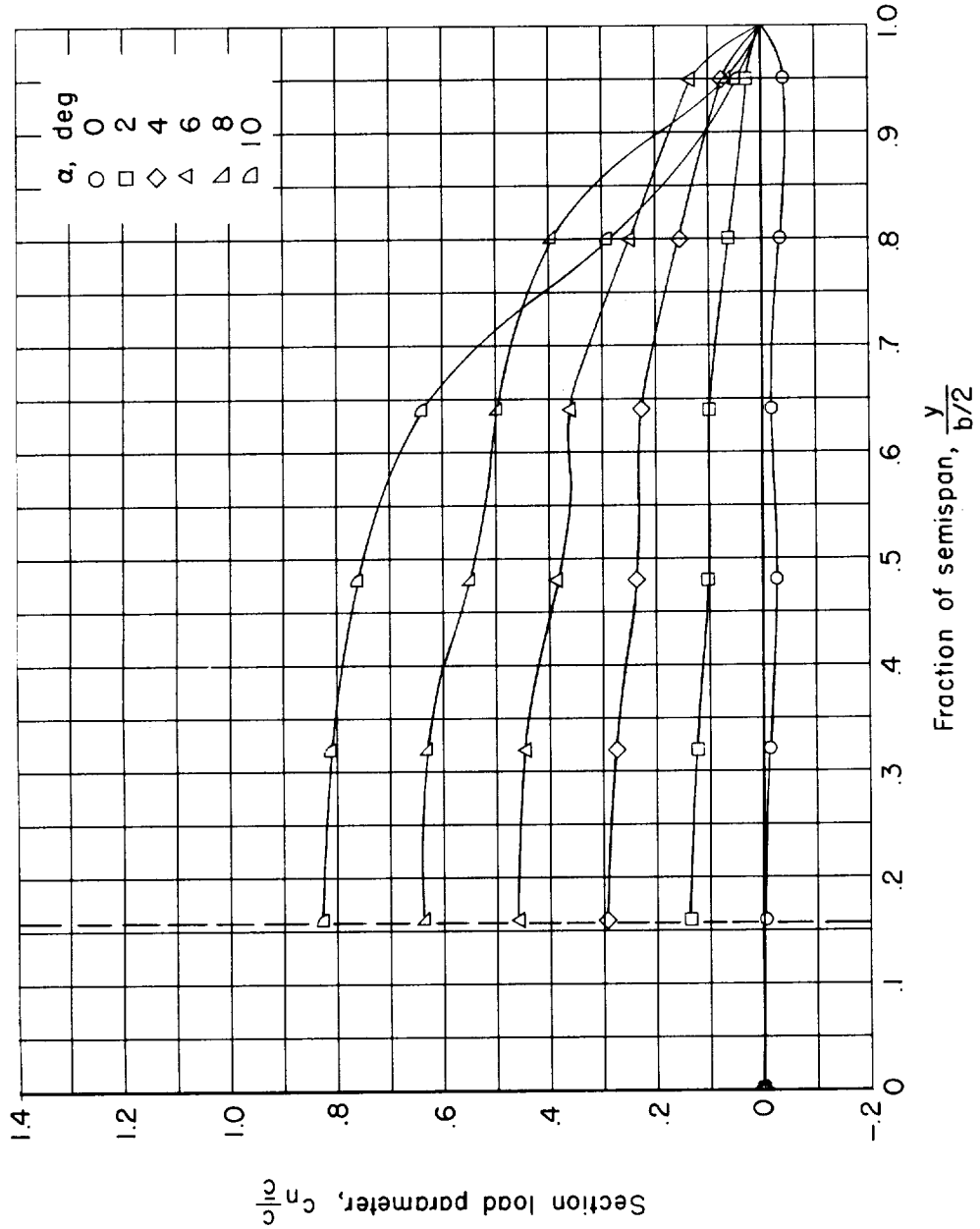

(d) M = 0.92.

Figure 10.- Continued.

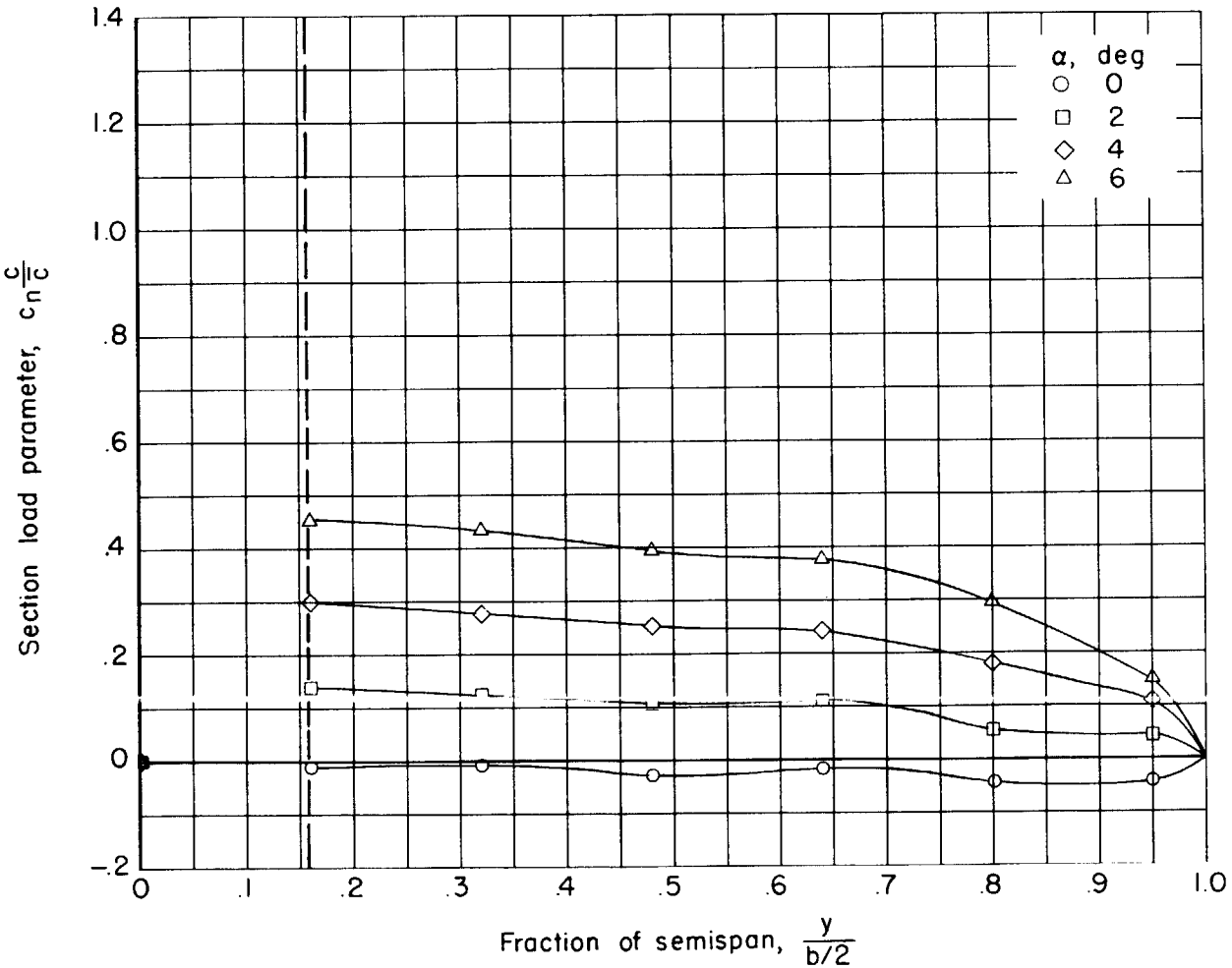

(e) M = 0.98.

Figure 10.- Continued.

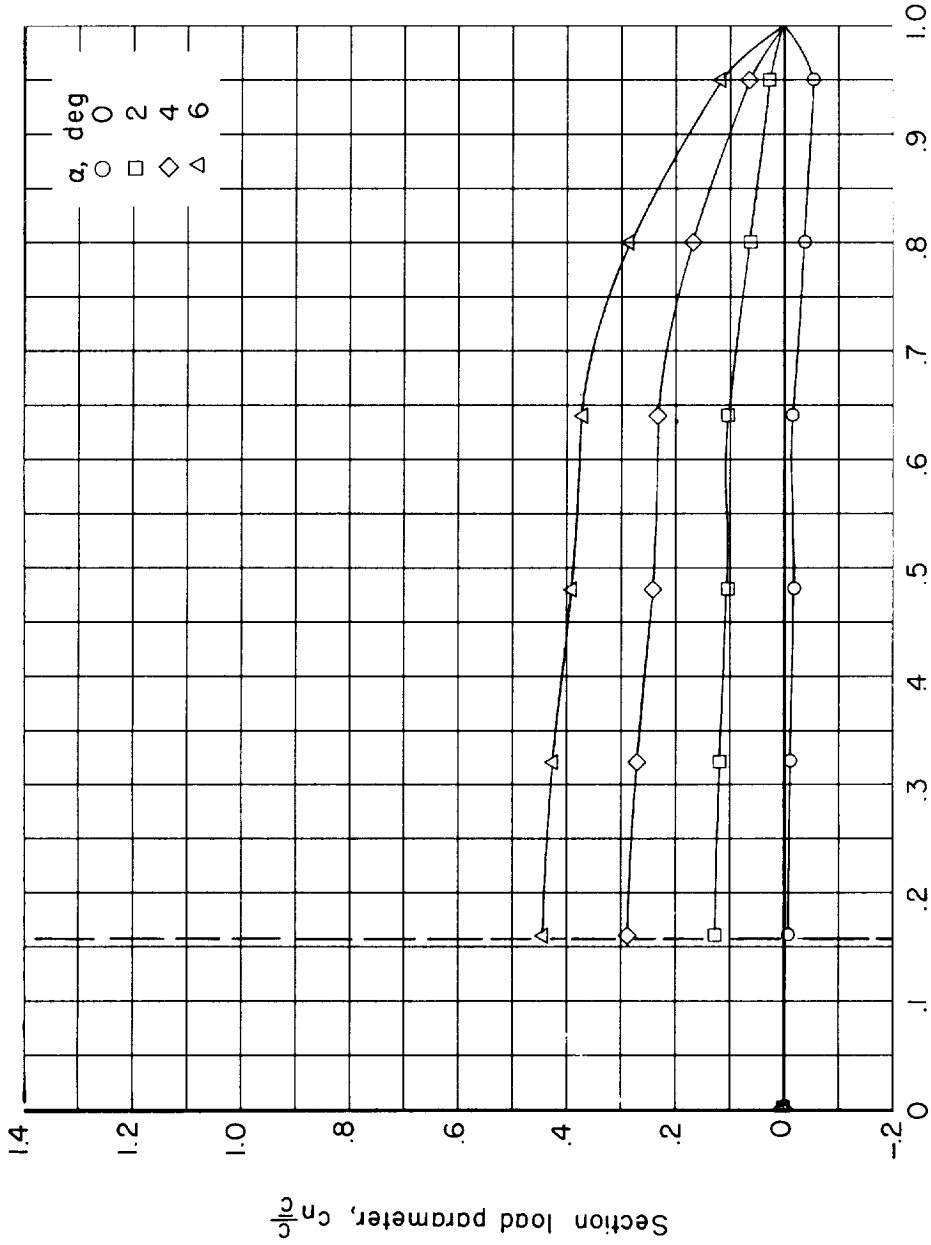

(f) M = 1.00.

Figure 10.- Continued.

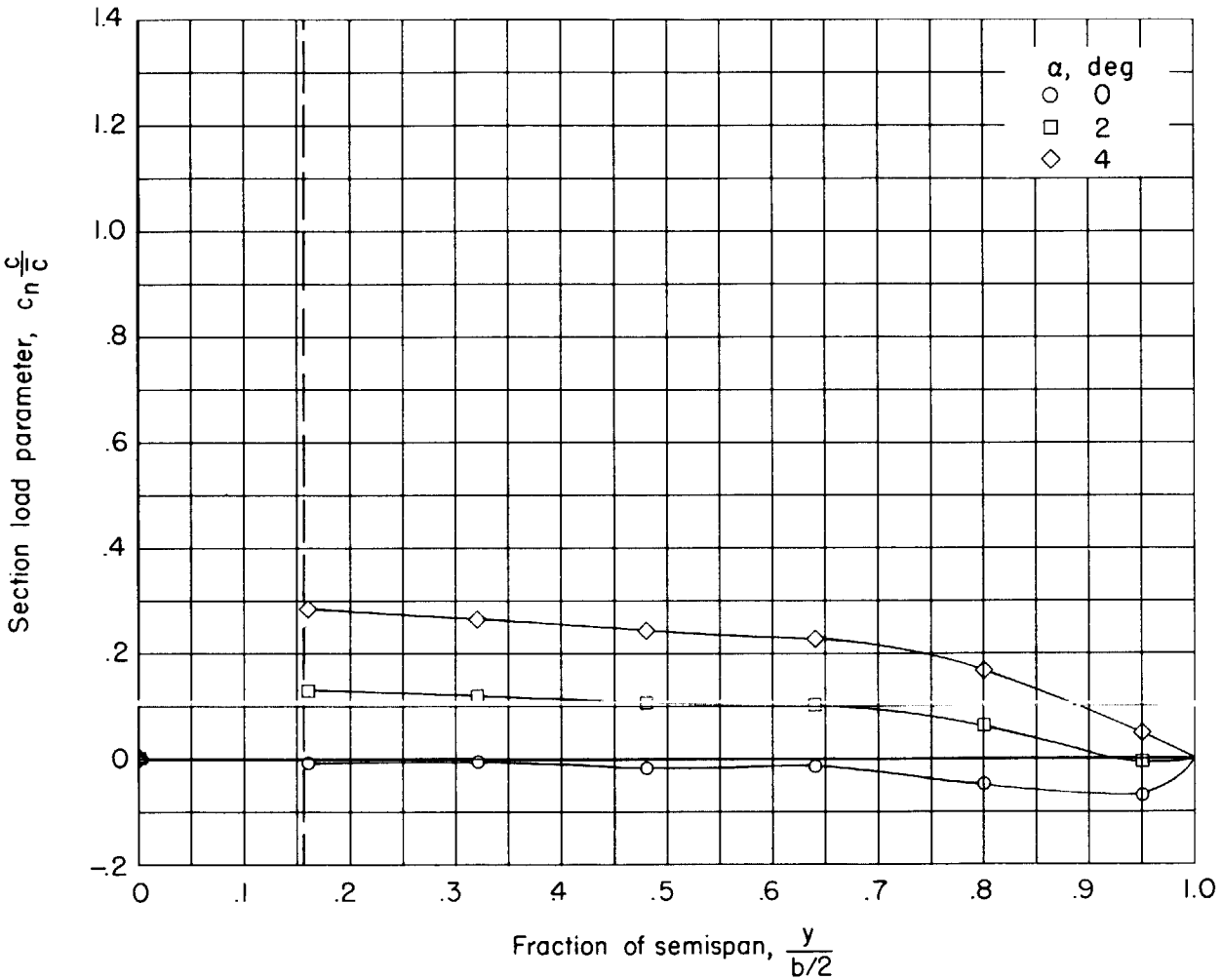

(g) M = 1.05.

Figure 10.- Concluded.

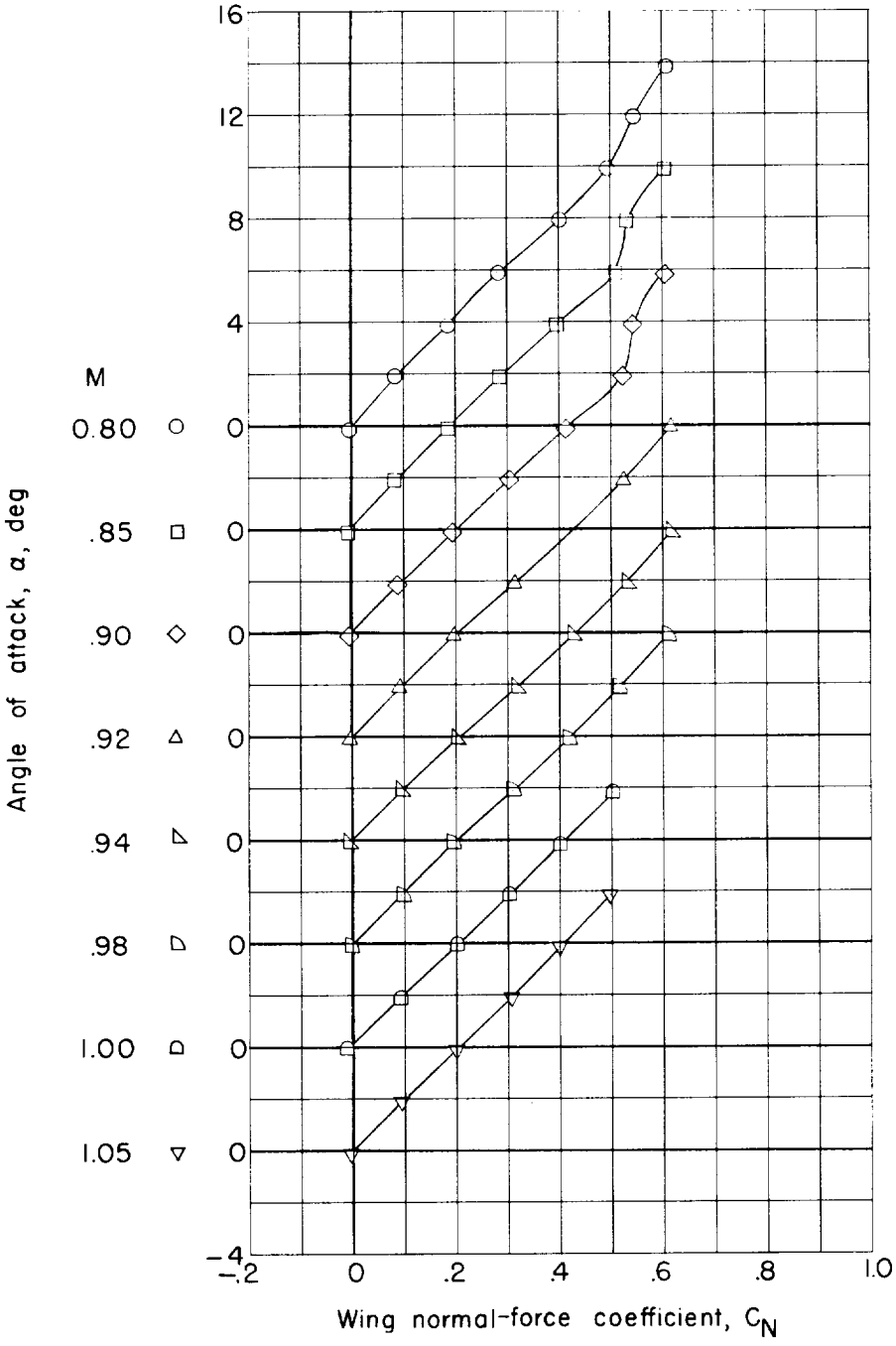

(a) Indented body and plane wing.

Figure 11.- Variation of angle of attack with wing normal-force coefficient for various Mach numbers.

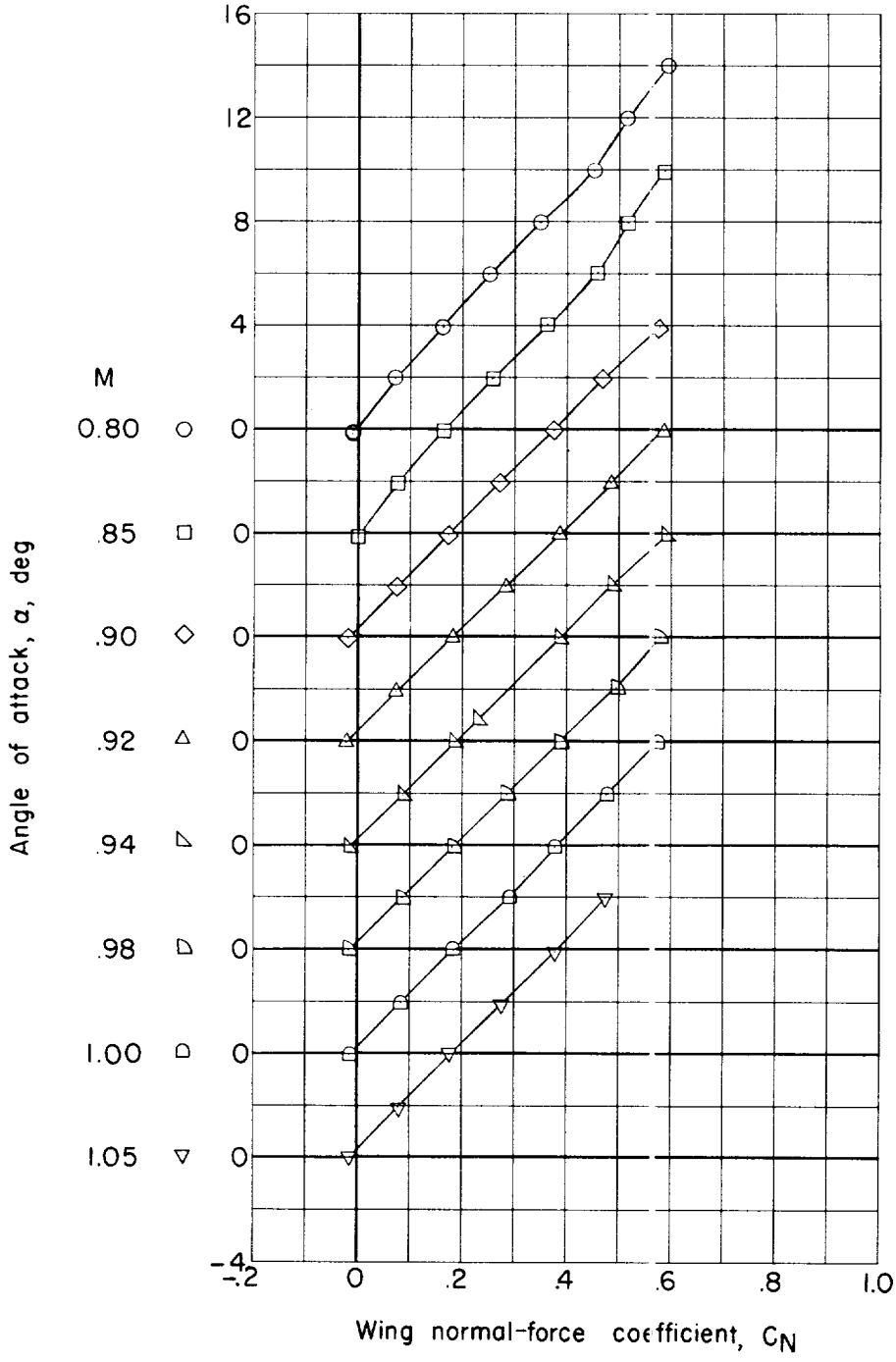

(b) Indented body and cambered wing.

Figure 11.- Continued.

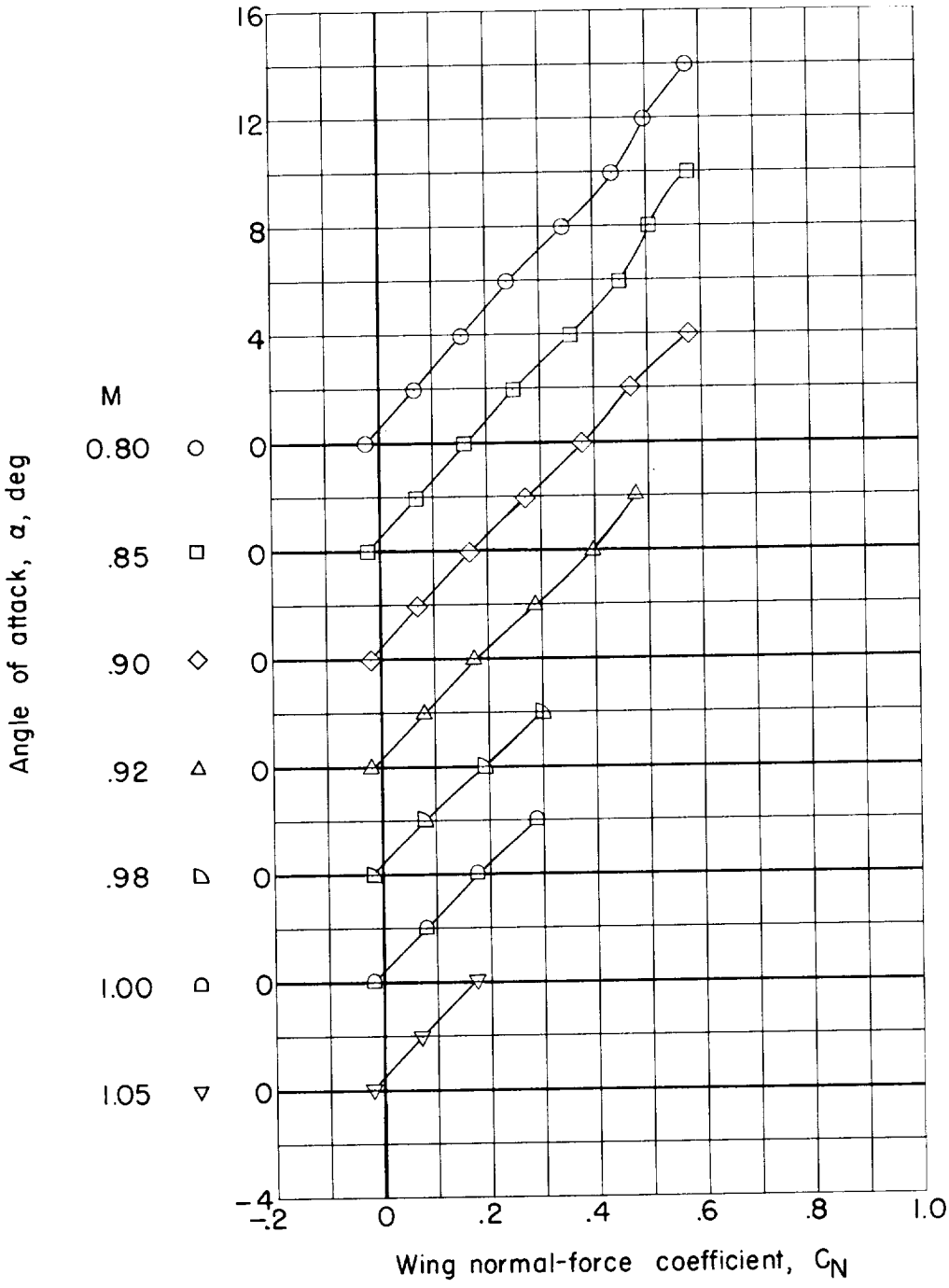

(c) Nonindented body and cambered wing.

Figure 11.- Concluded.

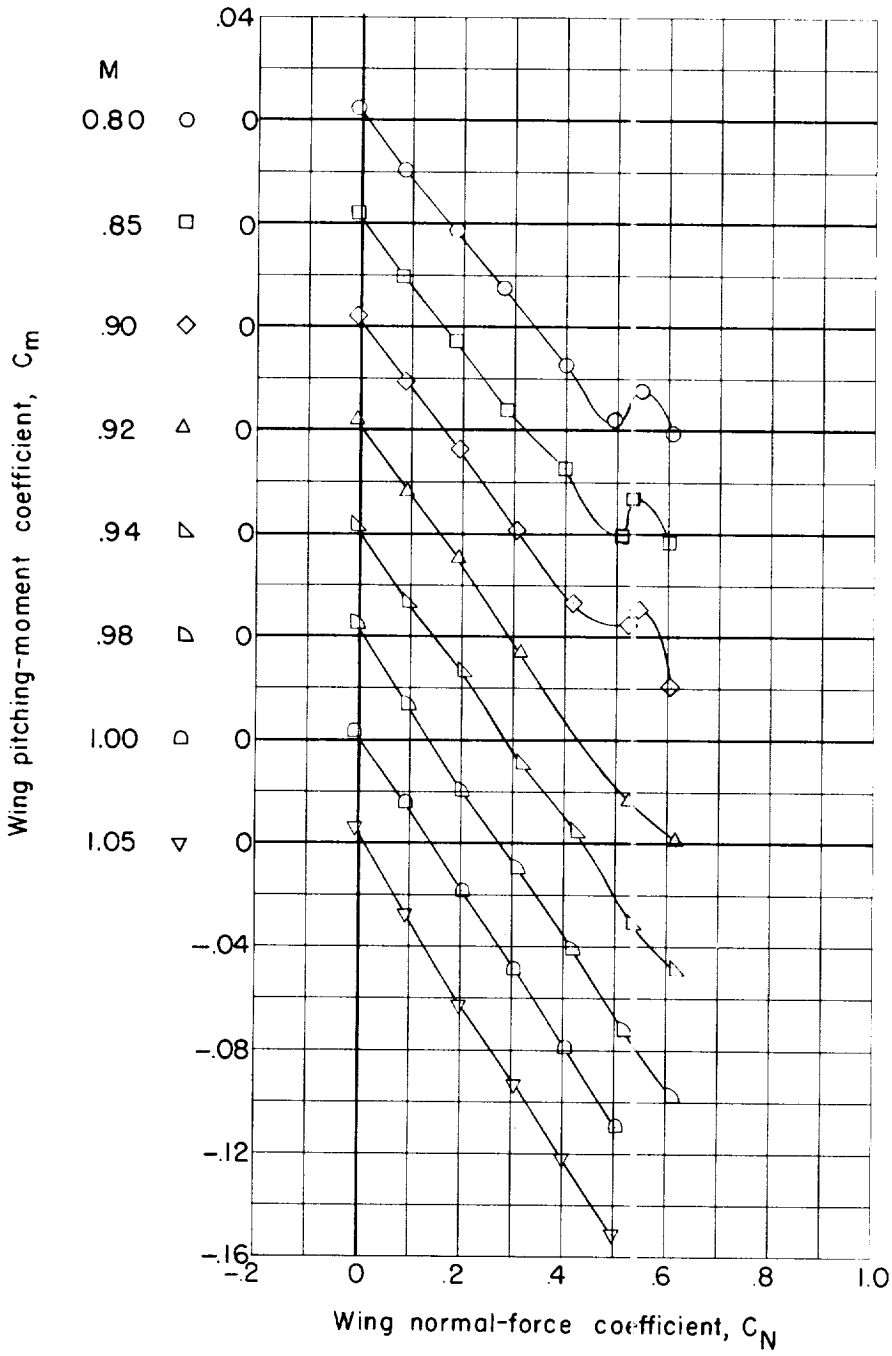

(a) Indented body and plane wing.

Figure 12.- Variation of wing pitching-moment coefficient with wing normal-force coefficient for various Mach numbers.

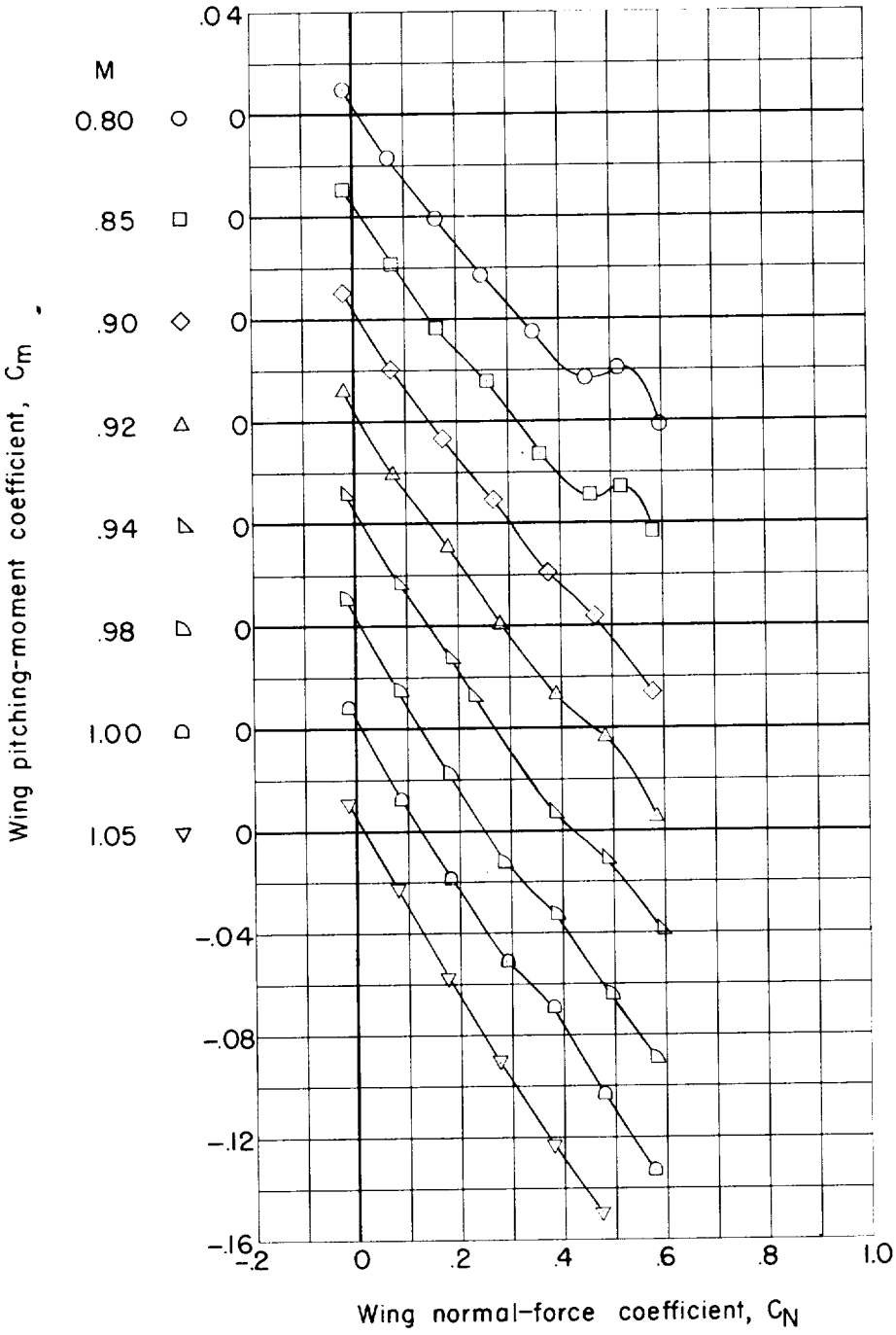

(b) Indented body and cambered wing.

Figure 12.- Continued.

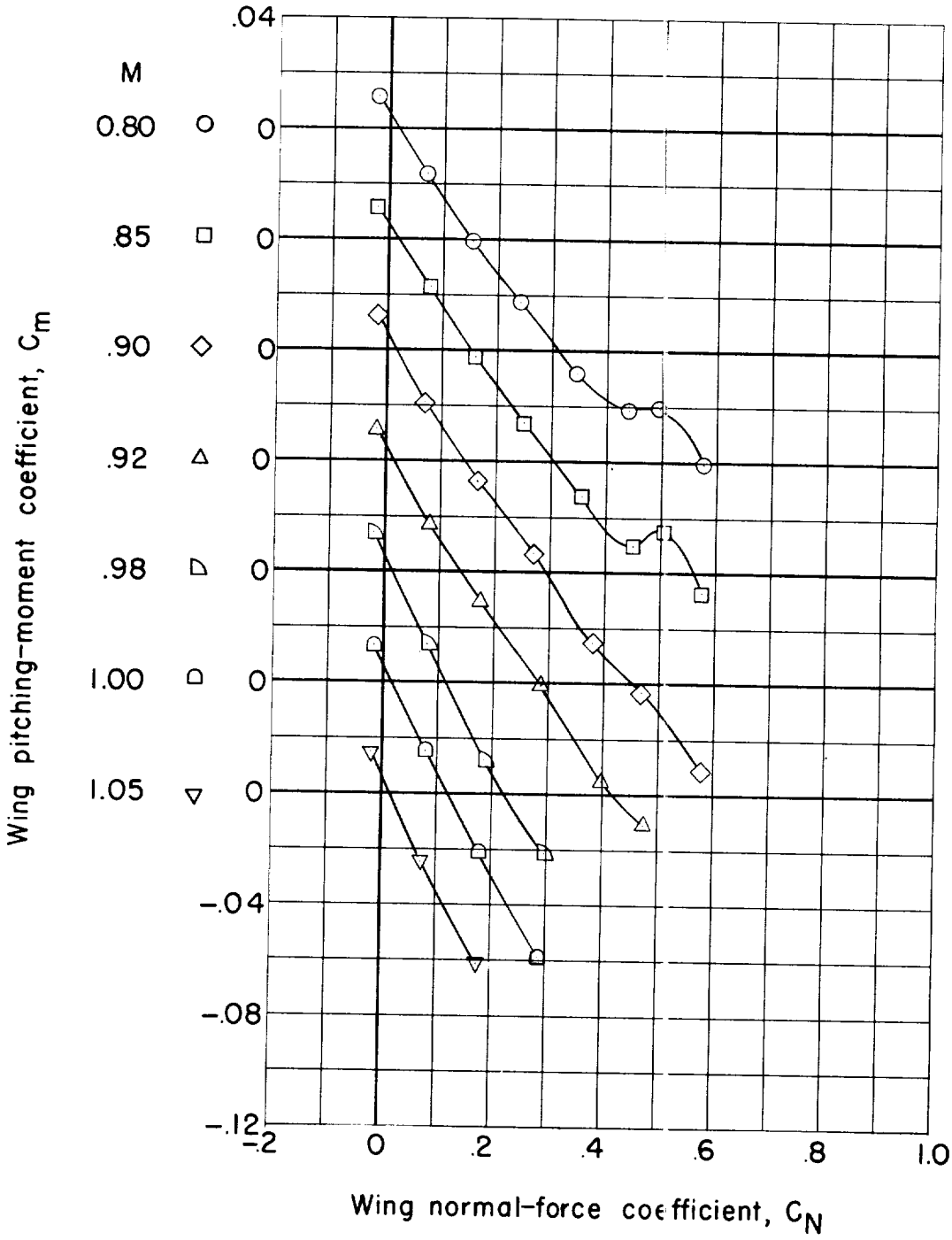

(c) Nonindented body and cambered wing.

Figure 12.- Concluded.

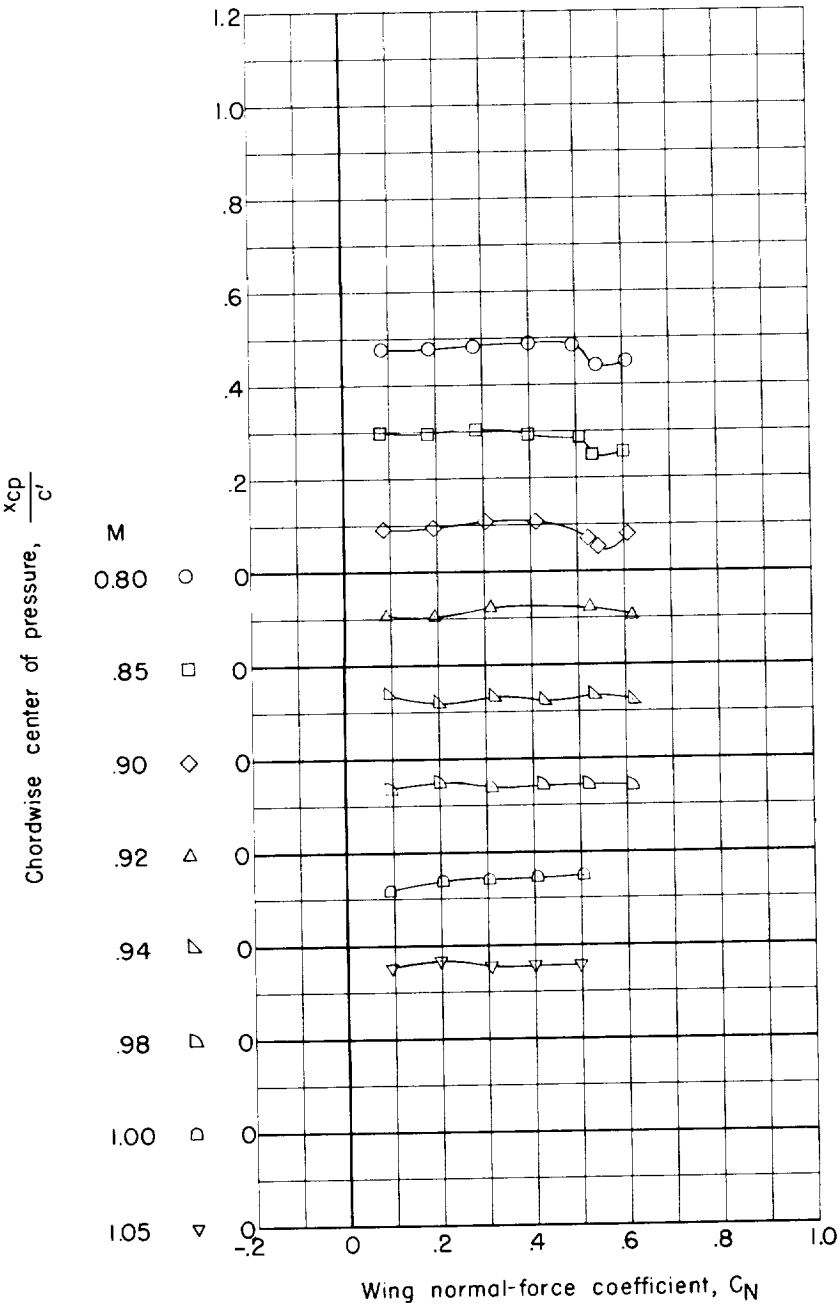

(a) Indented body and plane wing.

Figure 13.- Variation of wing chordwise center-of-pressure location with wing normal-force coefficient for various Mach numbers.

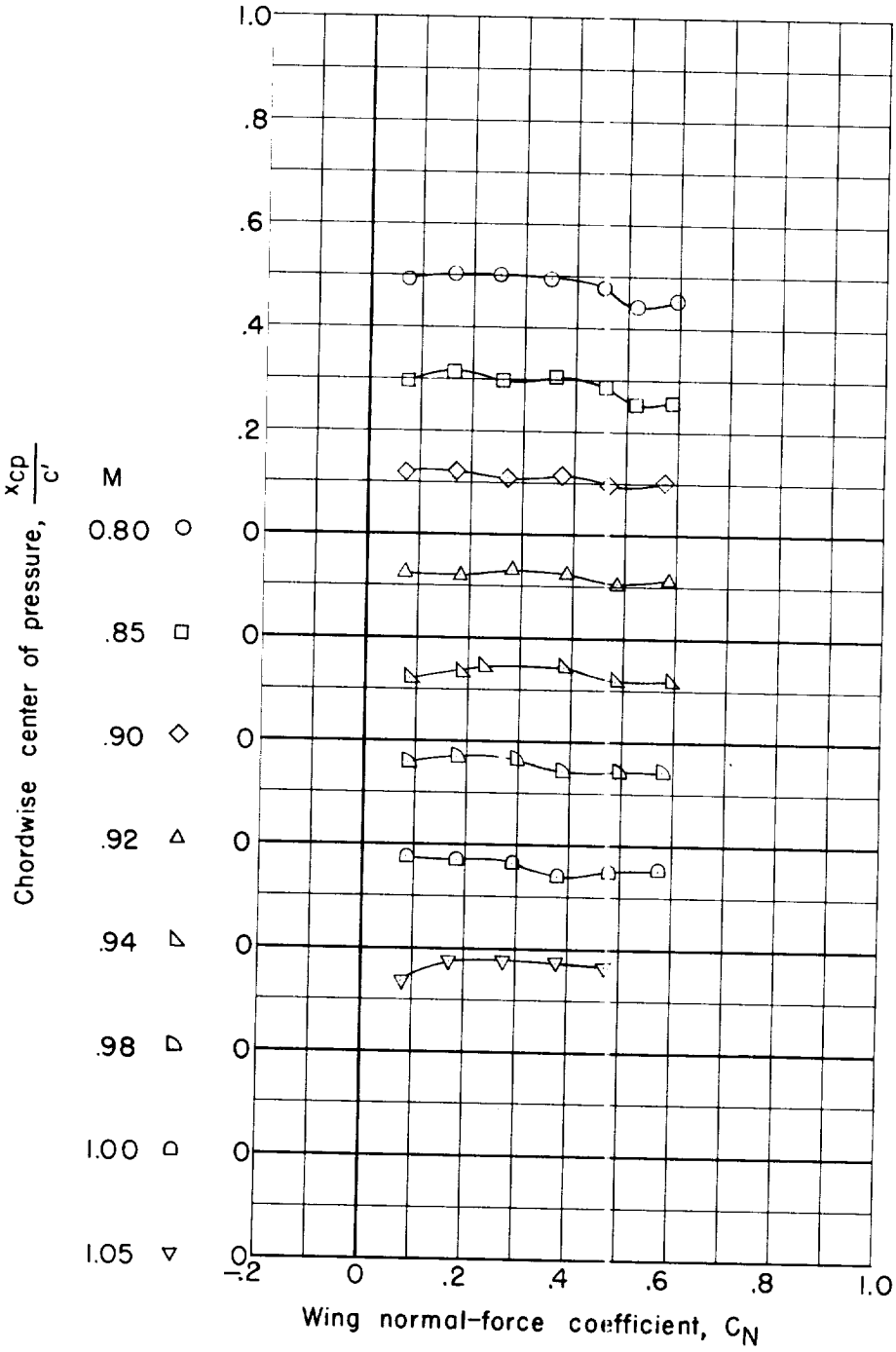

(b) Indented body and cambered wing.

Figure 13.- Continued.

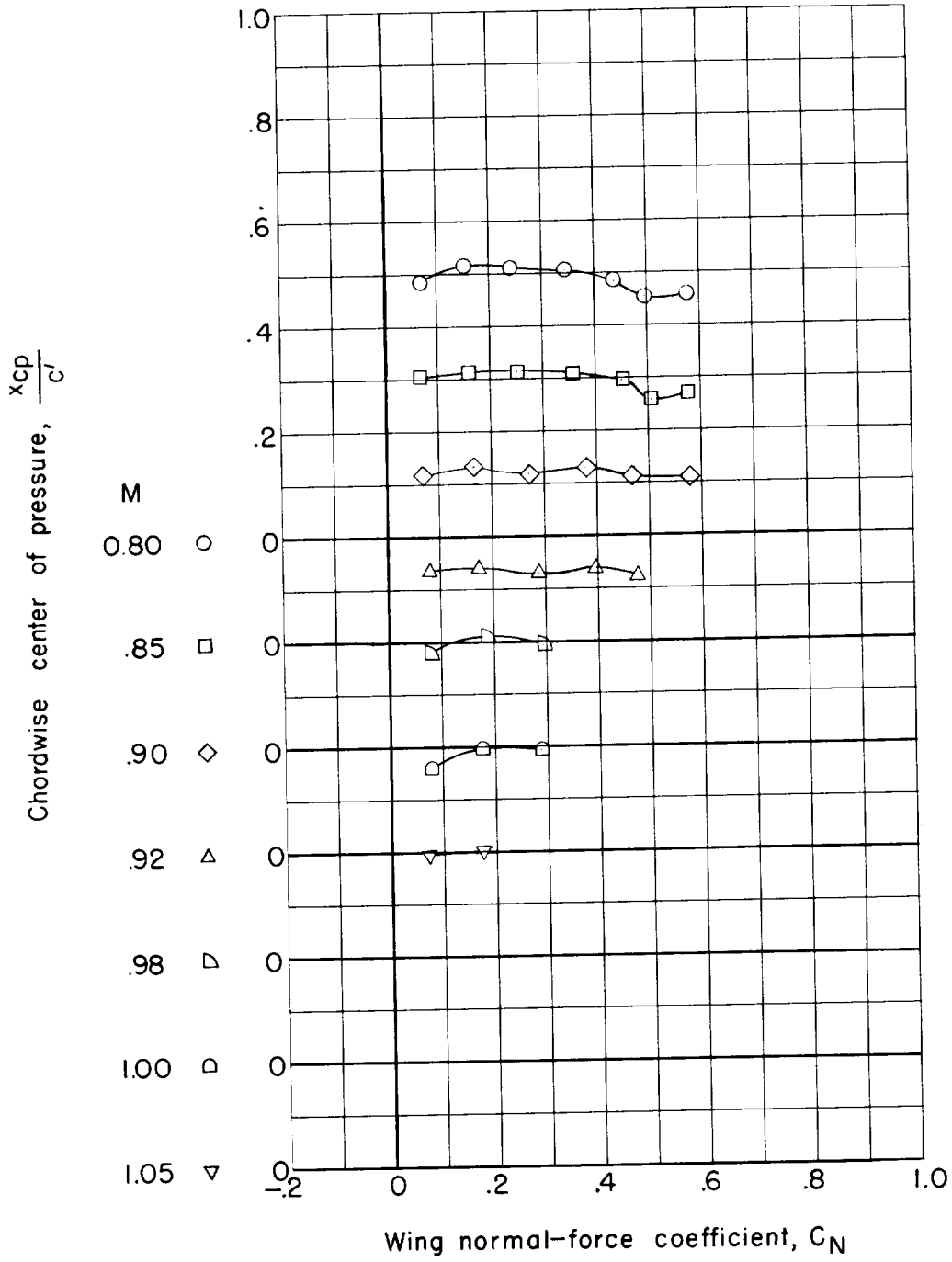

(c) Nonindented body and cambered wing.

Figure 13.- Concluded.

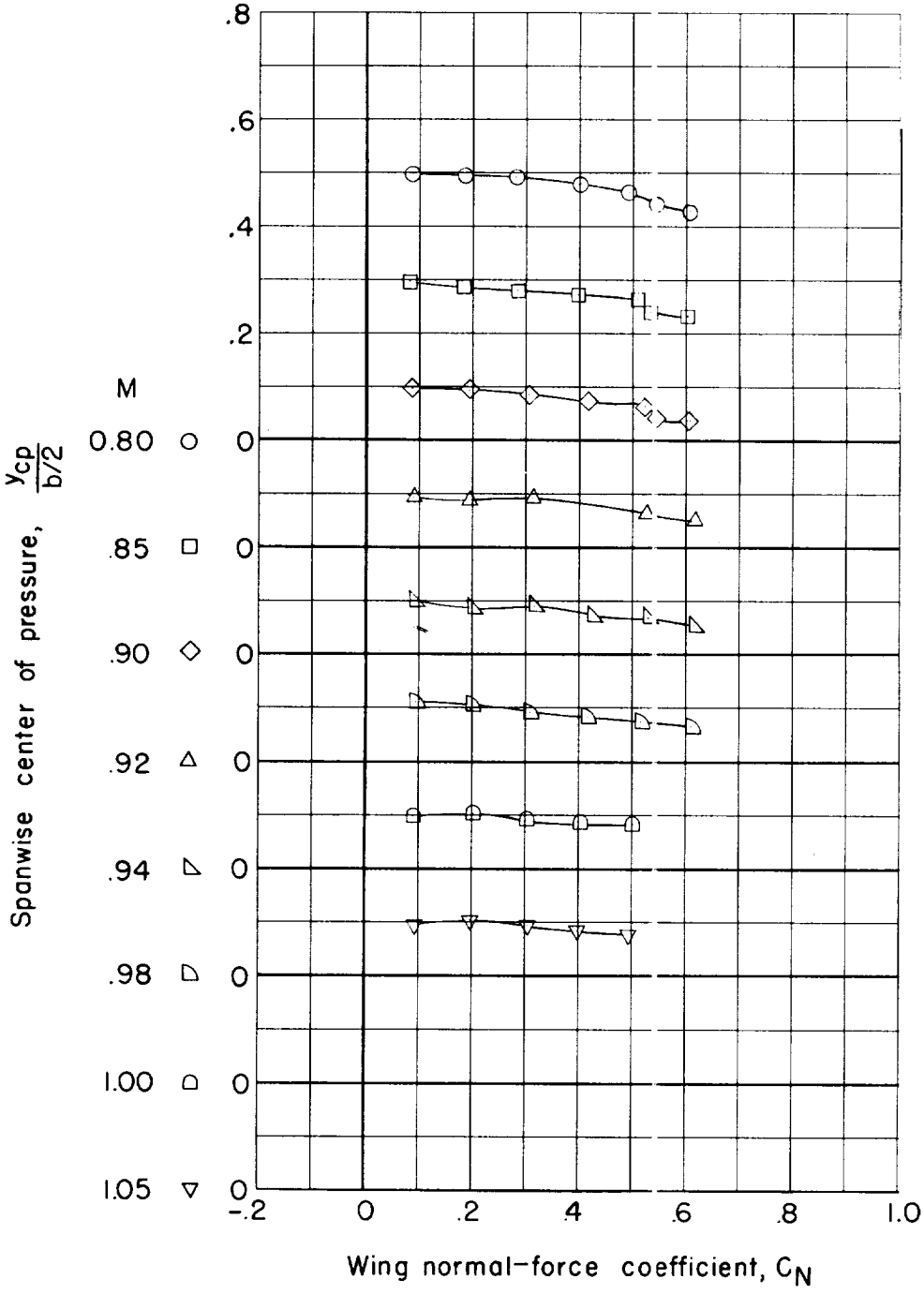

(a) Indented body and plane wing.

Figure 14.- Variation of spanwise center-of-pressure location with wing normal-force coefficient for various Mach numbers.

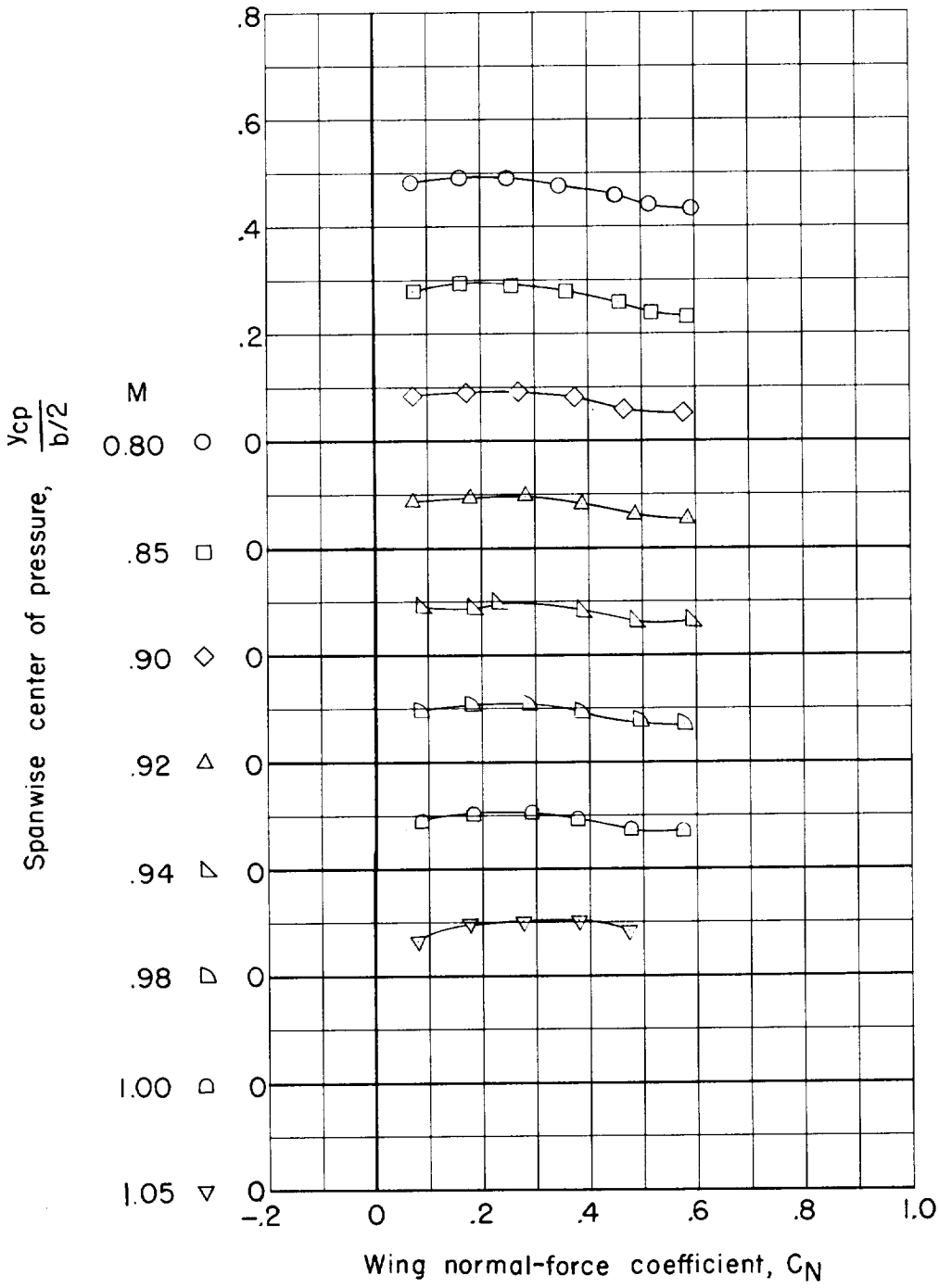

(b) Indented body and cambered wing.

Figure 14.- Continued.

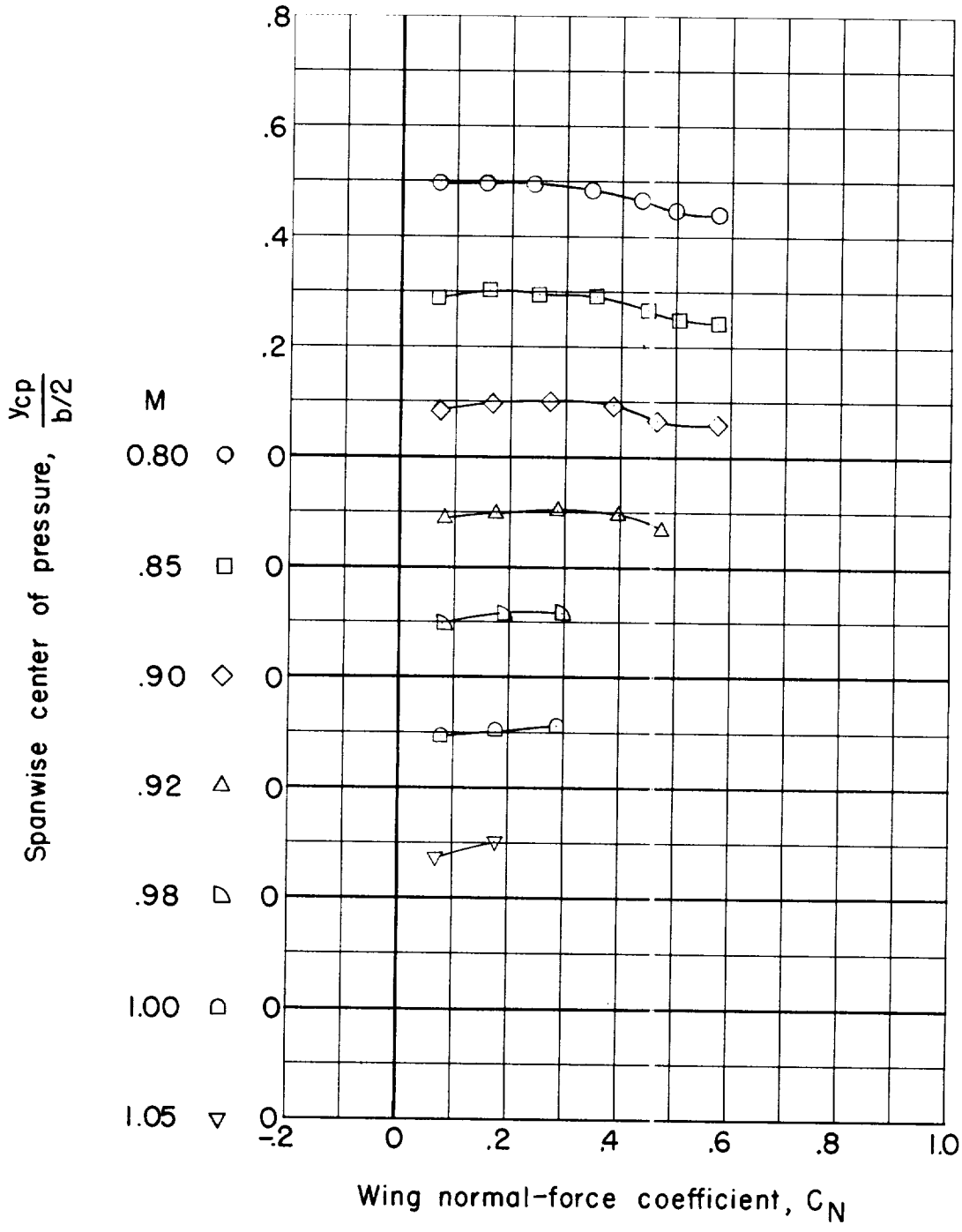

(c) Nonindented body and cambered wing.

Figure 14.- Concluded.

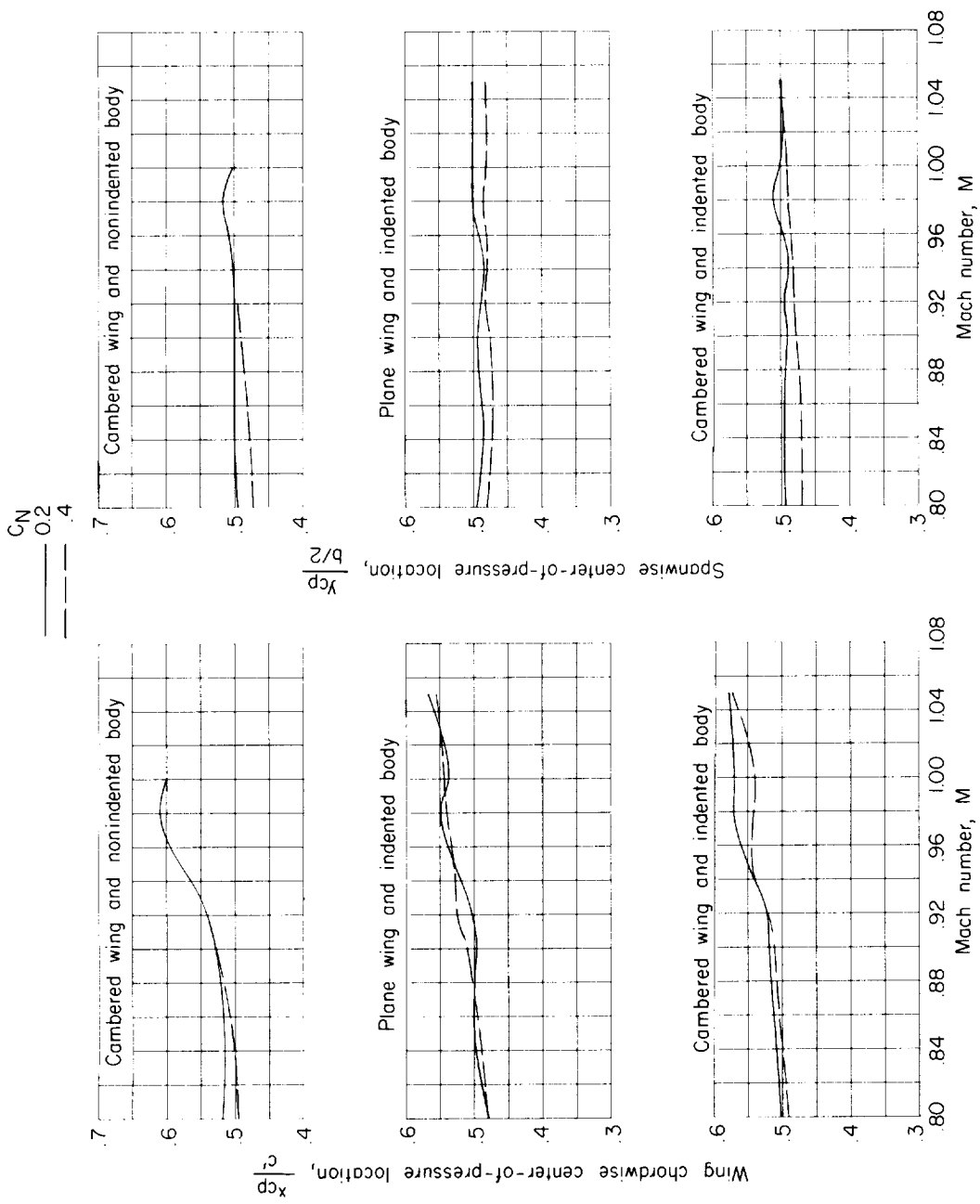

Figure 15.- Variation of wing chordwise center of pressure and spanwise center of pressure with Mach number for constant values of wing normal-force coefficient.

NASA-Langley, 1961 L-1564

L-1564